

Scuola di Scienze  
Corso di Laurea Magistrale in Fisica

**Analysis of the spectrum of the spin-1  
biquadratic antiferromagnetic chain**

**Relatore:**  
Prof. Elisa Ercolessi

**Presentata da:**  
Ferri Silvia

**Correlatore:**  
Dott. Davide Vodola

**Sessione III**  
**Anno Accademico 2013/2014**



to Giulia whose passion had me starting and to Ezio whose death had me finishing



## Abstract

In questo elaborato vengono discusse le catene di spin-1, modelli quantistici definiti su un reticolo unidimensionale con interazione tra siti primi vicini. Fra la ricca varietà di tipologie esistenti è stato scelto di porre attenzione primariamente sul modello antiferromagnetico con interazione puramente biquadratica. Vengono presentati diversi metodi di classificazione degli autostati di tale modello, a partire dalle simmetrie che ne caratterizzano l'Hamiltoniana. La corrispondenza con altri modelli noti, quali il modello XXZ di spin 1/2, la catena di Heisenberg  $SU(3)$  ed i modelli di Potts, è utile ad individuare strutture simmetriche nascoste nel formalismo di spin-1, le quali consentono di ricavare informazioni sullo spettro energetico. Infine, vengono presentati risultati numerici accompagnati da alcune considerazioni sulle modifiche dello spettro quando si aggiunge un termine bilineare alla Hamiltoniana biquadratica.



# Contents

	iii
	v
<b>Introduction</b>	<b>ix</b>
<b>1 A brief overview of spin-1 models</b>	<b>1</b>
1.1 The bilinear-biquadratic spin-1 Hamiltonian . . . . .	1
<b>2 <math>SU(2)</math> symmetry and correspondence with the XXZ model</b>	<b>11</b>
2.1 Correspondence between XXZ model and pure-biquadratic model . . . . .	13
2.2 The XXZ model: Bethe ansatz . . . . .	15
2.3 The purely biquadratic Hamiltonian: Bethe ansatz . . . . .	19
2.3.1 Single-deviation states . . . . .	20
2.3.2 Two-deviation states . . . . .	20
2.3.3 Three-deviation states . . . . .	21
2.3.4 Four-deviation states . . . . .	23
2.4 Note on the correspondence of states . . . . .	26
<b>3 <math>SU(3)</math> symmetry and the bilinear Heisenberg chain</b>	<b>27</b>
3.1 $SU(3)$ Heisenberg chain . . . . .	27
3.2 $SU(3)$ -symmetry of the pure biquadratic spin-1 model . . . . .	30
3.3 Mapping of the biquadratic Hamiltonian into a $SU(3)$ spin chain . . . . .	31
3.4 Complete mapping of quantum numbers . . . . .	34
<b>4 Equivalence with the nine-state Potts model</b>	<b>43</b>
4.1 $q$ -state Potts models . . . . .	43
4.2 Fermionic formulation of $SU(3)$ Heisenberg Hamiltonian . . . . .	49
4.3 Correspondence between the Potts model and the biquadratic Hamiltonian . . . . .	53
4.4 $q$ -state vertex models correspondence with the biquadratic Hamiltonian . . . . .	59

---

<b>5</b>	<b>Two-site, four-site and six-site biquadratic Hamiltonian</b>	<b>63</b>
5.1	Biquadratic Hamiltonian on a two-site chain . . . . .	64
5.2	Biquadratic Hamiltonian on a four-site chain . . . . .	79
5.3	Biquadratic Hamiltonian on a six-site chain . . . . .	91
<b>6</b>	<b>Eight-site Hamiltonian and new results</b>	<b>99</b>
6.1	Comments on the ground state of the pure-biquadratic model	99
6.2	Eight-site Hamiltonian . . . . .	102
<b>A</b>	<b>Spin-1 Representations</b>	<b>109</b>
A.1	Spin variables . . . . .	109
A.2	Spin-1 operators . . . . .	110
A.3	$SU(2)$ -multiplets . . . . .	112
A.4	Useful commutation rules for spin operators . . . . .	113
<b>B</b>	<b><math>SU(3)</math> group</b>	<b>115</b>
B.1	Group generators . . . . .	115
B.2	Lie Subalgebras of $SU(3)$ . . . . .	116
B.3	$SU(3)$ -multiplets . . . . .	119
<b>C</b>	<b>Alternative mapping</b>	<b>125</b>
C.1	Alternative form of the $SU(3)$ Heisenberg chain . . . . .	125
C.2	Mapping between spin-1 operators and Gell-Mann matrices . . . . .	126

# Introduction

Spin-1 models are not as studied as the widespread spin-1/2 ones, which are known to be integrable thanks to the Bethe ansatz technique [40], even in some anisotropic cases. Nevertheless, they are indeed an interesting matter of discussion. In fact, they represent the simplest non trivial case of integer spin systems, which are expected, according to Haldane [23], to behave quite differently from the half-integer ones. The main difference emerges when comparing spin-1 and spin-1/2 Heisenberg models: while the spin-1/2 XXX chain is well-known to be gapless, the spin-1 bilinear model represents a massive, i.e. gapped, theory.

There are mainly two types of spin-1 models which are currently objects of study.

The first one appears as a generalisation of the spin-1/2 XXZ Hamiltonian to the case of spin-1 variables and it is named  $\lambda - D$  model after the parameters that characterise it.

$$\mathcal{H}(\lambda, D) = \sum_{i=1}^N [S_i^x S_{i+1}^x + S_i^y S_{i+1}^y + \lambda S_i^z S_{i+1}^z + D(S_i^z)^2] \quad (1)$$

As it happens for the spin-1/2 Heisenberg model, the first parameter  $\lambda$  quantifies the anisotropy along the  $z$ -direction. The main difference with the former model, though, is given by the presence of a quadratic self-interaction term (its coefficient conventionally labelled with  $D$ ), that is responsible for a richer phase diagram of this model. It displays, among others, an Ising-like phase, a large- $D$  phase and a so-called Haldane phase.

The Ising-like phase (large  $\lambda$  and small  $D$ ) shows the usual long-range antiferromagnetic order with a ground state given by the perturbation of the two Néel states, having alternate spins with  $S^z = \pm 1$ . The other two antiferromagnetic phases have both a null Néel order parameter, however there is another operator, that is the string order parameter [26], allowing us to distinguish among them. Whereas it is null in the large- $D$  phase, for which the system configuration with all zero  $z$ -component of spin is energetically favourite, it has a non-null value for the Haldane phase, which lies in the intermediate parameter region in the phase diagram.

The second type of spin-1 Hamiltonian, which will be taken under ex-

amination throughout this work, contains both a bilinear and a biquadratic exchange term:

$$\mathcal{H}(J_i, \Theta) = \sum_{i=1}^N J_i \left[ \cos \Theta \vec{S}_i \cdot \vec{S}_{i+1} - \sin \Theta (\vec{S}_i \cdot \vec{S}_{i+1})^2 \right] \quad (2)$$

with  $J_{2i} = \delta \leq 1$  and  $J_{2i-1} = 1$ .

Depending on the values of the angle  $\Theta$ , parametrising the ratio of the coupling constants of the two terms of the Hamiltonian, and the anisotropy parameter  $\delta$  for the even sublattice, the bilinear-biquadratic model displays various behaviours, again with different antiferromagnetic phases. One of them is the dimerised phase (the system shows a tendency to spontaneously split into pairs of interacting spins), which has both order parameters null and it is the analogue of the large- $D$  phase. Then, the Haldane phase, the phase region in which lies the spin-1 Heisenberg model, which has always a null Néel order parameter, but a non-vanishing string order parameter. This model presents a trimerised phase too, distinguishable from the former two by the absence of a gap between the ground and the first excited state, while the other two previously mentioned antiferromagnetic phases are gapped.

The symmetry properties of these models will be a massive topic of discussion throughout this whole work. In fact, the analysis of the bilinear-biquadratic Hamiltonian starts with the consideration that this is globally an  $SU(2)$ -invariant model. This was the basis on which we held the Bethe ansatz approach to the spin-1 biquadratic chain, eventually mapped into a spin-1/2 XXZ model. However, some special points in the parameter space are endowed with additional symmetries, not immediately clear in the conventional spin-1 formalism. This is the reason why a mapping into the bilinear  $SU(3)$  Heisenberg chain was proposed. By means of a whole new perspective on the spin-1 model, we may be able to extract information about the classification of states in  $SU(3)$  multiplets and the degeneracies of the energy spectrum. The biquadratic point in the phase diagram is quite special because its spectrum can be studied with other devices, such as the correspondence with the quantum nine-states Potts model, also equivalent to the three-state vertex one.

In the first chapter, we will provide the reader with a brief overview of the characteristic features of the wide variety of spin-1 models exhibiting bilinear and biquadratic nearest-neighbour interactions. These models can be described by means of a general form of the Hamiltonian, depending on a single angular parameter, which determines the dominance of either the bilinear or the biquadratic term. Plotting the phase diagram for the global model as a function of the angle  $\Theta$ , we can locate different regions, both ferromagnetic and antiferromagnetic, corresponding to different behaviours of the system under investigation. A brief summary is presented, listing the remarkable points on the phase diagram mainly studied in literature,

because of their relevance or because of the additional symmetries which make them integrable via different methods.

The second chapter focuses, as most of the following discussion, on the antiferromagnetic spin-1 chain with pure biquadratic exchange and its  $SU(2)$  symmetry in particular. This kind of approach, based on  $SU(2)$  quantum numbers, allows us to deal with this model by means of the Bethe ansatz technique, following the idea presented in [32]. As a result of the application of this method, we come across to a possible partial mapping between states of the spin-1 pure-biquadratic model and those of the well-known spin-1/2 XXZ Hamiltonian.

The third chapter develops the analysis of the equivalence of the spin-1 biquadratic model and deals with the  $SU(3)$ -symmetric Heisenberg chain with alternate representations on even and odd sites. This mapping, enlightens the underlying  $SU(3)$  symmetry of the spin-1 Hamiltonian and allows a classification of states in multiplets exploiting a whole new good quantum number for the biquadratic Hamiltonian, other than the usual  $z$ -component of the total spin. It turns out to be strictly related to the parity of the location of  $S^z = 0$  spins on the length of the chain.

The fourth chapter follows the list of the correspondences of the pure-biquadratic Hamiltonian with other known models. The equivalence with the quantum Hamiltonian arising from a nine-state Potts model will be proved by means of other relevant properties of the spin-1 operators, which are encompassed by the Temperley-Lieb algebra. As a conclusion there is an hint at the procedure developed in [27] to prove the correspondence with a three-state vertex model.

The fifth chapter presents a complete outline of the simplest cases of biquadratic spin-1 chains with an even number of sites. In particular, for the two-site, four-site and six-site chains, the spectrum has been evaluated numerically and the correspondence with the  $SU(3)$  multiplets has been established. Finally, it is shown a complete mapping between the states formerly classified according to  $SU(2)$  and then according to  $SU(3)$  quantum numbers.

The last chapter is dedicated to the numerical analysis of the eight-site spin-1 chain. Exploiting the mapping with  $SU(3)$  operators, the spectrum was evaluated numerically. Furthermore, the analysis of the spectrum was extended from the pure-biquadratic point, studying the behaviour of the energies of the ground and the lowest excited states in a neighbourhood of the biquadratic antiferromagnetic point.



# Chapter 1

## A brief overview of spin-1 models

The most interesting spin-1 quantum models with nearest-neighbour interactions can be classified in two groups according to their symmetry properties [26]. The first one is essentially a generalisation of the spin-1/2 XXZ model to the case of spin-1 variables:

$$\mathcal{H}(\lambda, D) = \sum_{i=1}^N [S_i^x S_{i+1}^x + S_i^y S_{i+1}^y + \lambda S_i^z S_{i+1}^z + D(S_i^z)^2] \quad (1.1)$$

in which an additional term appears, that is the quadratic self-interaction, which was trivial in the spin-1/2 case. The second class of spin-1 models is represented by the bilinear-biquadratic model, which has the following Hamiltonian form:

$$\mathcal{H}(J_1, J_2) = \sum_{i=1}^N [J_1 \vec{S}_i \cdot \vec{S}_{i+1} - J_2 (\vec{S}_i \cdot \vec{S}_{i+1})^2] \quad (1.2)$$

Throughout this work we will deal just with the latter type of model and, in particular, with the special case of purely biquadratic interaction.

### 1.1 The bilinear-biquadratic spin-1 Hamiltonian

The most general  $SU(2)$ -invariant quantum spin-1 Hamiltonian with nearest-neighbour interactions is represented by the bilinear-biquadratic model:

$$\mathcal{H}(J_1, J_2) = \sum_{i=1}^N [J_1 \vec{S}_i \cdot \vec{S}_{i+1} - J_2 (\vec{S}_i \cdot \vec{S}_{i+1})^2] \quad (1.3)$$

in which a spin-1 variable  $\vec{S}_i = \{S_i^x, S_i^y, S_i^z\}$  is located on each site of a one-dimensional chain. Sites are numbered from 1 to  $N$ . Interactions occur only

between nearest neighbour sites, therefore the Hamiltonian can be written as a sum of terms, each of them involving only the spins located at positions  $i$  and  $i + 1$  on the chain.  $J_1$  and  $J_2$  are the coupling constants for the bilinear and biquadratic term of the Hamiltonian respectively; they may vary defining different types of models starting from the same form (1.3).

Spin variables lying on different sites are independent, which means that their components commute among themselves.

$$[S_i^{(\alpha)}, S_j^{(\beta)}] = 0 \quad \text{for } i \neq j \quad \text{and} \quad \alpha, \beta = x, y, z \quad (1.4)$$

The operators of spin for  $S = 1$  have a 3-dimensional representation, and their components on the same site obey the well-known algebra:

$$[S_i^{(\alpha)}, S_i^{(\beta)}] = i\epsilon_{\alpha\beta\gamma} S_i^{(\gamma)}. \quad (1.5)$$

It is immediately understood by means of the spin-1 operator algebra (1.5), that the whole bilinear-biquadratic model is invariant under the action of the  $SU(2)$  group. Since the Hamiltonian is just a combination of scalar products of spin operators, it is clearly invariant under rotations in a 3-dimensional space, represented by the  $SO(3)$  group, that has the same Lie algebra of  $SU(2)$ . (See appendix A for a detailed description of  $SU(2)$  group properties).

Boundary conditions at the extremes of the chain are needed when dealing with finite systems. The most commonly employed boundary conditions for this model are:

- periodic boundary conditions:  $\vec{S}_{N+1} = \vec{S}_1$
- Dirichelet boundary conditions (free ends):  $\vec{S}_0 = 0$  and  $\vec{S}_{N+1} = 0$

The Hamiltonian (1.3) can be rewritten by means of a very useful parametrization, reminding that only the ratio between coupling constants  $J_1$  and  $J_2$  matters. Thus, we have an overall constant, that is  $J$  (we will assume  $J > 0$  throughout the whole description of this model), meanwhile the dominance of either the linear or the biquadratic term, as well as the ferromagnetic or antiferromagnetic properties of the model are determined by choosing the amplitude of the angle  $\Theta \in [0, 2\pi]$ .

$$\mathcal{H}(J, \Theta) = J \sum_{i=1}^N \left[ \cos \Theta \vec{S}_i \cdot \vec{S}_{i+1} - \sin \Theta (\vec{S}_i \cdot \vec{S}_{i+1})^2 \right] \quad (1.6)$$

A graphical representation of the phase diagram [35] as a function of  $\Theta$  will be more immediate.

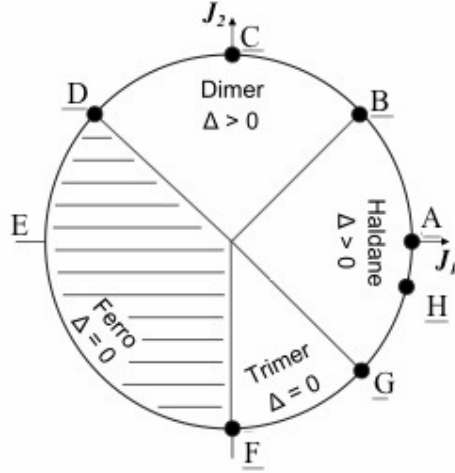


**Figure 1.1:** Round phase diagram of the bilinear-biquadratic spin-1 model as a function of the parameter  $\Theta$ , with  $\tan \Theta$  representing the ratio between the coupling constants  $J_2$  and  $J_1$  respectively related to the biquadratic and bilinear terms of the Hamiltonian (1.3). It shows four phases: one ferromagnetic and three antiferromagnetic, named trimer, Haldane and dimer phase. The latter two antiferromagnetic phases display a gap ( $\Delta > 0$ ) between the ground and the first excited state, whereas the ferromagnetic and trimer phases are gapless ( $\Delta = 0$ ). Points on the diagram labelled by capital letters, single out special models of which we give a quick overview in this chapter. (Picture taken from [7]).

Now we may attempt to describe it. First of all, there are two main regions in which we may split it, remembering that  $\Theta$  measures the dominance of the two competing terms of the bilinear-biquadratic Hamiltonian. The region included between  $\frac{3}{4}\pi$  and  $\frac{3}{2}\pi$  shows a ferromagnetic behavior, while the remaining region with  $-\frac{\pi}{2} < \Theta < \frac{3}{4}\pi$  is the antiferromagnetic phase, which has been divided into three further regions:

- $-\frac{\pi}{2} < \Theta < -\frac{\pi}{4} \rightarrow$  **trimerised phase**
- $-\frac{\pi}{4} < \Theta < \frac{\pi}{4} \rightarrow$  **Haldane phase**
- $\frac{\pi}{4} < \Theta < \frac{3}{4}\pi \rightarrow$  **dimerised phase**

In the entire **ferromagnetic** phase the fully aligned state

$$|GS\rangle = |+++++\dots\rangle,$$

is always an eigenstate of the Hamiltonian (1.6), with energy given by

$$E_0 = JN(\cos \Theta - \sin \Theta). \quad (1.7)$$

Using the highest-weight-state basis, we are allowed to evaluate the action of the whole Hamiltonian (1.6) on an excitation of  $S_{tot} = N - 1$ , for which

we simply switch one of the quintet bonds of the ferromagnetic state into a triplet bond. The result gives the following expression for the corresponding eigenvalue of the Hamiltonian [7]:

$$E(k) = E_0 - 2J(\cos \Theta)(1 - \cos k) \quad (1.8)$$

where  $k$  is the momentum of the Bethe ansatz wave function of the spin wave excitation, that is an eigenstate of the Hamiltonian defined, using the valence bond notation, by the following expression:

$$|k\rangle = \sum_{i_1 \neq i_2} e^{ik i_1} [i_1, i_2](i_3, i_4, \dots, i_N) \quad (1.9)$$

where the square brackets indicates a triplet bond connection between the spins located on sites  $i_1$  and  $i_2$ , meanwhile the parentheses indicates spins all connected by quintet valence bonds.

As we can see, the energy of this excitation is always positive in the range  $\frac{3}{4}\pi < \Theta < \frac{3}{2}\pi$ , which means that moving away from the fully aligned state demands energy, therefore  $|GS\rangle$  is the system ground state in this phase.

Thus, from the dispersion relation (1.8) we realise that the model remains gapless in this region of the phase diagram, which means that it should be always possible to create arbitrarily small excitations starting from the system ground state  $|GS\rangle$ .

A finite gap opens [19, 20] when, crossing the continuous phase transition at  $\Theta = \frac{3}{4}\pi$ , the model enters the antiferromagnetic **dimerised** region, i.e.  $\Theta \in [\frac{\pi}{4}, \frac{3}{4}\pi]$ . The main difference distinguishing this phase from the other gapped phase is the fact that the translational symmetry is broken because the system shows a spontaneous tendency to split into pairs of mutually interacting spins. As a consequence the ground state becomes two-fold degenerate. In this range we find the purely biquadratic antiferromagnetic Hamiltonian ( $\Theta = \frac{\pi}{2}$ ).

An integrable, massless model [41, 8] separates the dimerised phase from the **Haldane** phase, again with a continuous phase transition. The second gapped phase is a disordered one: the translational symmetry is unbroken, the ground state is unique and there are exponentially decaying correlation functions. This range varies from  $\Theta = -\frac{\pi}{4}$  to  $\Theta = \frac{\pi}{4}$  and it contains the antiferromagnetic Heisenberg model ( $\Theta = 0$ ) and the AKLT model ( $\Theta = -\arctan \frac{1}{3}$ ).

The valence-bond basis provides a simple device to describe the two different types of states belonging to the two different gapped phases, as shown in figure 1.2.

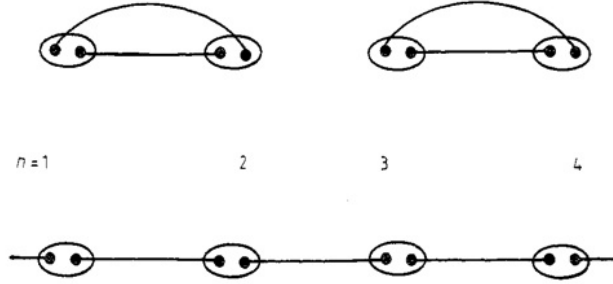


**Figure 1.2:** Two different states of a spin-1 chain with four sites in the valence-bond pictorial representation. Each site is occupied by two spin-1/2 variables, encircled together by the projector on their triplet state ( $S = 1$ ). This is a graphical representation of the constraint that each locus is occupied by one spin-1 variable. Therefore, spin-1/2 variables can form singlet states represented by valence bonds only with variables located on different sites. The constraint of one particle per site implies one further rule to be obeyed while connecting spins, that is the non crossing relation, i.e. the valence bonds cannot cross one another an odd number of times. (Picture taken from [17]).

The first one represents a state with broken symmetry: each pair of neighbouring spins is connected by two valence bonds. This state is not translationally invariant, because we have two allowed configurations related by a shift of one lattice site. The second image represents a state with unbroken symmetry: all spins are connected with one bond to the preceding and with another to the following spin. The resulting state is clearly translationally invariant.

Although the last one is the exact VBS ground state for the AKLT model [3, 4], neither of these states is the exact ground state for the bilinear-biquadratic model with arbitrary  $\Theta$ . However, they may be employed as variational ground states for those generic models, the first state having lower energy for  $\Theta > \arctan \frac{1}{2}$  and the second one for  $\Theta < \arctan \frac{1}{2}$  [17]. The exact ground state will, however, fit the same symmetry requirements of these two cases.

Eventually, there is one more antiferromagnetic phase, that is the **trimerised** phase in the range  $-\frac{\pi}{2} < \Theta < -\frac{\pi}{4}$ . Separated from the Haldane phase by a continuous phase transition corresponding to an integrable critical  $SU(3)$ -symmetric model [29, 39], this last phase is expected to be gapless and spontaneously trimerised, as it is suggested by the symmetry of the values of the soft modes at  $k = 0, \pm \frac{2}{3}\pi$  [36].

Now, let's try to make a list of all the remarkable points of the phase diagram and the characteristic features of each phase, starting from  $\Theta = 0$ .

- $\Theta = 0$  (point A)

This is the spin-1 antiferromagnetic quantum Heisenberg model.

$$\mathcal{H}(J, \Theta = 0) = J \sum_{i=1}^N \vec{S}_i \cdot \vec{S}_{i+1} \quad (1.10)$$

It is a non-integrable model, but it has been deeply investigated in literature [23, 24]. It was proved that it is a massive model, that is, it shows a finite excitation gap ( $\Delta E/J \approx 0.41$ ) [30] between the fundamental and the first excited state, exponentially decaying correlation functions and a disordered non-degenerate ground state.

- $\Theta = \frac{\pi}{4}$  (point B)

$$\mathcal{H}(J', \Theta = \frac{\pi}{4}) = J' \sum_{i=1}^N \left[ \vec{S}_i \cdot \vec{S}_{i+1} - (\vec{S}_i \cdot \vec{S}_{i+1})^2 \right] \quad (1.11)$$

where we have rescaled the coupling constant  $J' = \frac{\sqrt{2}}{2}J$ .

This Hamiltonian is integrable by means of a Bethe ansatz technique, developed by Takhtajan and Babudjian [41, 8]. It represents the continuous phase transition point between the two gapped antiferromagnetic phases, the Haldane and the dimerised phase. Here, the model becomes conformally invariant with a  $SU(2)_2$  symmetry and its related critical theory is a Wess-Zumino-Witten model with  $k = 2$  [1]. The obvious consequence is that the spectrum of the model represented at this point is gapless and has a unique ground state.

- $\Theta = \frac{\pi}{2}$  (point C)

This is an antiferromagnetic spin-1 model with pure biquadratic exchange.

$$\mathcal{H}(J, \Theta = \frac{\pi}{2}) = -J \sum_{i=1}^N (\vec{S}_i \cdot \vec{S}_{i+1})^2 \quad (1.12)$$

It can be partially mapped into a quantum spin-1/2 XXZ Hamiltonian with  $\Delta < -1$ , which is known to represent a massive system with  $\Delta E/(-J) = 0.173\dots$  [31, 32]. Thus, there is a gapped spectrum and a doubly-degenerate ground state, given the fact that we are in a dimerised phase [36].

There are also two other special mappings available at this special point: this system may be shown to be equivalent to a  $SU(3)$ -symmetric spin chain [13] and to a quantum nine-state Potts model [9].

- $\Theta = \frac{3}{4}\pi$  (point D)

The corresponding Hamiltonian has the following form:

$$\mathcal{H}(J', \Theta = \frac{3}{4}\pi) = -J' \sum_{i=1}^N \left[ \vec{S}_i \cdot \vec{S}_{i+1} + (\vec{S}_i \cdot \vec{S}_{i+1})^2 \right] \quad (1.13)$$

where we have rescaled again the coupling constant in the same way as before  $J' = \frac{\sqrt{2}}{2}J$ . At this point there is a continuous phase transition between the antiferromagnetic and the ferromagnetic phase, therefore there is a crossing of ferromagnetic and antiferromagnetic energies. There are degenerate ground states of each type [7]. The system is obviously gapless and correlation functions are the same for every couple of spins, because they are independent of distance.

A peculiarity of the model at this point is that we may express the Hamiltonian as a sum of projection operators on triplets of two neighbouring spins, given that:

$$\hat{P}_1(\vec{S}_i + \vec{S}_{i+1}) = 1 - \frac{1}{2}(\vec{S}_i \cdot \vec{S}_{i+1}) - \frac{1}{2}(\vec{S}_i \cdot \vec{S}_{i+1})^2. \quad (1.14)$$

Again, this model turns out to be SU(3) invariant [21].

- $\Theta = \pi$  (point E)

This point represents the ferromagnetic spin-1 Heisenberg model.

$$\mathcal{H}(J, \Theta = \pi) = -J \sum_{i=1}^N \vec{S}_i \cdot \vec{S}_{i+1} \quad (1.15)$$

The ground state is the fully aligned state with maximum  $z$ -spin component ( $S_{tot}^z = N$ ) and the related energy is  $E_0 = -JN$ . The spectrum is clearly gapless, as it happens for the whole ferromagnetic phase, meaning that it is possible to create excitations arbitrarily close to the ground state. A simple example is set by a spin wave excitation of momentum  $k$ , with total spin  $S_{tot} = N - 1$ , that obeys the following dispersion relation [36] :

$$E = E_0 + 2J(1 - \cos k) \quad (1.16)$$

- $\Theta = \frac{3}{2}\pi$  (point F)

Here there is the other continuous transition point between the ferromagnetic and the antiferromagnetic phase. The related Hamiltonian corresponds to a purely biquadratic ferromagnetic model:

$$\mathcal{H}(J, \Theta = \frac{3}{2}\pi) = J \sum_{i=1}^N (\vec{S}_i \cdot \vec{S}_{i+1})^2 \quad (1.17)$$

Just like the corresponding antiferromagnetic model it is endowed with a  $SU(3)$  symmetry and it has massive spectrum with the same dispersion relation (provided  $-J \rightarrow J$ ):

$$E = E_0 + J(3 + 2 \cos k) \quad \text{where} \quad E_0 = JN \quad (1.18)$$

At point F there is again the possibility of expressing the Hamiltonian as a sum of projection operators [7] of pairs of neighbouring spins on a common singlet state, knowing that:

$$\hat{P}_0(\vec{S}_i + \vec{S}_{i+1}) = -\frac{1}{3} + \frac{1}{3}(\vec{S}_i \cdot \vec{S}_{i+1})^2 \quad (1.19)$$

- $\Theta = -\frac{\pi}{4}$  (point G)

This point corresponds to a continuous phase transition which separates a gapless antiferromagnetic phase (trimer) from a gapped one (Haldane). Again, we find an exactly integrable model

$$\mathcal{H}(J', \Theta = -\frac{\pi}{4}) = J' \sum_{i=1}^N \left[ \vec{S}_i \cdot \vec{S}_{i+1} + (\vec{S}_i \cdot \vec{S}_{i+1})^2 \right], \quad (1.20)$$

which is usually referred to as Lai-Sutherland Hamiltonian. It is solvable with the Bethe ansatz [29, 39]. The resulting spectrum is gapless and the ground state is unique. As its diametrically opposite point (D), this Hamiltonian can be written as a sum of permutation operators and it has a mapping onto a  $SU(3)$ -symmetric spin chain. As a consequence of being a massless model, its critical behaviour should be related to a  $SU(3)$ -symmetric conformal theory with  $k = 1$ .

- $\Theta = -\arctan(1/3)$  (point H)

$$\mathcal{H}(J'', \Theta = -\arctan(1/3)) = J'' \sum_{i=1}^N \left[ \vec{S}_i \cdot \vec{S}_{i+1} + \frac{1}{3}(\vec{S}_i \cdot \vec{S}_{i+1})^2 \right] \quad (1.21)$$

where a rescaling of the coupling constant has been performed according to  $J'' = \frac{3}{\sqrt{10}}$ .

This particular model, named AKLT model (after Affleck, Kennedy, Lieb and Tasaki), has known solutions thanks to the valence-bond-solid basis, which can be used to express the exact form of the ground state, that is unique in the thermodynamic limit. It represents a massive model, thus its spectrum has a finite gap and the spin correlations are purely exponential [3, 4].

One last interesting property of this Hamiltonian is that it may be expressed as a sum of projection operators onto a quintet state of spins lying on neighbouring sites. In fact,

$$\hat{P}_2(\vec{S}_i + \vec{S}_{i+1}) = \frac{1}{3} + \frac{1}{2}(\vec{S}_i \cdot \vec{S}_{i+1}) + \frac{1}{6}(\vec{S}_i \cdot \vec{S}_{i+1})^2 \quad (1.22)$$



## Chapter 2

# $SU(2)$ symmetry and correspondence with the XXZ model

It was proved that there are some special values of  $\Theta$ , such as  $\Theta = \pm\frac{\pi}{4}, \pm\frac{\pi}{2}$ , for which the model (1.6) is solvable by means of the Bethe ansatz [31, 41, 8, 29, 39].

This technique, which was created in order to find explicitly eigenvalues and eigenstates of the spin-1/2 Heisenberg chain, is mainly founded on the definition of a primary state, that is usually one of the two fully aligned states, for example we choose the one with the maximum value of the  $S_{tot}^z$ , on which we act a certain number of times with the ladder operators  $S_i^-$  to get other states with lower values of  $S_{tot}^z$ . The classification of states arising in this framework is based on  $SU(2)$  quantum numbers, i.e.  $\vec{S}_{tot}^2$  and  $S_{tot}^z$ .

Since the Hamiltonian (1.6) commutes with the  $z$ -component of the total spin, we may choose a basis of eigenstates of  $S_{tot}^z$  on which we decompose the Hamiltonian eigenstates. This kind of approach is allowed just for an  $SU(2)$ -invariant system because the commutation properties of the Hamiltonian with the group generators leads to a decomposition of the total Hilbert space of eigenstates into sectors with fixed values of  $S_{tot}^z$ . Thus, the Hamiltonian appears in a block diagonal form and eigenstates of the same  $S_{tot}^z$  transform among themselves under the action of the this matrix operator.

Following this decomposition method, well-known for the spin-1/2 chain, we may be able to apply the Bethe ansatz technique in order to solve the bilinear-biquadratic model in some special cases; among them lies the **pure biquadratic model**.

Let's focus our attention, for the moment, on the resulting Hamiltonian (1.6) for  $\Theta = \frac{\pi}{2}$ :

$$\mathcal{H}(J, \Theta = \frac{\pi}{2}) = -J \sum_{i=1}^N (\vec{S}_i \cdot \vec{S}_{i+1})^2 \quad (2.1)$$

which represents a biquadratic antiferromagnetic model, that is a spin-1 chain with a pure biquadratic exchange interaction.

Employing the technique outlined before, paying attention to some necessary changes due to the different spin representation, we can find a pattern to describe all eigenstates of this Hamiltonian. The spin variables fixed on each site of the one dimensional lattice can now take three different values of  $S_i^z$ , and we can represent them through a symbolic notation:  $|+\rangle, |0\rangle, |-\rangle$ .

Starting with the fully aligned state:

$$|GS\rangle = |+++++\dots\rangle,$$

we can build up all other  $S_{tot}^z$  eigenstates by operating an arbitrary number of times on this state with a combination of the ladder operators  $S_i^-$ . We get, then, the classification of states according to their values of  $S_{tot}^z$ , which correspond to a precise number of deviations from the fundamental state.

Asking that a linear combination of states belonging to the same eigenvalue of  $S_{tot}^z$  forms an eigenstate of the global Hamiltonian, one eventually gets some constraints on the wavevector  $k$ , connected to the wave function defined in the Bethe ansatz solution. The general behavior of the pure-biquadratic model eigenstates, which will be fully developed in the following sections, can be summarised as follows:

- **states with a single deviation:**

these states have the same energy as the fully aligned state. The action of the pure biquadratic term on these state is null, which means that these states do not propagate.

- **states with an arbitrary number of isolated deviations:**

states with isolated deviations are states for which the applications of the ladder operators  $S_i^-$  occur neither on the same nor on adjacent sites. There are up to  $N/2$  possible isolated deviations on a  $N$ -spin chain. All of these states are obviously degenerate with the fully aligned state.

- **states with two non-isolated deviations:**

these states contain a couple of the type  $|+-\rangle, |00\rangle$  or  $|-\rangle$ . According to the expression of the biquadratic Hamiltonian, these are the only couples of nearest-neighbour states propagating, therefore they form a two-string, with energy expressed by:

$$\Delta E_2 = -J(3 + 2 \cos k) \quad (2.2)$$

where

$$k = \frac{2\pi l}{N} \quad l = 0, 1, 2, \dots, N-1 \quad (2.3)$$

• **states with three non-isolated deviations:**

these states are inevitably made up of one propagating two-string and an isolated deviation. They have, thus, the same energy expression the two-deviation states have, but with some modifications given by the fact that when a two-string propagates through the isolated deviation, it shifts its position on the lattice by two lattice sites.

$$\Delta E_3 = -J(3 + 2 \cos \theta) \quad (2.4)$$

where

$$\theta = \frac{2\pi r \pm 2k}{N-2} \quad l = 0, 1, 2, \dots, N-3 \quad (2.5)$$

• **states with four non-isolated deviations:**

these may be interpreted as states with a pair of two-string, which interact among themselves while propagating on the chain. It occurs that in special cases the two two-string can unite forming a bound state and the energy expression of the whole state is given by:

$$\Delta E_4 = -J[(3 + 2 \cos k_1) + (3 + 2 \cos k_2)] \quad (2.6)$$

where

$$Nk_1 = 2\pi l_1 + \varphi \quad l_1 = 0, 1, \dots, N-1 \quad (2.7)$$

$$Nk_2 = 2\pi l_2 - \varphi \quad l_2 = 0, 1, \dots, N-1 \quad (2.8)$$

$$\cot \varphi/2 = \frac{-3 \sin \frac{1}{2}(k_1 - k_2)}{2 \cos \frac{1}{2}(k_1 + k_2) + 3 \cos \frac{1}{2}(k_1 - k_2)} \quad (2.9)$$

• **states with a higher number of non-isolated deviation:**

they are basically made up of the former building blocks. Isolated deviations, which do not propagate, on the one hand and propagating two-strings on the other, which may be forming new structures, such as two-string bound states.

## 2.1 Correspondence between XXZ model and pure-biquadratic model

The rather characteristic features of the formerly described structure of eigenstates of the biquadratic Hamiltonian can be immediately related to

the typical one of the XXZ model. The former is a one-dimensional lattice model described by the Hamiltonian:

$$\mathcal{H}(J^{xxz}, \Delta) = -J^{xxz} \sum_{i=1}^N [S_i^x S_{i+1}^x + S_i^y S_{i+1}^y + \Delta S_i^z S_{i+1}^z] \quad (2.10)$$

The undeniable similarities between the two families of eigenstates become clear once the identifications

$$\Delta = -\frac{3}{2} \quad J^{xxz} = 2J. \quad (2.11)$$

are made. Assuming these special values of the parameters, the solutions of the spin 1/2 XXZ model, which is known to be integrable via Bethe ansatz techniques [40], resemble exactly the eigenstates of the biquadratic spin-1 model under examination. It is well known [40] that the XXZ model for  $\Delta < -1$  is massive, i.e. it has a gap, so this mapping is in agreement with the prediction that the biquadratic spin-1 model lies into the parameter region  $\frac{\pi}{4} < \Theta < \frac{3}{4}\pi$ , where the bilinear-biquadratic model is supposed to have a finite gap.

An other interesting consequence of this mapping is the interpretation as **spin waves** of the deviations, which form essentially a localised structure, named two-string, propagating itself jointly along the spin chain. This has a strong analogy with what happens in spin-1/2 magnetic systems, where a single spin flip creates a magnonic excitation. There, magnons interact among themselves forming bound states; the same happens here for states with four or more deviations, in which a couple of two-strings may appear, with the corresponding momenta obeying exactly the same dispersion relation of the XXZ model (2.6).

This correspondence between the eigenstates of these two models was pointed out at first by Parkinson [31], who used the Bethe ansatz to compute the energies of the previously listed states, classified by the number of deviations, that is directly related to the value of the  $z$ -component of the total spin. This discovered correspondence between XXZ eigenstates with  $M$  deviations and biquadratic Hamiltonian eigenstates with  $M$  two-strings supposedly allows us to find the eigenstates and eigenvalues of the biquadratic model by means of the Bethe ansatz.

Even though the pure-biquadratic has not yet been proved to be an integrable model, the mapping proposed by Parkinson leads to a vast knowledge of the model (2.1), but with some significant reservations.

Following the work outlined by Parkinson [32] we will stay within the framework of periodic boundary conditions comparing the results with the XXZ-model Bethe ansatz equations, which are strictly related to the different type of boundary conditions imposed on the model (cfr. eq. (2.22)).

Thus, in order to allow the comparison we will restrict ourselves to chains with an even number of sites and periodic boundary conditions.

Secondly, the mapping on XXZ model is working as long as the states with an **even number of deviations** are concerned. States with an odd number of deviations have no representation in the XXZ model; therefore the suggested mapping is only partial. This can be easily understood by the dimensional analysis of the problem. The XXZ Hamiltonian is a spin-1/2 model, therefore each spin variable can take on just two values, whereas the pure-biquadratic Hamiltonian is a spin-1 model, which means that each variable can take on three different values. With  $N$  defining the length of the chain, the XXZ Hamiltonian operator is  $2^N \times 2^N$  dimensional: the number of its eigenstates, amounting to  $2^N$ , is definitely lesser than the one given by the biquadratic spin-1 Hamiltonian, which belongs to a  $3^N \times 3^N$  dimensional Hilbert space. Being the latter eigenstates in a larger number, we realise that not every biquadratic eigenstate can be mapped into the XXZ chain, but only those ones with peculiar features that will be defined later on. We stress the fact that we can map each XXZ eigenstate into a biquadratic model eigenstate, but the converse is not true, because of the dimensional discrepancy.

There is one further complication: thanks to numerical simulations on finite length chains [32] it was possible to check out computationally that the energy levels do, in fact, match for each even number of deviations, apart from  $M = N/2$ . The mapping into the XXZ model is not working for states with  $S_{tot}^z = 0$ , which is a big disappointment, since this is certainly the largest sector of eigenstates of the Hamiltonian and the most important one because it contains the ground state for the antiferromagnetic model.

The reason why this mapping is not complete is not clear yet, but it should be crucial to understand it. We could make some assumptions based on the fact that the number of couples  $|+-\rangle$  would then fill entirely the available sites, preventing thus to the two-strings to propagate freely along the chain. This argument is not really convincing, because if this unresolved matter has to be ascribed to the progressively reducing "available room for propagation" on the chain, there would have been some kind of deviation from the XXZ correspondence pattern as the number of two-strings approached  $N/2$ . This question remains still unsolved.

## 2.2 The XXZ model: Bethe ansatz

The XXZ model is a spin-1/2 quantum model defined on a one dimensional lattice of length  $N$ . It is essentially a chain of  $N$  sites with a spin variable on each locus. Differently from the simpler Heisenberg model, that is completely isotropic -the coupling constants along all three cartesian axes are equal-, the XXZ model introduces an isotropy along the  $z$ -axis, which may

be quantified by the parameter  $\Delta$ . The XXZ Hamiltonian is:

$$\mathcal{H}(J^{xxz}, \Delta) = -J^{xxz} \sum_{i=1}^N [S_i^x S_{i+1}^x + S_i^y S_{i+1}^y + \Delta S_i^z S_{i+1}^z] \quad (2.12)$$

The anisotropic coupling along the  $z$ -axis, achieved by means of a parameter  $\Delta \neq 1$ , breaks the  $SU(2)$  invariance of this spin model. Therefore, the XXZ Hamiltonian does not commute with the  $x$  and  $y$  components of the total spin  $S_{tot}^x$  and  $S_{tot}^y$  anymore, but it still commutes with  $S_{tot}^z$ , which means that the eigenvalues of  $S_{tot}^z$  are still good quantum numbers for this model. Thanks to this crucial property of the XXZ Hamiltonian we are allowed to decompose the Hilbert space of its eigenstates into sectors with fixed  $S_{tot}^z$

$$\mathfrak{H} = \bigoplus_{n=0}^{\infty} \mathfrak{H}^{(n)} \quad (2.13)$$

and proceed with the usual Bethe ansatz technique, that is founded on the assumption that a general eigenstate of the Hamiltonian may be found by setting an ansatz on the wave function form. The amount of work will be reduced if we could be able to find operators that commute with the Hamiltonian, allowing us to restrict the Hilbert space of states, in order to work within sufficiently narrow subspaces, which will be later extended employing the symmetries of the system, only once the solutions are found.

This is the reason why we proceed assuming that a given value of deviations, represented by  $M$ , from the fully aligned state

$$|0\rangle = |\uparrow\uparrow\uparrow\uparrow\uparrow\uparrow \dots\rangle,$$

is uniquely characterising the subspace in which we work. We immediately realise that  $S_{tot}^z = n = N/2 - M$ . Thus fixing  $M$  is a simple way of choosing a sector of the block diagonal XXZ Hamiltonian, for which  $S_{tot}^z$  is fixed. Whereas the fully aligned states ( $M = 0, M = N$ ) are the two ground states of a ferromagnetic system, the fundamental state of the antiferromagnetic model would be located in the  $S_{tot}^z = 0$ , that means of course  $M = N/2$ .

A generic eigenstate belonging to a fixed- $M$  sector can be written as a linear combination of all the states with different locations of the  $M$  down spins on the chain sites, labelled by the integers  $n_i, i = 1, 2, \dots, M$ .

$$|\Psi\rangle = \sum_{\{n\}} f(n_1, n_2, \dots, n_M) S_{n_1}^- S_{n_2}^- \dots S_{n_M}^- |0\rangle \quad (2.14)$$

The sum runs over all the  $M!$  permutations of the  $M$  position indices, that are supposed to be ordered  $0 \leq i_1 < i_2 < \dots < i_M \leq N$ . The coefficients

of this combination are functions of indices and their global form can be determined by imposing that  $|\Psi\rangle$  is an eigenstate of the Hamiltonian.

$$\mathcal{H}(J^{xxz}, \Delta)|\Psi\rangle = E|\Psi\rangle \quad (2.15)$$

It is convenient to use the XXZ-model Hamiltonian formulation written in terms of ladder operators:

$$\mathcal{H}(J^{xxz}, \Delta) = -\frac{1}{2}J^{xxz} \sum_{i=1}^N \left[ S_i^+ S_{i+1}^- + S_i^- S_{i+1}^+ + 2\Delta S_i^z S_{i+1}^z \right] \quad (2.16)$$

The action of the former Hamiltonian operator on a state given by (2.14), gives the following eigenvalue equation:

$$\begin{aligned} & -\frac{1}{2}J \sum_i (1 - \delta_{n_i, n_{i+1}}) [f(n_1, \dots, n_i + 1, n_{i+1}, \dots, n_M) + \\ & + f(n_1, \dots, n_i, n_{i+1} - 1, \dots, n_M)] + \\ & + J\Delta \left[ -\frac{1}{4}N + M - \sum_i \delta_{n_{i+1}, n_{i+1}} \right] f(n_1, \dots, n_i, n_{i+1}, \dots, n_M) = \\ & = Ef(n_1, \dots, n_i, n_{i+1}, \dots, n_M) \end{aligned} \quad (2.17)$$

Let us formulate now the basic ansatz regarding the wave function form:

$$f(n_1, \dots, n_M) = \sum_P A(P) e^{i \sum_{i=1}^M k_{P(i)} n_i} \quad (2.18)$$

where the sum runs over the  $M!$  permutations  $P$  of the  $M$  site indices.  $k$  are named quasi-momenta, because the former expression formally resembles a superposition of plane waves with momenta  $k_{P(i)}$  with  $i = 1, \dots, M$ .

Starting from the eigenstate equation (2.17) for the case  $n_i + 1 \neq n_{i+1} \forall i = 1, \dots, M$ , we can ignore the presence of the  $\delta_{n_{i+1}, n_{i+1}}$  terms, and using the ansatz on the wave function, we find the expression of the **energy of a general eigenstate** as a function of the quasi momenta:

$$E = E_0 + \sum_{i=1}^M [J^{xxz} (\Delta - \cos k_j)] \quad (2.19)$$

in which we have defined the energy of the fully aligned state  $|0\rangle = |\uparrow\uparrow\uparrow\uparrow\uparrow\uparrow \dots\rangle$  as  $E_0 = -\frac{1}{4}N J^{xxz}$ .

In order to find the whole expression of the wave functions we need to calculate the coefficients  $A(P)$ , which do not enter explicitly in the former determination of the energy dispersion relation. They are fixed by the analysis of the occurrence of deviations on two neighbouring sites, that is  $n_i + 1 = n_{i+1}$  for just one value of  $i$ . Taking into account the  $\delta_{n_{i+1}, n_{i+1}}$ ,

equation (2.17) can be rewritten as a series of constraints for the wave function:

$$\begin{aligned} f(n_1, \dots, n_i + 1, n_i + 1, \dots, n_M) + f(n_1, \dots, n_i, n_i, \dots, n_M) = \\ = 2\Delta f(n_1, \dots, n_i, n_{i+1}, \dots, n_M) \end{aligned} \quad (2.20)$$

for  $i = 1, \dots, M$ , which can be easily satisfied choosing the following expression for the amplitude coefficients:

$$A(P) = \epsilon(P) \prod_{l < j} \left( e^{i(k_{P(l)} + k_{P(j)})} - 2\Delta e^{ik_{P(l)}} + 1 \right) \quad (2.21)$$

with  $\epsilon(P)$  being the sign of the permutation  $P$ .

The quasi momenta are not determined directly by means of the application of the Bethe ansatz technique to the Hamiltonian of the XXZ model, but they may be found employing different conditions, which they must satisfy. This last set of equations is determined by the assumption of a certain type of boundary conditions on the system, which univocally fix the values of the quasi-momenta.

Assuming periodic boundary conditions, i.e.  $\vec{S}_{N+1} = \vec{S}_1$ , the XXZ system is known to be an exactly integrable model.

The imposition of periodic boundary conditions on the wave function results in a set of equations:

$$e^{ik_j N} = (-1)^{M-1} \prod_{l \neq j} \frac{e^{i(k_j + k_l)} + 1 - 2\Delta e^{ik_j}}{e^{i(k_j + k_l)} + 1 - 2\Delta e^{ik_l}} \quad j = 1, 2, \dots, M \quad (2.22)$$

which leads to:

$$k_j N = - \sum_{l=1}^M \Theta(k_j, k_l) + 2\pi I_j \quad (2.23)$$

where we have defined:

$$\Theta(k_j, k_l) = 2 \tan^{-1} \frac{\Delta \sin \frac{1}{2}(k_j - k_l)}{\cos \frac{1}{2}(k_j + k_l) - \Delta \cos \frac{1}{2}(k_j - k_l)} \quad (2.24)$$

with

$$I_j = \frac{M + 1 - 2j}{2}, \quad j = 1, 2, \dots, M. \quad (2.25)$$

Tuning the parameters which the XXZ model Hamiltonian depends on, we may be able to get the same energy spectrum of the biquadratic Hamiltonian (restricted to states with an even number of deviations). Therefore, we set

$$\Delta = -\frac{3}{2} \quad J^{xxz} = 2J.$$

This identification used in equations (2.19) and (2.24) with  $M = 1$  and  $M = 2$  leads directly to the expressions for  $E_2$  and  $E_4$  for states of the biquadratic Hamiltonian with two and four deviations, respectively (2.2) (2.6).





or

$$|\beta(i)\rangle = |++++00++++\dots\rangle,$$

where the first deviation is located at the site  $i$  in both cases.

Clearly, there are  $2N$  states of this kind. A general eigenstate will be a linear combination of  $|\alpha(i)\rangle$  and  $|\beta(i)\rangle$ :

$$|\Psi\rangle = \sum_i (a_i |\alpha(i)\rangle + b_i |\beta(i)\rangle) \quad (2.33)$$

with coefficients  $a_i$  and  $b_i$  determined by the constraint that this is an eigenstate of the biquadratic Hamiltonian:

$$\mathcal{H}(J, \Theta = \frac{\pi}{2}) |\Psi\rangle = E_2 |\Psi\rangle \quad (2.34)$$

which has to satisfy the periodic boundary conditions, too.

A solution of this equation is given by  $a_i = A e^{ik_i}$ , if the wavevector  $k$  satisfies the relation:

$$\Delta E = E_2 - E_0 = -J(3 + 2 \cos k). \quad (2.35)$$

These states are not degenerate with the aligned state anymore. This is a consequence of the fact that these states contain pairs, like  $| - + \rangle$ ,  $| + - \rangle$  or  $| 0 0 \rangle$ , which transform among themselves under the action of the operator  $h_i$ , producing a shift of the position of the deviation, too. The result is a propagating wave, which is very similar in its dispersion relation to spin waves of magnetic models. As we stated, this is exactly the case for the XXZ model.

### 2.3.3 Three-deviation states

Again we must distinguish between isolated deviations and non isolated deviations. The former considerations still apply for the isolated-deviation states. Let's focus now on states with three deviations occurring on neighbouring sites or (two of them at most) on the same site. We find states of these types:

$$\begin{aligned} |\alpha(i, j)\rangle &= |++++\underset{i}{0}++\underset{j}{0}0++++\dots\rangle \\ |\beta(i, j)\rangle &= |++++\underset{i}{0}++\underset{j}{-}++++\dots\rangle, \\ |\gamma(i, j)\rangle &= |++\underset{i}{0}0++\underset{j}{0}++++\dots\rangle \\ |\delta(i, j)\rangle &= |++++\underset{i}{-}++\underset{j}{0}0++++\dots\rangle \end{aligned}$$

which we can linearly combine with coefficients  $a_{ij}$ ,  $b_{ij}$ ,  $c_{ij}$  and  $d_{ij}$  respectively. Imposition of periodic boundary conditions yields relations among them:

$$a_{ij} = c_{j+1, i+N}$$

$$c_{ij} = a_{j,i+N-1}$$

$$b_{ij} = d_{j,i+N}$$

$$d_{ij} = b_{j,i+N}$$

Only two of these weight coefficients are independent, because the set of states  $|\alpha(i, j)\rangle$  and  $|\gamma(i, j)\rangle$  are essentially the same, modulo periodic boundary conditions. The same happens for  $|\beta(i, j)\rangle$  and  $|\delta(i, j)\rangle$ .

As usual we get our set of constraints on the coefficients by imposing that a linear combination  $|\Psi\rangle$  of these four types of states is an eigenstate of the biquadratic Hamiltonian. We eventually get to solve a set of equations for a single parameter  $a_{ij}$ .

A further simplification comes from the requirement of the translational invariance, that means:

$$a_{ij} = e^{iki} a_n \quad \text{where} \quad n = j - i \quad (2.36)$$

By means of this procedure we are allowed to find a solution of the Bethe ansatz type:

$$a_n = A_1 e^{i\theta n} + A_2 e^{-i\theta n} \quad (2.37)$$

provided  $\theta$  satisfies:

$$\frac{\Delta E}{-J} - 3 = e^{i\theta} + e^{-i\theta}, \quad (2.38)$$

which is the dispersion relation for a three-deviation state:

$$E_3 = E_0 - J(3 + 2 \cos \theta) \quad (2.39)$$

Furthermore, the constraint on  $|\Psi\rangle$  to be an Hamiltonian eigenstate translates into an equation which fixes the value of  $\theta$ :

$$e^{i\theta(N-2)} = e^{-2ik} \iff \theta = \frac{2\pi r \pm 2k}{N-2} \quad r = 0, 1, 2, \dots, N-3 \quad (2.40)$$

Since  $k$  is defined as  $k = \frac{2\pi l}{N}$ , with integer  $l$ , it may happen that  $r$  and  $l$  combine in giving a multiple of  $N-2$ , that means  $\theta = \frac{2\pi p}{N}$ , with integer  $p$ , which reproduces the result previously discussed for two-deviation states. Thus, apart from this kind of states, obviously degenerate with two-deviation states, eigenstates of the biquadratic Hamiltonian with three deviations correspond to a propagating couple interacting with a stationary deviation. When the two-string has to pass through the single deviation, it causes its shift by two site positions; this is pointed out by the presence of the  $N-2$  factor. These states belong to the  $S_{tot}^z = N-3$  sector, but some

of them belong to  $S_{tot} = N - 2$  and the rest of them to  $S_{tot} = N - 3$ . The total number of them amounts to  $2N(N - 2)$ .

Since  $\theta$  is defined by equation (2.38),  $\theta$  is always real, which means that there are not three-deviation bound states. This is an important result because it states that an odd number of deviations cannot combine to form a system bound state.

### 2.3.4 Four-deviation states

Once again, we have to discard at first states with isolated deviations, and then we may apply the same Bethe ansatz technique outlined in the previous cases. Computational complications arise since the more deviations we take under consideration, the wider the variety of states is. Nevertheless, it is still possible to find an analytical solution of the case  $S^z = N - 4$ . We can incorporate right from the beginning the periodic boundary conditions restricting the possible cases of four deviations to the following ones:

$$\begin{aligned} |\alpha(i, j)\rangle &= |++\underset{i}{00}++\underset{j}{00}+++ \dots\rangle \\ |\beta(i, j)\rangle &= |++\underset{i}{-}++\underset{j}{00}+++ \dots\rangle \\ |\gamma(i, j)\rangle &= |++\underset{i}{-}++\underset{j}{-}+++ \dots\rangle, \end{aligned}$$

where two two-strings are separated. When the two two-strings interact we have the following cases:

$$\begin{aligned} |\alpha(i, i + 2)\rangle &= |++\underset{i}{0000}++++ \dots\rangle \\ |\beta(i, i + 1)\rangle &= |++\underset{i}{-}00++++ \dots\rangle \\ |\beta(i, i + N - 2)\rangle &= |++00\underset{i}{-}++++ \dots\rangle \\ |\gamma(i, i + 1)\rangle &= |++\underset{i}{-}-++++ \dots\rangle \\ |\rho(i)\rangle &= |++\underset{i}{0}+-0++++ \dots\rangle \\ |\sigma(i)\rangle &= |++\underset{i}{0}-+0++++ \dots\rangle \end{aligned}$$

with the respective weight coefficients  $a_{i,j}$ ,  $b_{i,j}$ ,  $c_{i,j}$ ,  $a_{i,i+2}$ ,  $b_{i,i+1}$ ,  $b_{i,i+N-2}$ ,  $c_{i,i+1}$ ,  $r_i$  and  $s_i$ .

The procedure is exactly the same applied for the case  $N = 2$  and  $N = 3$ . Imposition of translational invariance and periodic boundary conditions are needed to find a solution of the eigenstate constraints given by the action of the Hamiltonian on a linear combination of the previously listed states, which transforms among themselves. Again, the most general Bethe ansatz solution can be expressed in the form:

$$a_{ij} = e^{iki} a_n \quad \text{where} \quad n = j - i \quad (2.41)$$

with

$$a_n = A_1 e^{ik_1 n} + A_2 e^{ik_2 n} \quad \text{where} \quad k_1 + k_2 = k. \quad (2.42)$$

Periodic boundary conditions require:  $\frac{A_1}{A_2} = e^{ik_2 N}$  and the vanishing condition on the determinant of the system of constraints coming from the eigenvalue equations, gives:

$$\varepsilon(\varepsilon - 3 - 2 \cos k_1)(\varepsilon - 3 - 2 \cos k_1)(\varepsilon - 6 - 2 \cos k_1 - 2 \cos k_2) = 0, \quad (2.43)$$

where we have defined  $\varepsilon = \frac{(E_4 - E_0)}{-J}$ . These four different values of  $\varepsilon$  correspond to four different cases:

- $\varepsilon = 0 \rightarrow$  **no two-strings**. Only isolated deviations make up a state with energy equal to  $E_0$ , thus degenerate with the fully aligned state.
- $\varepsilon = 3 + 2 \cos k_1 \rightarrow$  **one two-string** with momentum  $k_1$  interacting with two stationary isolated deviations. The energy of this kind of states resembles the one of the two-deviation or three-deviation states, when a two-string is formed. It can be noticed that the dispersion relation is basically the same as (2.35).
- $\varepsilon = 3 + 2 \cos k_2 \rightarrow$  **one two-string** with momentum  $k_2$  and two isolated deviations. Same observations stand.
- $\varepsilon = 6 + 2 \cos k_1 + \cos k_2 \rightarrow$  **two two-strings**, each one with its own momentum  $k_1$  or  $k_2$ . There are two two-strings formed with the available four deviations. They interact on the chain exactly in the same way spin waves do on a spin-1/2 chain, since the energy is precisely the sum of the single energies of the two two-string. They can even bond together and form bound states with complex momenta  $k_1$  and  $k_2$ , provided their sum, representing the total momentum, stays real.

The last case is also the most interesting one. Some other conditions on the determinant of the eigenvalue equations concerning special low value of  $n$ , making use of the definitions (2.42) in the case

$$\varepsilon = 6 + 2 \cos k_1 + 2 \cos k_2 \quad (2.44)$$

yields the condition:

$$e^{ik_2 N} = - \frac{e^{i(k_1+k_2)} + 1 + 3e^{ik_2}}{e^{i(k_1+k_2)} + 1 + 3e^{ik_1}} \quad (2.45)$$

Naming  $e^{ik_2 N} = e^{-i\varphi}$ , and keeping in mind relation (2.42) between  $k_1$  and  $k_2$ , we finally get a simple expression of the wavevectors describing a state containing two two-strings:

$$Nk_1 = 2\pi l_1 + \varphi \quad Nk_2 = 2\pi l_2 - \varphi \quad l_1, l_2 \in \mathbb{Z} \quad (2.46)$$

where  $\varphi$  is defined by

$$\cot \varphi/2 = \frac{-3 \sin \frac{1}{2}(k_1 - k_2)}{2 \cos \frac{1}{2}(k_1 + k_2) + 3 \cos \frac{1}{2}(k_1 - k_2)} \quad (2.47)$$

The energy of two interacting 2-string is given by (2.44):

$$E_4 = E_0 - J[(3 + 2 \cos k_1) + (3 + 2 \cos k_2)]. \quad (2.48)$$

In the thermodynamic limit, the real values of  $k_1$  and  $k_2$  should form a continuum of states lying inside a cosine-shaped upper and lower profile, meanwhile the bound states will form a line below or above this diagram according to the positive or negative sign of the coupling constant  $J$ .

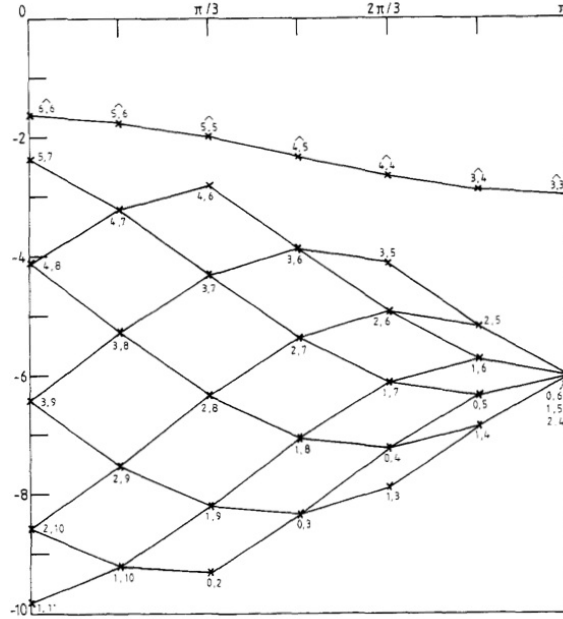


**Figure 2.1:** Energy-momentum relation for a twelve-site pure biquadratic spin-1 chain. The figure shows the scaled energy  $E/J$  as a function of momentum  $k$  calculated by means of the Bethe ansatz for states with four deviations. This picture displays only the couples of integer values  $l_1$  and  $l_2$  yielding two interacting two-strings with momenta  $k_1$  and  $k_2$  given by (2.46). Although the picture displays only one half of the allowed values for the momenta, the other part being symmetric, it is clearly visible the usual cosine-shaped structure of eigenstates, which will be filled by states in the continuous limit. The bound states of two-strings form a line lying above the graph, which is characterised by equal or scaled by one at most integer numbers  $l_1$  and  $l_2$ . (Picture taken from [32])

## 2.4 Note on the correspondence of states

As previously stated, we cannot find a complete correspondence between the biquadratic Hamiltonian eigenstates and the spin-1/2 XXZ model ones, because the first model has definitely many more states. Just a small amount of them will be mapped into the XXZ states thanks to the equivalence established in section 2.1, paying attention to the fact that the correspondence occurs between spin-1 pairs of the biquadratic modes and single deviations on the XXZ model. We have to bear in mind that the analytical expression of the Bethe ansatz wave function coefficients which links the two models uniquely applies to some special case of spin-1 couples, i.e. only the propagating couples

$$|+-\rangle, |00\rangle, |-+\rangle$$

suitably combined to form an Hamiltonian eigenstate, can be mapped into single deviations, i.e. a  $|-\rangle$ , on the spin-1/2 chain.

The equivalence lies just in the propagation modes along the chain, which resemble the spin waves of the XXZ model, because of the localisation property and the interaction among two-strings in the biquadratic model, which shows the same rules of spin-waves composition in magnetic systems. However, a large amount of states of the biquadratic Hamiltonian cannot be mapped into the XXZ model because there is not enough room in the Hilbert space of states. In particular, the non-propagating spin-1 pairs:

$$|++\rangle, |+0\rangle, |0+\rangle, |0-\rangle, |-0\rangle, |--\rangle$$

may be thought as having all the same representation on the spin-1/2 chain. In fact, they are all equivalent to the background set, made up of all  $|\uparrow\rangle$ , within which the deviations, represented by  $|\downarrow\rangle$ , run forming the spin waves.

The lack of means to represent the latter set of couples, which are necessary in particular to build up the states with an odd number of deviations, but also appear every time an isolated deviation occurs on the chain, is preventing us from completing the entire mapping between the two models.

## Chapter 3

# $SU(3)$ symmetry and the bilinear Heisenberg chain

In the introduction about the bilinear-biquadratic Hamiltonian, we have stressed the importance of the symmetry properties related to this particular quantum model. In the previous chapter it was developed an  $SU(2)$ -symmetric approach, because the entire model is invariant under that group, regardless of the value of  $\Theta$ , which selects a point on the phase diagram (See fig.1.1).

However, it can be shown that the bilinear-biquadratic Hamiltonian (1.6) at some special points is endowed with more symmetry properties, namely it is invariant under the larger  $SU(3)$  group, which contains  $SU(2)$  as a subgroup. These special points are located on the phase diagram at:

- $\Theta = \frac{\pi}{2}$  (point C) and  $\Theta = -\frac{\pi}{2}$  (point F). Antiferromagnetic ( $-J$ ) and ferromagnetic ( $+J$ ) pure-biquadratic spin-1 Hamiltonian, respectively.

$$\mathcal{H}^{biQ}(\pm J) = \pm J \sum_{i=1}^N (\vec{S}_i \cdot \vec{S}_{i+1})^2 \quad (3.1)$$

- $\Theta = \frac{3}{4}\pi$  (point D) and  $\Theta = -\frac{\pi}{4}$  (point G). Antiferromagnetic-ferromagnetic transition point ( $-J$ ) and Lai-Sutherland model ( $+J$ ) respectively.

$$\mathcal{H}^{LS}(\pm J) = \pm J \sum_{i=1}^N \left[ \vec{S}_i \cdot \vec{S}_{i+1} + (\vec{S}_i \cdot \vec{S}_{i+1})^2 \right], \quad (3.2)$$

### 3.1 $SU(3)$ Heisenberg chain

Exactly in the same way as it happens for  $SU(2)$ , we may build up a  $SU(3)$  Heisenberg model employing the same Hamiltonian structure with nearest-neighbour interactions, replacing the well-known  $SU(2)$  spin operators with

the  $SU(3)$  generators. Bearing in mind that there are eight of them, the resulting Heisenberg Hamiltonian structure is:

$$\mathcal{H}^{SU(3)}(J) = J \sum_{i=1}^N \sum_{\alpha=1}^8 \lambda_i^\alpha \lambda_{i+1}^\alpha, \quad (3.3)$$

where  $i = 1, 2, \dots, N$  labels the lattice site to which the Gell-Mann matrix  $\lambda^\alpha$  is referred, whereas  $\alpha$  running from 1 to 8 indicates that the sum is taken all over the  $SU(3)$  generators. (See the related appendix B for definitions and conventional notations applied for the  $SU(3)$  group).

Since  $SU(3)$  has two non equivalent fundamental representations [3] and  $[\bar{3}]$  (for further details, see appendix B), there are basically two possible ways of defining this  $SU(3)$  Hamiltonian:

- the first one is built up using the same representation, either fundamental or antifundamental, on all sites of the chain;
- the second one is build up using alternatively fundamental and anti-fundamental representations respectively on odd and even sites.

These two different models can be related to the two different types of  $SU(3)$ -invariant spin-1 Hamiltonians expressed by (3.1) and (3.2). A simple way of showing the equivalence between the  $SU(3)$  Heisenberg chain and the spin-1 models [13] is based on the identification of the spin operators  $S^1, S^2$  and  $S^3$  with the three Gell-Mann matrices:

$$\lambda_i^7 = \begin{pmatrix} 0 & 0 & 0 \\ 0 & 0 & -i \\ 0 & i & 0 \end{pmatrix} \quad -\lambda_i^5 = \begin{pmatrix} 0 & 0 & i \\ 0 & 0 & 0 \\ -i & 0 & 0 \end{pmatrix} \quad \lambda_i^2 = \begin{pmatrix} 0 & -i & 0 \\ i & 0 & 0 \\ 0 & 0 & 0 \end{pmatrix} \quad (3.4)$$

It is sufficient to have three of the  $SU(3)$  generators to reproduce the  $SU(2)$  subalgebra. Moreover, it is important to stress that we may have chosen other perfectly fine representations (some examples are described in appendix A) of the spin-1 operators, which fulfill the same algebra, but lead us to a different mapping into the  $SU(3)$  generators, maybe involving other Gell-Mann matrices. The chosen mapping, with

$$S_i^1 = \lambda_i^7 \quad S_i^2 = -\lambda_i^5 \quad S_i^3 = \lambda_i^2 \quad (3.5)$$

is particularly convenient to prove the equivalence relation between the two models under investigation. The mapping of all other Gell-Mann matrices is performed explicitly by calculating the squares and the mixed products of the spin components (for details see appendix C). The final expression for a  $SU(2)$ -symmetric model of the form

$$\mathcal{H}(\alpha, \beta) = \sum_{i=1}^N \left[ \alpha (\vec{S}_i \cdot \vec{S}_{i+1}) + \beta (\vec{S}_i \cdot \vec{S}_{i+1})^2 \right] \quad (3.6)$$

as a function of the  $SU(3)$  generators is:

$$\begin{aligned} \mathcal{H}(\alpha, \beta) = & \sum_{i=1}^N \alpha (\lambda_i^2 \lambda_{i+1}^2 + \lambda_i^5 \lambda_{i+1}^5 + \lambda_i^7 \lambda_{i+1}^7) + \\ & + \sum_{i=1}^N \frac{1}{2} \beta (\lambda_i^8 \lambda_{i+1}^8 + \lambda_i^3 \lambda_{i+1}^3 + \frac{8}{3} + \lambda_i^1 \lambda_{i+1}^1 - \lambda_i^2 \lambda_{i+1}^2 + \lambda_i^4 \lambda_{i+1}^4 + \\ & - \lambda_i^5 \lambda_{i+1}^5 + \lambda_i^6 \lambda_{i+1}^6 - \lambda_i^7 \lambda_{i+1}^7) \end{aligned} \quad (3.7)$$

For  $\alpha = 0$  and  $\beta = \pm J$  the Hamiltonian (3.6) reproduces the pure biquadratic (anti-)ferromagnetic model, therefore the same choice of the parameters  $\alpha$  and  $\beta$  in equation (3.7) guarantees that the resulting expression as function of the  $SU(3)$  generators is representing exactly the biquadratic Hamiltonian:

$$\begin{aligned} \mathcal{H}^{biQ}(\pm J) = \mathcal{H}(\alpha = 0, \beta = \pm J) = & \pm \frac{1}{2} J \sum_{i=1}^N [ \lambda_i^8 \lambda_{i+1}^8 + \lambda_i^3 \lambda_{i+1}^3 + \\ & + \lambda_i^1 \lambda_{i+1}^1 - \lambda_i^2 \lambda_{i+1}^2 + \lambda_i^4 \lambda_{i+1}^4 - \lambda_i^5 \lambda_{i+1}^5 + \lambda_i^6 \lambda_{i+1}^6 - \lambda_i^7 \lambda_{i+1}^7 ] \pm \frac{4}{3} JN \end{aligned} \quad (3.8)$$

Now, let's define properly the  $SU(3)$ -symmetric **Heisenberg chain** with **alternate** fundamental and antifundamental **representations**:

$$\mathcal{H}^{F \otimes A}(\pm J) = \pm J \sum_{i=1}^{N/2} \sum_{\alpha=1}^8 \left[ \lambda_{2i-1}^\alpha \bar{\lambda}_{2i}^\alpha + \bar{\lambda}_{2i}^\alpha \lambda_{2i+1}^\alpha \right] \quad (3.9)$$

where the antifundamental representations  $\bar{[3]}$  have been placed on even sites, whereas fundamental representations  $[3]$  were employed to describe odd sites.

It is clear, from equation (3.8), that the equivalence relation between the spin-1 biquadratic and the  $SU(3)$  chain

$$\mathcal{H}^{biQ}(\pm J) = -\frac{1}{2} \mathcal{H}^{F \otimes A}(\pm J) \pm \frac{4}{3} JN \quad (3.10)$$

may be performed by means of two very simple modifications, such as an overall rescaling factor of  $-\frac{1}{2}$  and an additive constant which basically just shifts the energy eigenvalues.

For the sake of completeness, we just hint at the fact that it is also possible to find the equivalence relation connecting the Lai-Sutherland model with the  $SU(3)$  chain using the same type of representation both on even and odd sites; that is:

$$\mathcal{H}^{LS}(\pm J) = \frac{1}{2} \mathcal{H}^{F \otimes F}(\pm J) \pm \frac{4}{3} JN \quad (3.11)$$

The equivalence is found by fixing the parameters  $\alpha = \beta = \pm J$  in equation (3.7). Thus, the formulation in terms of Gell-Mann matrices becomes:

$$\mathcal{H}^{F \otimes F}(\pm J) = \pm J \sum_{i=1}^N \sum_{\alpha=1}^8 \lambda_i^\alpha \lambda_{i+1}^\alpha \quad (3.12)$$

### 3.2 $SU(3)$ -symmetry of the pure biquadratic spin-1 model

Let's focus now on the antiferromagnetic model with pure biquadratic exchange:

$$\mathcal{H}^{biQ}(J) = -J \sum_{i=1}^N (\vec{S}_i \cdot \vec{S}_{i+1})^2 \quad (3.13)$$

in its  $SU(2)$ -symmetric structure.

The mapping (3.5) proposed in the previous section is very useful to the aim of showing the equivalence between the spin-1 purely biquadratic model and a Heisenberg Hamiltonian endowed with  $SU(3)$  symmetry. However, it turns out to have a complicated interpretation of in terms of  $SU(2)$  operators. This framework, in fact, leads to a mapping of quantum numbers, which is not very effective in order to classify the pure biquadratic model eigenstates, that spontaneously organise themselves according to the  $SU(2)$ -symmetric structure outlined in section 2.3.

The formerly discussed mapping leads to the following relations between  $SU(3)$  and  $SU(2)$  operators:

$$T_{2i+1}^3 = \frac{1}{2} \lambda_{2i+1}^3 = \frac{1}{2} [(S_{2i+1}^2)^2 - (S_{2i+1}^1)^2] \quad (3.14)$$

$$Y_{2i+1} = \frac{1}{\sqrt{3}} \lambda_{2i+1}^8 = (S_{2i+1}^3)^2 - \frac{2}{3} \quad (3.15)$$

These identities work only for odd sites, on which we deliberately chose to have a fundamental representation of the  $SU(3)$  group, whereas, for even sites, operators belonging to the antifundamental representation are involved, which lead to an extra minus sign due to the fact that both  $\lambda^3$  and  $\lambda^8$  are real matrices (cfr. appendix B):

$$\bar{T}_{2i}^3 = \frac{1}{2} \bar{\lambda}_{2i}^3 = -\frac{1}{2} \lambda_{2i}^3 \quad (3.16)$$

$$\bar{Y}_{2i} = \frac{1}{\sqrt{3}} \bar{\lambda}_{2i}^8 = -\frac{1}{\sqrt{3}} \lambda_{2i}^8 \quad (3.17)$$

The consequence of using alternate representations on global quantum numbers of the entire  $SU(3)$  chain can be actually incorporated in an alternate minus sign for odd and even sites:

$$T_{tot}^3 = \frac{1}{2} \sum_{i=1}^N (-1)^{i+1} \lambda_i^3 = \sum_{i=1}^N (-1)^{i+1} \frac{1}{2} [(S_i^2)^2 - (S_i^1)^2] \quad (3.18)$$

$$Y_{tot} = \frac{1}{\sqrt{3}} \sum_{i=1}^N (-1)^{i+1} \lambda_i^8 = \sum_{i=1}^N (-1)^{i+1} [(S_i^3)^2 - \frac{2}{3}] \quad (3.19)$$

Although this mapping between  $SU(3)$  and  $SU(2)$  quantum numbers is quite easy to find, there is the main disadvantage of having a non diagonal form of  $S^3$ ,

$$S_3 = \begin{pmatrix} 0 & -i & 0 \\ i & 0 & 0 \\ 0 & 0 & 0 \end{pmatrix} \quad (3.20)$$

that makes the interpretation in terms of  $S^z$  eigenstates very intricate, because of the eigenstates form (A.9).

The matter is, then, finding a representation of the spin algebra that has one of the three spin components, usually  $S^z$  in a diagonal form. The most convenient choice is done organising the  $S^z$  eigenvalues  $0, \pm 1$  on the diagonal in a slightly different order from usual:

$$S^z = \begin{pmatrix} 1 & 0 & 0 \\ 0 & -1 & 0 \\ 0 & 0 & 0 \end{pmatrix} \quad (3.21)$$

leading to the set of eigenvalue (A.11). The remaining consistent choice for the matrices representing the  $S^x$  and  $S^y$  spin operators are defined in (A.10) in appendix A. Now the obvious advantage of selecting this particular form of the spin components is that the  $S^z$  operator coincide with the third Gell-Mann matrix  $\lambda^3$ .

### 3.3 Mapping of the biquadratic Hamiltonian into a $SU(3)$ spin chain

Once established the fundamental relation  $S^z = \lambda^3$ , we can write down the complete mapping between the spin-1 operators of the pure-biquadratic Hamiltonian and the Gell-Mann matrices of the  $SU(3)$  Heisenberg chain:

$$S^x = \frac{1}{\sqrt{2}}(\lambda^4 + \lambda^6) \quad S^y = \frac{1}{\sqrt{2}}(\lambda^5 - \lambda^7) \quad (3.22)$$

$$(S^x)^2 = \frac{1}{2}(\lambda^1 - \frac{1}{\sqrt{3}}\lambda^8 + \frac{4}{3}) \quad (S^y)^2 = \frac{1}{2}(-\lambda^1 - \frac{1}{\sqrt{3}}\lambda^8 + \frac{4}{3}) \quad (3.23)$$

$$(S^z)^2 = \frac{1}{3}(\sqrt{3}\lambda^8 + 2) \quad (3.24)$$

$$S^x S^y = \frac{1}{2}(\lambda^2 + i\lambda^3) \quad S^y S^x = \frac{1}{2}(\lambda^2 - i\lambda^3) \quad (3.25)$$

$$S^y S^z = \frac{1}{2\sqrt{2}}(i\lambda^4 + \lambda^5 + i\lambda^6 + \lambda^7) \quad S^z S^y = \frac{1}{2\sqrt{2}}(-i\lambda^4 + \lambda^5 - i\lambda^6 + \lambda^7) \quad (3.26)$$

$$S^x S^z = \frac{1}{2\sqrt{2}}(\lambda^4 - i\lambda^5 - \lambda^6 + i\lambda^7) \quad S^z S^x = \frac{1}{2\sqrt{2}}(-\lambda^4 + i\lambda^5 - \lambda^6 - i\lambda^7) \quad (3.27)$$

Let's proceed with the mapping of the pure-biquadratic model (3.13) into a  $SU(3)$  symmetric model. The computational effort would be a little more using this mapping than the previously discussed one (3.5), but it makes very immediate the mapping of the biquadratic Hamiltonian eigenstates with  $SU(3)$  quantum numbers  $T^3$  and  $Y$ .

In order to simplify at minimum the algebra, we need to invert the logical process and using the inverse map, expressing the  $SU(3)$  operators as combinations of the three spin components, their squares and mixed products. The reason behind this choice lies in the fact that we will obtain an expression containing  $SU(2)$  operators, which will be considerably easier to manipulate in order to recover the pure-biquadratic Hamiltonian form. This is due to the much simpler Lie algebra of  $SU(2)$ , built upon three commutation rules (A.2) and one basic relation among the spin squares (A.13). From the structure constant table B.1, we see that the  $SU(3)$  algebra would be certainly more difficult to deal with.

Inverting the former relations, we obtain the conventional map for the fundamental representation generators:

$$\lambda_i^1 = (S_i^x)^2 - (S_i^y)^2 \quad (3.28)$$

$$\lambda_i^2 = S_i^x S_i^y + S_i^y S_i^x \quad (3.29)$$

$$\lambda_i^3 = S^z = -i(S_i^x S_i^y - S_i^y S_i^x) \quad (3.30)$$

$$\lambda_i^4 = \frac{1}{\sqrt{2}}(S_i^x + S_i^x S_i^z + S_i^z S_i^x) \quad (3.31)$$

$$\lambda_i^5 = \frac{1}{\sqrt{2}}(S_i^y + S_i^y S_i^z + S_i^z S_i^y) \quad (3.32)$$

$$\lambda_i^6 = \frac{1}{\sqrt{2}}(S_i^x - S_i^x S_i^z - S_i^z S_i^x) \quad (3.33)$$

$$\lambda_i^7 = \frac{1}{\sqrt{2}}(-S_i^y + S_i^y S_i^z + S_i^z S_i^y) \quad (3.34)$$

$$\lambda_i^8 = \sqrt{3}((S_i^z)^2 - \frac{2}{3}) = \sqrt{3}(\frac{4}{3} - (S_i^x)^2 - (S_i^y)^2) \quad (3.35)$$

As previously explained, we will start with the  $SU(3)$  Hamiltonian in the form:

$$\mathcal{H}^{F \otimes A}(J) = J \sum_{i=1}^{N/2} \sum_{\alpha=1}^8 \left[ \lambda_{2i-1}^\alpha \bar{\lambda}_{2i}^\alpha + \bar{\lambda}_{2i}^\alpha \lambda_{2i+1}^\alpha \right] \quad (3.36)$$

that may be written using only the fundamental generators, recalling the relation between fundamental and antifundamental representation generators  $\overline{\lambda^\alpha} = -(\lambda^\alpha)^*$  :

$$\begin{aligned} \mathcal{H}^{F \otimes A}(J) = & J \sum_{i=1}^N [ -\lambda_i^1 \lambda_{i+1}^1 + \lambda_i^2 \lambda_{i+1}^2 - \lambda_i^3 \lambda_{i+1}^3 - \lambda_i^4 \lambda_{i+1}^4 + \\ & + \lambda_i^5 \lambda_{i+1}^5 - \lambda_i^6 \lambda_{i+1}^6 + \lambda_i^7 \lambda_{i+1}^7 - \lambda_i^8 \lambda_{i+1}^8 ] \end{aligned} \quad (3.37)$$

We will deal with couples of term separately.

$$\begin{aligned} -\lambda_i^1 \lambda_{i+1}^1 - \lambda_i^8 \lambda_{i+1}^8 = & -(S_i^x)^2 (S_{i+1}^x)^2 - (S_i^y)^2 (S_{i+1}^y)^2 + (S_i^x)^2 (S_{i+1}^y)^2 + \\ & (S_i^y)^2 (S_{i+1}^x)^2 - 3(S_i^z)^2 (S_{i+1}^z)^2 - \frac{4}{3} + 2(S_{i+1}^z)^2 + 2(S_i^z)^2 \end{aligned} \quad (3.38)$$

$$\lambda_i^2 \lambda_{i+1}^2 - \lambda_i^3 \lambda_{i+1}^3 = -S_i^z S_{i+1}^z + (S_i^x S_i^y + S_i^y S_i^x)(S_{i+1}^x S_{i+1}^y + S_{i+1}^y S_{i+1}^x) \quad (3.39)$$

$$-\lambda_i^4 \lambda_{i+1}^4 - \lambda_i^6 \lambda_{i+1}^6 = S_i^y S_{i+1}^y - (S_i^x S_i^z + S_i^z S_i^x)(S_{i+1}^x S_{i+1}^z + S_{i+1}^z S_{i+1}^x) \quad (3.40)$$

$$\lambda_i^5 \lambda_{i+1}^5 + \lambda_i^7 \lambda_{i+1}^7 = -S_i^x S_{i+1}^x + (S_i^y S_i^z + S_i^z S_i^y)(S_{i+1}^y S_{i+1}^z + S_{i+1}^z S_{i+1}^y) \quad (3.41)$$

Manipulating the first identity with the help of the property  $(S^x)^2 + (S^y)^2 + (S^z)^2 = 2$ , we may get to the form:

$$-\lambda_i^1 \lambda_{i+1}^1 - \lambda_i^8 \lambda_{i+1}^8 = \frac{8}{3} - 2(S_i^x)^2 (S_{i+1}^x)^2 - 2(S_i^y)^2 (S_{i+1}^y)^2 - 2(S_i^z)^2 (S_{i+1}^z)^2 \quad (3.42)$$

Regarding the three following identities, the best way to proceed is using the commutator definition, for example equation (3.39) becomes:

$$\begin{aligned} \lambda_i^2 \lambda_{i+1}^2 - \lambda_i^3 \lambda_{i+1}^3 = & (S_i^x S_i^y - S_i^y S_i^x)(S_{i+1}^x S_{i+1}^y - S_{i+1}^y S_{i+1}^x) + \\ & + (S_i^x S_i^y + S_i^y S_i^x)(S_{i+1}^x S_{i+1}^y + S_{i+1}^y S_{i+1}^x) = \\ & = 2S_i^x S_i^y S_{i+1}^x S_{i+1}^y + 2S_i^y S_i^x S_{i+1}^y S_{i+1}^x \end{aligned} \quad (3.43)$$

Rearranging in the same manner equation (3.40) and (3.41) we get analogous identities:

$$\begin{aligned} -\lambda_i^4 \lambda_{i+1}^4 - \lambda_i^6 \lambda_{i+1}^6 = & -(S_i^x S_i^z - S_i^z S_i^x)(S_{i+1}^x S_{i+1}^z - S_{i+1}^z S_{i+1}^x) + \\ & -(S_i^x S_i^z + S_i^z S_i^x)(S_{i+1}^x S_{i+1}^z + S_{i+1}^z S_{i+1}^x) = \\ & = -2S_i^x S_i^z S_{i+1}^x S_{i+1}^z - 2S_i^z S_i^x S_{i+1}^z S_{i+1}^x \end{aligned} \quad (3.44)$$

$$\begin{aligned}
\lambda_i^5 \lambda_{i+1}^5 + \lambda_i^7 \lambda_{i+1}^7 &= (S_i^y S_i^z - S_i^z S_i^y)(S_{i+1}^y S_{i+1}^z - S_{i+1}^z S_{i+1}^y) + \\
&+ (S_i^y S_i^z + S_i^z S_i^y)(S_{i+1}^y S_{i+1}^z + S_{i+1}^z S_{i+1}^y) = \quad (3.45) \\
&= 2S_i^y S_i^z S_{i+1}^y S_{i+1}^z + 2S_i^z S_i^y S_{i+1}^z S_{i+1}^y
\end{aligned}$$

Finally, when all pieces come together, we get the following expression:

$$\mathcal{H}^{F \otimes A}(J) = -2J \sum_{i=1}^N (S_i^x S_{i+1}^x - S_i^y S_{i+1}^y + S_i^z S_{i+1}^z)^2 + \frac{8}{3} JN \quad (3.46)$$

which resembles the equivalence relation (3.10) previously found with the mapping illustrated in appendix C. There is one difference, though. In order to recover exactly the biquadratic Hamiltonian (3.13), we need to change some of the signs. Recalling that the  $SU(2)$  Lie algebra (A.2) is *invariant under the exchange of the signs of two of its generators*, we may arbitrarily change the signs of two of the spin components, in particular we will choose  $S^x$  and  $S^z$ , to restore the sum of terms with concurring signs.

However, since there is a product of the same spin components of two neighbouring sites, the global sign would not be altered. The trick we have to exploit is changing the signs only for the  $x$ - and  $z$ -components of one of two adjacent spins which interact through the Hamiltonian. Since this must be true for each couple of neighbouring spins, we need to **alternatively** exchange the suitable signs on the whole length of the chain.

We will show that the best possible choice is switching signs of  $x$ - and  $z$ -components **only on even sites**. In conclusion, the mapping we just performed works uniquely under these premises:

$$\mathcal{H}^{F \otimes A}(J) = -2J \sum_{i=1}^N (\vec{S}_i \cdot \vec{S}_{i+1})^2 + \frac{8}{3} JN \quad (3.47)$$

provided  $S_{2i}^x \rightarrow -S_{2i}^x$  and  $S_{2i}^z \rightarrow -S_{2i}^z$

We stress again the essential assumption for the exact mapping of the pure-biquadratic spin-1 Hamiltonian into a  $SU(3)$  Heisenberg chain: *it is necessary to switch the signs of two of the spin components on either odd or even sites of the biquadratic model in order to recover the  $SU(3)$ -invariant Heisenberg model with alternate representations on even and odd sites*. We will see in the following section how to deal with these changes of sign.

### 3.4 Complete mapping of quantum numbers

This section is dealing with the mapping between  $SU(2)$  and  $SU(3)$  quantum numbers, that allows a classification of the pure-biquadratic Hamiltonian eigenstates, which may be calculated via the Bethe ansatz technique,

according to a hidden symmetry structure enlightened by the equivalence with the  $SU(3)$  group.

Let's start again from the equivalence relation (3.47). We already know that the eigenstates of the  $SU(3)$  Hamiltonian

$$\mathcal{H}^{F \otimes A}(J) = J \sum_{i=1}^{N/2} \sum_{\alpha=1}^8 \left[ \lambda_{2i-1}^{\alpha} \bar{\lambda}_{2i}^{\alpha} + \bar{\lambda}_{2i}^{\alpha} \lambda_{2i+1}^{\alpha} \right] \quad (3.48)$$

with alternate representations on even and odd sites can be classified according to the good quantum numbers:

$$T_{tot}^3 = \frac{1}{2} \sum_{i=1}^N (-1)^{i+1} \lambda_i^3 \quad Y_{tot} = \sum_{i=1}^N (-1)^{i+1} Y_i \quad (3.49)$$

It is easy to prove that  $T_{tot}^3$  and  $Y_{tot}$  do indeed commute with the Hamiltonian in the form (3.48). It is necessary to make extensive use of the  $SU(3)$  Lie algebra, that is encoded in its structure constants defined and listed table B.1. The only useful ones to proceed with this commutator evaluation are those involving  $\lambda^3$ , namely:

$$f_{123} = 1, \quad f_{345} = \frac{1}{2}, \quad f_{367} = -\frac{1}{2} \quad (3.50)$$

$$\begin{aligned} & [\mathcal{H}^{F \otimes A}(J), T_{tot}^3] = \\ & J \left[ \sum_{i=1}^{N/2} \sum_{\alpha=1}^8 \left( \lambda_{2i-1}^{\alpha} \bar{\lambda}_{2i}^{\alpha} + \bar{\lambda}_{2i}^{\alpha} \lambda_{2i+1}^{\alpha} \right), \frac{1}{2} \sum_{j=1}^N (-1)^{j+1} \lambda_j^3 \right] = \\ & = J \sum_{i=1}^{N/2} \sum_{\alpha=1}^8 \left( (-1)^{2i} \left[ \lambda_{2i-1}^{\alpha} \bar{\lambda}_{2i}^{\alpha}, \lambda_{2i-1}^3 \right] + (-1)^{2i+1} \left[ \lambda_{2i-1}^{\alpha} \bar{\lambda}_{2i}^{\alpha}, \lambda_{2i}^3 \right] + \right. \\ & \left. + (-1)^{2i+1} \left[ \bar{\lambda}_{2i}^{\alpha} \lambda_{2i+1}^{\alpha}, \lambda_{2i}^3 \right] + (-1)^{2i+2} \left[ \bar{\lambda}_{2i}^{\alpha} \lambda_{2i+1}^{\alpha}, \lambda_{2i+1}^3 \right] \right) = \\ & = J \sum_{i=1}^{N/2} \sum_{\alpha=1}^8 \left( \left[ \lambda_{2i-1}^{\alpha}, \lambda_{2i-1}^3 \right] \bar{\lambda}_{2i}^{\alpha} - \lambda_{2i-1}^{\alpha} \left[ \bar{\lambda}_{2i}^{\alpha}, \lambda_{2i}^3 \right] + \right. \\ & \left. - \left[ \bar{\lambda}_{2i}^{\alpha}, \lambda_{2i}^3 \right] \lambda_{2i+1}^{\alpha} + \bar{\lambda}_{2i}^{\alpha} \left[ \lambda_{2i+1}^{\alpha}, \lambda_{2i+1}^3 \right] \right) \end{aligned} \quad (3.51)$$

Finally the evaluation of commutators results into a null expression, i.e.

$$\begin{aligned}
&= \sum_{j=1}^{N/2} \left( -2i\lambda_{2i-1}^2 \bar{\lambda}_{2i}^1 + 2i\lambda_{2i-1}^1 \bar{\lambda}_{2i}^2 - i\lambda_{2i-1}^5 \bar{\lambda}_{2i}^4 + i\lambda_{2i-1}^4 \bar{\lambda}_{2i}^5 + i\lambda_{2i-1}^7 \bar{\lambda}_{2i}^6 - i\lambda_{2i-1}^6 \bar{\lambda}_{2i}^7 + \right. \\
&- 2i\lambda_{2i-1}^1 \lambda_{2i}^2 - 2i\lambda_{2i-1}^2 \lambda_{2i}^1 - i\lambda_{2i-1}^4 \lambda_{2i}^5 - i\lambda_{2i-1}^5 \lambda_{2i}^4 + i\lambda_{2i-1}^6 \lambda_{2i}^7 + i\lambda_{2i-1}^7 \lambda_{2i}^6 + \\
&- 2i\lambda_{2i}^2 \lambda_{2i+1}^1 - 2i\lambda_{2i}^1 \lambda_{2i+1}^2 - i\lambda_{2i}^5 \lambda_{2i+1}^4 - i\lambda_{2i}^4 \lambda_{2i+1}^5 + i\lambda_{2i}^7 \lambda_{2i+1}^6 + i\lambda_{2i}^6 \lambda_{2i+1}^7 + \\
&\left. - 2i\bar{\lambda}_{2i}^1 \lambda_{2i+1}^2 + 2i\bar{\lambda}_{2i}^2 \lambda_{2i+1}^1 - i\bar{\lambda}_{2i}^4 \lambda_{2i+1}^5 + i\bar{\lambda}_{2i}^5 \lambda_{2i+1}^4 + i\bar{\lambda}_{2i}^6 \lambda_{2i+1}^7 - i\bar{\lambda}_{2i}^7 \lambda_{2i+1}^6 \right) \\
&= 0
\end{aligned} \tag{3.52}$$

Now, using the  $SU(2)$  formalism we should be able to show that also the equivalent Hamiltonian of the pure-biquadratic spin-1 model (3.13), commutes with the  $SU(3)$  quantum number  $T_{tot}^3$ , once the suitable changes of sign

$$S_{2i}^x \rightarrow -S_{2i}^x \quad S_{2i}^z \rightarrow -S_{2i}^z \tag{3.53}$$

have been made. Therefore, the first  $SU(3)$  quantum number  $T_{tot}^3$  happens to be exactly the component of the total spin along the  $z$ -axis for the bi-quadratic Hamiltonian eigenstates:

$$\begin{aligned}
T_{tot}^3 &= \frac{1}{2} \sum_{i=1}^N (-1)^{i+1} \lambda_i^3 = \frac{1}{2} \sum_{i=1}^N (-1)^{i+1} S_i^z \quad (S_{2i}^z \rightarrow -S_{2i}^z) \\
\implies T_{tot}^3 &= \frac{1}{2} \sum_{i=1}^N (-1)^{i+1} (-1)^{i+1} S_i^z = \frac{1}{2} \sum_{i=1}^N S_i^z = \frac{1}{2} S_{tot}^z
\end{aligned} \tag{3.54}$$

This result is very useful in order to label the states, because according to the Bethe ansatz technique we proceed by deviations from the fully aligned states, that are easily connected with the value of  $S_{tot}^z$ . Now, let's prove this result working in the  $SU(2)$  operators environment; we should be able to verify the following commutation relation:

$$\left[ \mathcal{H}^{biQ}(-J), S_{tot}^z \right] = \left[ -J \sum_{i=1}^N (\vec{S}_i \cdot \vec{S}_{i+1})^2, \sum_{j=1}^N S_j^z \right] = 0 \tag{3.55}$$

Since spin operators acting on different sites commute among themselves, the only surviving terms of the summation appear among the following ones:

$$\begin{aligned}
\left[ (S_i^x)^2 (S_{i+1}^x)^2, S_i^z + S_{i+1}^z \right] &= -i(S_i^x S_i^y + S_i^y S_i^x)(S_{i+1}^x)^2 + \\
&- i(S_i^x)^2 (S_{i+1}^x S_{i+1}^y + S_{i+1}^y S_{i+1}^x)
\end{aligned} \tag{3.56}$$

$$\begin{aligned} [(S_i^y)^2 (S_{i+1}^y)^2, S_i^z + S_{i+1}^z] = & + i(S_i^y S_i^x + S_i^x S_i^y)(S_{i+1}^y)^2 + \\ & + i(S_i^y)^2 (S_{i+1}^y S_{i+1}^x + S_{i+1}^x S_{i+1}^y) \end{aligned} \quad (3.57)$$

$$\begin{aligned} [(S_i^x S_i^y)(S_{i+1}^x S_{i+1}^y), S_i^z + S_{i+1}^z] = & + i((S_i^x)^2 - (S_i^y)^2)(S_{i+1}^x S_{i+1}^y) + \\ & + i(S_i^x S_i^y)((S_{i+1}^x)^2 - (S_{i+1}^y)^2) \end{aligned} \quad (3.58)$$

$$\begin{aligned} [(S_i^y S_i^x)(S_{i+1}^y S_{i+1}^x), S_i^z + S_{i+1}^z] = & + i((S_i^x)^2 - (S_i^y)^2)(S_{i+1}^y S_{i+1}^x) + \\ & + i(S_i^y S_i^x)((S_{i+1}^x)^2 - (S_{i+1}^y)^2) \end{aligned} \quad (3.59)$$

$$\begin{aligned} [(S_i^x S_i^z)(S_{i+1}^x S_{i+1}^z), S_i^z + S_{i+1}^z] = & - i(S_i^y S_i^z)(S_{i+1}^x S_{i+1}^z) + \\ & - i(S_i^x S_i^z)(S_{i+1}^y S_{i+1}^z) \end{aligned} \quad (3.60)$$

$$\begin{aligned} [(S_i^z S_i^x)(S_{i+1}^z S_{i+1}^x), S_i^z + S_{i+1}^z] = & - i(S_i^z S_i^y)(S_{i+1}^z S_{i+1}^x) + \\ & - i(S_i^z S_i^x)(S_{i+1}^z S_{i+1}^y) \end{aligned} \quad (3.61)$$

$$\begin{aligned} [(S_i^y S_i^z)(S_{i+1}^y S_{i+1}^z), S_i^z + S_{i+1}^z] = & + i(S_i^x S_i^z)(S_{i+1}^y S_{i+1}^z) + \\ & + i(S_i^y S_i^z)(S_{i+1}^x S_{i+1}^z) \end{aligned} \quad (3.62)$$

$$\begin{aligned} [(S_i^z S_i^y)(S_{i+1}^z S_{i+1}^y), S_i^z + S_{i+1}^z] = & + i(S_i^z S_i^x)(S_{i+1}^z S_{i+1}^y) + \\ & + i(S_i^z S_i^y)(S_{i+1}^z S_{i+1}^x) \end{aligned} \quad (3.63)$$

The sum of the first four commutators (3.56), (3.57), (3.58) and (3.59), once properly rearranged, manifestly vanish. The same happens to the following four ones (3.60), (3.61), (3.62) and (3.63). Hence, it was somehow easy to prove that the equation (3.55) holds.

However, there is one more quantum number characterising the  $SU(3)$  Heisenberg chain and it will be very interesting to see what is its correspondent one for the spin-1 biquadratic Hamiltonian.

Here, there is an important difference from the previous case. Since the second  $SU(3)$  quantum number  $Y_i$  is defined in (3.35) as proportional to the square of the  $z$ -component of the spin operator on each site, now the change of sign (3.53) to be performed in order to relate the spin-1 one chain to the  $SU(3)$ -symmetric model, appears to be irrelevant.

$$\begin{aligned}
Y_{tot} &= \frac{1}{\sqrt{3}} \sum_{i=1}^N (-1)^{i+1} \lambda_i^8 = \sum_{i=1}^N (-1)^{i+1} \left( (S_i^z)^2 - \frac{2}{3} \right) \quad (S_{2i}^z \rightarrow -S_{2i}^z) \\
\Rightarrow Y_{tot} &= \sum_{i=1}^N (-1)^{i+1} \left( ((-1)^{i+1} S_i^z)^2 - \frac{2}{3} \right) = \sum_{i=1}^N (-1)^{i+1} (S_i^z)^2 \equiv (S^z)_{stag}^2
\end{aligned} \tag{3.64}$$

Therefore, the minus sign introduced by alternate fundamental and antifundamental representations would not vanish, leading to a distinction between states based on the parity of the sites of the chain. That is, the new staggered operator  $(S^z)_{stag}^2$  would not distinguish among states with  $S_i^z = 1$  and  $S_i^z = -1$ , but eigenstates of  $S^z$  with null eigenvalue would definitely stand out.

Recalling the Bethe ansatz approach outlined in section 2.3, we may draw the conclusion that  $Y$  is definitely related to the two-string interpretation because, while it is null for neighbouring couples with the same spin eigenvalues on both sites and minus-plus couples, it does have a non-null eigenvalue for a couple with just one zero and a plus or a minus. The value of  $Y$  is either  $+1$  or  $-1$  depending on the location of the zero. We will see some examples of this action of the operator  $Y$  later on, when dealing with finite chains.

For now, let's focus our attention on the upcoming proof of the commutation relation that shows that  $Y$  is a good quantum number for the  $SU(3)$  Heisenberg model. This should be really immediate, recalling the appropriate commutation relations among Gell-mann matrices and employing the suitable structure constants:

$$f_{458} = \frac{\sqrt{3}}{2} \quad f_{678} = \frac{\sqrt{3}}{2} \tag{3.65}$$

$$\begin{aligned}
[\mathcal{H}^{F \otimes A}(J), Y_{tot}] &= J \left[ \sum_{i=1}^{N/2} \sum_{\alpha=1}^8 \left( \lambda_{2i-1}^\alpha \bar{\lambda}_{2i}^\alpha + \bar{\lambda}_{2i}^\alpha \lambda_{2i+1}^\alpha \right), \frac{1}{\sqrt{3}} \sum_{j=1}^N (-1)^{j+1} \lambda_j^8 \right] = \\
&= \frac{J}{\sqrt{3}} \sum_{i=1}^{N/2} \sum_{\alpha=1}^8 \left( [\lambda_{2i-1}^\alpha, \lambda_{2i-1}^8] \bar{\lambda}_{2i}^\alpha - \lambda_{2i-1}^\alpha [\bar{\lambda}_{2i}^\alpha, \lambda_{2i}^8] + \right. \\
&\quad \left. - [\bar{\lambda}_{2i}^\alpha, \lambda_{2i}^8] \lambda_{2i+1}^\alpha + \bar{\lambda}_{2i}^\alpha [\lambda_{2i+1}^\alpha, \lambda_{2i+1}^8] \right)
\end{aligned} \tag{3.66}$$

This expression, once again, leads to a sum of Gell-Mann matrices which is easily shown to be null.

$$\begin{aligned}
 & \frac{J}{\sqrt{3}} 2i \frac{\sqrt{3}}{2} \sum_{i=1}^{N/2} \left( -\lambda_{2i-1}^5 \bar{\lambda}_{2i}^4 + \lambda_{2i-1}^4 \bar{\lambda}_{2i}^5 - \lambda_{2i-1}^5 \lambda_{2i}^4 - \lambda_{2i-1}^4 \lambda_{2i}^5 + \right. \\
 & - \lambda_{2i}^5 \lambda_{2i+1}^4 - \lambda_{2i}^4 \lambda_{2i+1}^5 - \bar{\lambda}_{2i}^4 \lambda_{2i+1}^5 + \bar{\lambda}_{2i}^5 \lambda_{2i+1}^4 + \\
 & \left. + (\lambda^5 \rightarrow \lambda^7, \lambda^4 \rightarrow \lambda^6) \right) = 0
 \end{aligned} \tag{3.67}$$

Now, because of the equivalence relation (3.47), the pure-biquadratic Hamiltonian is bound to commute with the spin operator corresponding to  $Y$ , provided the appropriate substitutions (3.53) have been made. This operator was identified to be  $(S^z)_{stag}^2$ . Here, there is the complete proof of that property.

$$\begin{aligned}
 & \left[ \mathcal{H}^{biQ}(-J), (S^z)_{stag}^2 \right] = \left[ -J \sum_{i=1}^N (\vec{S}_i \cdot \vec{S}_{i+1})^2, \sum_{j=1}^N (-1)^{j+1} (S_j^z)^2 \right] = \\
 & = -J \sum_{i=1}^N (-1)^{i+1} \left[ \left( (S_i^x)^2 (S_{i+1}^x)^2 + (S_i^y)^2 (S_{i+1}^y)^2 + (S_i^z)^2 (S_{i+1}^z)^2 + \right. \right. \\
 & + (S_i^x S_i^y) (S_{i+1}^x S_{i+1}^y) + (S_i^y S_i^x) (S_{i+1}^y S_{i+1}^x) + \\
 & + (S_i^x S_i^z) (S_{i+1}^x S_{i+1}^z) + (S_i^z S_i^x) (S_{i+1}^z S_{i+1}^x) + \\
 & \left. \left. + (S_i^y S_i^z) (S_{i+1}^y S_{i+1}^z) + (S_i^z S_i^y) (S_{i+1}^z S_{i+1}^y) \right), (S_i^z)^2 - (S_{i+1}^z)^2 \right]
 \end{aligned} \tag{3.68}$$

We may treat each of the nine terms of the biquadratic Hamiltonian separately. Recalling the spin commutation relations collected in appendix A, we get the following set of identities:

$$\begin{aligned}
 & \left[ (S_i^x)^2 (S_{i+1}^x)^2, (S_i^z)^2 - (S_{i+1}^z)^2 \right] = -i S_i^x S_i^y S_i^z (S_{i+1}^x)^2 - i S_i^y S_i^x S_i^z (S_{i+1}^x)^2 + \\
 & - i S_i^z S_i^x S_i^y (S_{i+1}^x)^2 - i S_i^z S_i^y S_i^x (S_{i+1}^x)^2 + i (S_i^x)^2 S_{i+1}^x S_{i+1}^y S_{i+1}^z + \\
 & + i (S_i^x)^2 S_{i+1}^y S_{i+1}^x S_{i+1}^z + i (S_i^x)^2 S_{i+1}^z S_{i+1}^x S_{i+1}^y + i (S_i^x)^2 S_{i+1}^z S_{i+1}^y S_{i+1}^x
 \end{aligned} \tag{3.69}$$

$$\begin{aligned}
 & \left[ (S_i^y)^2 (S_{i+1}^y)^2, (S_i^z)^2 - (S_{i+1}^z)^2 \right] = +i S_i^x S_i^y S_i^z (S_{i+1}^y)^2 + i S_i^y S_i^x S_i^z (S_{i+1}^y)^2 + \\
 & + i S_i^z S_i^x S_i^y (S_{i+1}^y)^2 + i S_i^z S_i^y S_i^x (S_{i+1}^y)^2 - i (S_i^y)^2 S_{i+1}^x S_{i+1}^y S_{i+1}^z + \\
 & - i (S_i^y)^2 S_{i+1}^y S_{i+1}^x S_{i+1}^z - i (S_i^y)^2 S_{i+1}^z S_{i+1}^x S_{i+1}^y - i (S_i^y)^2 S_{i+1}^z S_{i+1}^y S_{i+1}^x
 \end{aligned} \tag{3.70}$$

$$\begin{aligned}
 & \left[ (S_i^x S_i^y) (S_{i+1}^x S_{i+1}^y), (S_i^z)^2 - (S_{i+1}^z)^2 \right] = +i (S_i^x)^2 S_i^z S_{i+1}^x S_{i+1}^y - i (S_i^y)^2 S_i^z S_{i+1}^x S_{i+1}^y + \\
 & + i S_i^z (S_i^x)^2 S_{i+1}^x S_{i+1}^y - i S_i^z (S_i^y)^2 S_{i+1}^x S_{i+1}^y - i S_i^x S_i^y (S_{i+1}^x)^2 S_{i+1}^z + \\
 & + i S_i^x S_i^y (S_{i+1}^y)^2 S_{i+1}^z - i S_i^x S_i^y S_{i+1}^z (S_{i+1}^x)^2 + i S_i^x S_i^y S_{i+1}^z (S_{i+1}^y)^2
 \end{aligned} \tag{3.71}$$

$$\begin{aligned}
& [(S_i^y S_i^x)(S_{i+1}^y S_{i+1}^x), (S_i^z)^2 - (S_{i+1}^z)^2] = +i(S_i^x)^2 S_i^z S_{i+1}^y S_{i+1}^x - i(S_i^y)^2 S_i^z S_{i+1}^y S_{i+1}^x + \\
& + iS_i^z (S_i^x)^2 S_{i+1}^y S_{i+1}^x - iS_i^z (S_i^y)^2 S_{i+1}^y S_{i+1}^x - iS_i^y S_i^x (S_{i+1}^x)^2 S_{i+1}^z + \\
& + iS_i^y S_i^x (S_{i+1}^y)^2 S_{i+1}^z - iS_i^y S_i^x S_{i+1}^z (S_{i+1}^x)^2 + iS_i^y S_i^x S_{i+1}^z (S_{i+1}^y)^2
\end{aligned} \tag{3.72}$$

$$\begin{aligned}
& [(S_i^x S_i^z)(S_{i+1}^x S_{i+1}^z), (S_i^z)^2 - (S_{i+1}^z)^2] = + - iS_i^y S_i^z S_i^z S_{i+1}^x S_{i+1}^z - iS_i^z S_i^y S_i^z S_{i+1}^x S_{i+1}^z + \\
& + iS_i^x S_i^z S_{i+1}^y S_{i+1}^z S_{i+1}^z + iS_i^x S_i^z S_{i+1}^z S_{i+1}^y S_{i+1}^z
\end{aligned} \tag{3.73}$$

$$\begin{aligned}
& [(S_i^z S_i^x)(S_{i+1}^z S_{i+1}^x), (S_i^z)^2 - (S_{i+1}^z)^2] = -iS_i^z S_i^y S_i^z S_{i+1}^z S_{i+1}^x - iS_i^z S_i^z S_i^y S_{i+1}^z S_{i+1}^x + \\
& + iS_i^z S_i^x S_{i+1}^z S_{i+1}^y S_{i+1}^z + iS_i^z S_i^x S_{i+1}^z S_{i+1}^y S_{i+1}^z
\end{aligned} \tag{3.74}$$

$$\begin{aligned}
& [(S_i^y S_i^z)(S_{i+1}^y S_{i+1}^z), (S_i^z)^2 - (S_{i+1}^z)^2] = +iS_i^x S_i^z S_i^z S_{i+1}^y S_{i+1}^z + iS_i^z S_i^x S_i^z S_{i+1}^y S_{i+1}^z + \\
& - iS_i^y S_i^z S_{i+1}^x S_{i+1}^z S_{i+1}^z - iS_i^y S_i^z S_{i+1}^z S_{i+1}^x S_{i+1}^z
\end{aligned} \tag{3.75}$$

$$\begin{aligned}
& [(S_i^z S_i^y)(S_{i+1}^z S_{i+1}^y), (S_i^z)^2 - (S_{i+1}^z)^2] = +iS_i^z S_i^x S_i^z S_{i+1}^z S_{i+1}^y + iS_i^z S_i^z S_i^x S_{i+1}^z S_{i+1}^y + \\
& - iS_i^z S_i^y S_{i+1}^z S_{i+1}^x S_{i+1}^z - iS_i^z S_i^y S_{i+1}^z S_{i+1}^x S_{i+1}^z
\end{aligned} \tag{3.76}$$

The strategy employed to prove this long list of terms is in fact null is based on cyclic permutations of the spin components, according to the  $SU(2)$  algebra, in order to recreate exactly the expression of the commutator of the Hamiltonian with the  $z$ -component of the total spin, which we have previously shown to be zero. We will reproduce two copies of that commutator preceded by a  $S_i^z$  and  $S_{i+1}^z$  operator respectively. To make this possible, we should commute the  $S^z$  operators to bring them in the first position of each term of the sum. Let's see an example of this procedure for equations (3.69) and (3.70).

$$\begin{aligned}
& [(S_i^x)^2 (S_{i+1}^x)^2, (S_i^z)^2 - (S_{i+1}^z)^2] = \\
& S_i^z (-iS_i^x S_i^y (S_{i+1}^x)^2 - iS_i^y S_i^x (S_{i+1}^x)^2 - iS_i^x S_i^y (S_{i+1}^x)^2 - iS_i^y S_i^x (S_{i+1}^x)^2) + \\
& + S_{i+1}^z (i(S_i^x)^2 S_{i+1}^x S_{i+1}^y + i(S_i^x)^2 S_{i+1}^y S_{i+1}^x + i(S_i^x)^2 S_{i+1}^x S_{i+1}^y + i(S_i^x)^2 S_{i+1}^y S_{i+1}^x) + \\
& + 2((S_i^x)^2 - (S_i^y)^2) (S_{i+1}^x)^2 - 2(S_i^x)^2 ((S_{i+1}^x)^2 - (S_{i+1}^y)^2)
\end{aligned} \tag{3.77}$$

$$\begin{aligned}
& [(S_i^y)^2 (S_{i+1}^y)^2, (S_i^z)^2 - (S_{i+1}^z)^2] = \\
& S_i^z (iS_i^y S_i^x (S_{i+1}^y)^2 + iS_i^x S_i^y (S_{i+1}^y)^2 + iS_i^y S_i^x (S_{i+1}^y)^2 + iS_i^x S_i^y (S_{i+1}^y)^2) + \\
& + S_{i+1}^z (-i(S_i^y)^2 S_{i+1}^y S_{i+1}^x - i(S_i^y)^2 S_{i+1}^x S_{i+1}^y - i(S_i^y)^2 S_{i+1}^y S_{i+1}^x - i(S_i^y)^2 S_{i+1}^x S_{i+1}^y) + \\
& - 2((S_i^x)^2 - (S_i^y)^2) (S_{i+1}^y)^2 + 2(S_i^y)^2 ((S_{i+1}^x)^2 - (S_{i+1}^y)^2)
\end{aligned} \tag{3.78}$$

The result of commutations on the first, second, fifth and sixth term produces some additional terms, making the expression apparently more complicated, but having a closer look at them we realise that there are, in fact, no surviving terms once they have been summed together.

The same exact technique of iterated permutations applied to the other couples of equations leads to similar expressions, where the left out terms delete each other. From identities (3.71) and (3.72) we get:

$$\begin{aligned}
 & [(S_i^x S_i^y)(S_{i+1}^x S_{i+1}^y), (S_i^z)^2 - (S_{i+1}^z)^2] = \\
 & S_i^z (i(S_i^x)^2 S_{i+1}^x S_{i+1}^y - i(S_i^y)^2 S_{i+1}^x S_{i+1}^y + i(S_i^x)^2 S_{i+1}^y S_{i+1}^x - i(S_i^y)^2 S_{i+1}^y S_{i+1}^x) + \\
 & + S_{i+1}^z (-iS_i^x S_i^y (S_{i+1}^x)^2 + iS_i^x S_i^y (S_{i+1}^y)^2 - iS_i^x S_i^y (S_{i+1}^x)^2 + iS_i^x S_i^y (S_{i+1}^y)^2) + \\
 & 2((S_i^x S_i^y + S_i^y S_i^x)(S_{i+1}^x S_{i+1}^y) - (S_i^x S_i^y)(S_{i+1}^x S_{i+1}^y + S_{i+1}^y S_{i+1}^x))
 \end{aligned} \tag{3.79}$$

$$\begin{aligned}
 & [(S_i^y S_i^x)(S_{i+1}^y S_{i+1}^x), (S_i^z)^2 - (S_{i+1}^z)^2] = \\
 & S_i^z (i(S_i^x)^2 S_{i+1}^y S_{i+1}^x - i(S_i^y)^2 S_{i+1}^y S_{i+1}^x + i(S_i^x)^2 S_{i+1}^x S_{i+1}^y - i(S_i^y)^2 S_{i+1}^x S_{i+1}^y) + \\
 & + S_{i+1}^z (-iS_i^y S_i^x (S_{i+1}^x)^2 + iS_i^y S_i^x (S_{i+1}^y)^2 - iS_i^y S_i^x (S_{i+1}^x)^2 + iS_i^y S_i^x (S_{i+1}^y)^2) + \\
 & + 2((S_i^x S_i^y + S_i^y S_i^x)(S_{i+1}^y S_{i+1}^x) - (S_i^y S_i^x)(S_{i+1}^y S_{i+1}^x + S_{i+1}^x S_{i+1}^y))
 \end{aligned} \tag{3.80}$$

From (3.73) and (3.74)

$$\begin{aligned}
 & [(S_i^x S_i^z)(S_{i+1}^x S_{i+1}^z), (S_i^z)^2 - (S_{i+1}^z)^2] + [(S_i^z S_i^x)(S_{i+1}^z S_{i+1}^x), (S_i^z)^2 - (S_{i+1}^z)^2] = \\
 & - S_i^z (iS_i^y S_i^z S_{i+1}^x S_{i+1}^z + iS_i^y S_i^z S_{i+1}^z S_{i+1}^x) + S_{i+1}^z (iS_i^x S_i^z S_{i+1}^y S_{i+1}^z + iS_i^x S_i^z S_{i+1}^z S_{i+1}^y) + \\
 & - S_i^z (iS_i^z S_i^y S_{i+1}^x S_{i+1}^z + iS_i^z S_i^y S_{i+1}^z S_{i+1}^x) + S_{i+1}^z (iS_i^z S_i^x S_{i+1}^y S_{i+1}^z + iS_i^z S_i^x S_{i+1}^z S_{i+1}^y) + \\
 & + (S_i^x S_i^z S_{i+1}^x S_{i+1}^z - S_i^x S_i^z S_{i+1}^z S_{i+1}^x) + (S_i^z S_i^x S_{i+1}^y S_{i+1}^z - S_i^z S_i^x S_{i+1}^z S_{i+1}^y)
 \end{aligned} \tag{3.81}$$

From (3.75) and (3.76)

$$\begin{aligned}
 & [(S_i^y S_i^z)(S_{i+1}^y S_{i+1}^z), (S_i^z)^2 - (S_{i+1}^z)^2] + [(S_i^z S_i^y)(S_{i+1}^z S_{i+1}^y), (S_i^z)^2 - (S_{i+1}^z)^2] = \\
 & + S_i^z (iS_i^x S_i^z S_{i+1}^y S_{i+1}^z + iS_i^x S_i^z S_{i+1}^z S_{i+1}^y) - S_{i+1}^z (iS_i^y S_i^z S_{i+1}^x S_{i+1}^z + iS_i^y S_i^z S_{i+1}^z S_{i+1}^x) + \\
 & + S_i^z (iS_i^z S_i^x S_{i+1}^y S_{i+1}^z + iS_i^z S_i^x S_{i+1}^z S_{i+1}^y) - S_{i+1}^z (iS_i^z S_i^y S_{i+1}^x S_{i+1}^z + iS_i^z S_i^y S_{i+1}^z S_{i+1}^x) + \\
 & + (S_i^y S_i^z S_{i+1}^y S_{i+1}^z - S_i^y S_i^z S_{i+1}^z S_{i+1}^y) + (S_i^z S_i^y S_{i+1}^x S_{i+1}^z - S_i^z S_i^y S_{i+1}^z S_{i+1}^x)
 \end{aligned} \tag{3.82}$$

So, after getting rid of the unwanted terms, the remaining expression can be rearranged to reproduce exactly twice the outcome of the commutator of the biquadratic Hamiltonian with the  $S^z$  operator, preceded by the common factor  $S_i^z$  in one case and by  $S_{i+1}^z$  in the other.

$$\begin{aligned}
& \left[ \mathcal{H}^{biQ}(-J), (S^z)_{stag}^2 \right] = \\
& -J \sum_{i=1}^N S_i^z \left[ (\vec{S}_i \cdot \vec{S}_{i+1})^2, S_i^z + S_{i+1}^z \right] - J \sum_{i=1}^N S_{i+1}^z \left[ (\vec{S}_i \cdot \vec{S}_{i+1})^2, S_i^z + S_{i+1}^z \right] = 0
\end{aligned} \tag{3.83}$$

The crucial point is that the cross elimination of the additional terms occurs solely thanks to the alternate signs introduced by the using the staggered  $(S^z)_{stag}^2$ ; otherwise they would not be compensated by each other but doubled, leading us to the conclusion that the commutator of the pure-biquadratic Hamiltonian with  $(S_{tot}^z)^2$  is not null. Thus, this is not a good quantum number for the model under examination and neither  $(S_{tot}^2)$  will be. This observation is quite remarkable, because in general we would not be able to organise the biquadratic Hamiltonian eigenvalues according to  $S_{tot}^2$  eigenvalues, which define the  $SU(2)$  multiplets structure.

## Chapter 4

# Equivalence with the nine-state Potts model

### 4.1 $q$ -state Potts models

The general  $q$ -state Potts model is a two-dimensional statistical model with nearest-neighbour interactions, that can be seen as a generalisation of the Ising model. In fact, it is effectively described in terms of classical spin variables, located on each site of the two-dimensional lattice. For our purposes we can restrict to a square lattice only, but Potts model can be defined on different geometries as well. Each site of the lattice, labelled by the index  $i$ , is occupied by a discrete variable  $\sigma_i$ , taking  $q$  different values, i.e.  $\sigma_i = 0, 1, 2, \dots, q - 1$ .

The expression of the  $q$ -state Potts Hamiltonian is thus given by:

$$\mathcal{H}^{q\text{-states}}(J) = -J \sum_{(i,j)} \delta(\sigma_i - \sigma_j) \quad (4.1)$$

where the notation  $(i, j)$  indicates the pairs of nearest-neighbour variables and  $\delta(x)$  is actually a Kronecker delta  $\delta_{x,0}$ . Thus, any couple of variables with the same value of  $\sigma_i$  yields a  $-J$  contribution to the total energy of the system, whereas any couple of different nearest-neighbour variables yields no contribution.

Just like the Ising model, which may be recovered in the  $q = 2$  case, this model shows an ordered-disordered (low-high temperature) phase transition, which is a first order transition for  $q > 4$  and a second order transition for  $q \leq 4$  [25].

Let's consider now a rectangular lattice with  $m$  rows and  $n$  columns, yielding a total number of sites  $N = m \times n$ , and possibly different coupling constants  $J_1$  and  $J_2$  along the two different lattice directions. We can define a dual lattice by connecting all the middle points on the links of the original

lattice. The resulting structure, named medial lattice, is a square lattice again, but rotated by  $45^\circ$  with respect to the direct lattice.

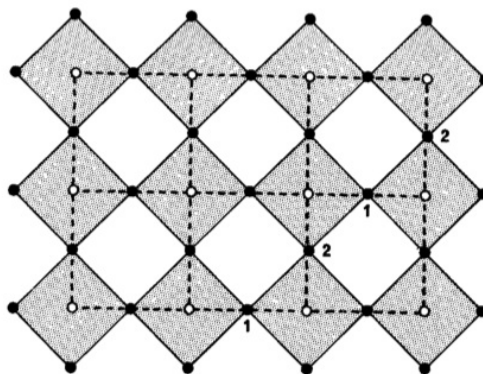


**Figure 4.1:** Classical Potts model defined on a square lattice with  $m$  rows and  $n$  columns. Each locus is occupied by a 'spin' variable, taking  $q$  different values. The direct lattice is represented by empty dots and dashed lines. The medial lattice connecting the the medial points of the direct lattice edges, is rotated by  $45^\circ$  and represented by filled dots and solid lines. In the medial lattice there are two different types of nodes that can be added row by row with the transfer matrix: they are horizontal (labelled by number one on the picture) or vertical (labelled by number two). (Picture taken from [11]).

In order to find the partition function for the  $q$ -state Potts model we need to define two different transfer matrices for the two different classes of edges that can be added.  $V$  adds a row of horizontal edges, while  $W$  adds a row of vertical ones. They are both  $(q^n \times q^n)$ -dimensional matrices, their elements being:

$$V_{\sigma,\sigma'} = \exp \left[ K_1 \sum_{j=1}^{n-1} \delta(\sigma_j, \sigma_{j+1}) \right] \prod_{j=1}^n \delta(\sigma_j, \sigma'_j) \quad (4.2)$$

$$W_{\sigma,\sigma'} = \exp \left[ K_2 \sum_{j=1}^n \delta(\sigma_j, \sigma'_j) \right] \quad (4.3)$$

in which  $\sigma$  and  $\sigma'$  represent the configuration of spin variables of a whole row namely  $\sigma = \sigma_1, \sigma_2, \dots, \sigma_n$ ;  $\sigma' = \sigma'_1, \sigma'_2, \dots, \sigma'_n$ .  $K_1 = \frac{J_1}{T}$  and  $K_2 = \frac{J_2}{T}$  keep track of the fact that the coupling constants along the two orthogonal directions of the lattice may be different.

The entire model transfer matrix is, thus, given by the a sequence of matrix products in which the operator  $V$  occurs  $m$  times, while the operator  $W$  occurs  $m - 1$  times. We have not imposed any kind of boundary conditions, for now. However, once boundary conditions have been established, we realise that the partition function for the classical  $q$ -state Potts model

on a two-dimensional lattice is clearly given by the trace on the  $(q^n \times q^n)$ -dimensional space, namely:

$$\mathcal{Z}_N = \text{Tr}[VWVWVW\dots VWV] \quad (4.4)$$

Now, let us define two algebras, [8] with operators labelled by odd and even indices respectively. The two sets of operators are:

$$(U_{2i-1})_{\sigma,\sigma'} = \frac{1}{\sqrt{q}} \prod_{j \neq i, j=1}^n \delta(\sigma_j, \sigma'_j) \quad (4.5)$$

$$(U_{2i})_{\sigma,\sigma'} = \sqrt{q} \delta(\sigma_i, \sigma_{i+1}) \prod_{j=1}^n \delta(\sigma_j, \sigma'_j) \quad (4.6)$$

for  $i = 1, 2, \dots, n$ . The matrix form of the first set of operators  $U_{2i-1}$  is a Kronecker product of  $N - 1$   $(q \times q)$ -dimensional identity matrices and a matrix with all entries equal to  $\frac{1}{\sqrt{q}}$  located at the  $i$ -th position within the product. The second set of matrices has a diagonal form instead, with all diagonal elements equal to  $\sqrt{q} \delta(\sigma_i, \sigma_{i+1})$ .

Let's have a look now at the odd and even site algebra defined in (4.5) and (4.6). It is possible to show, by means of their explicit representation, that the operators  $U_i, i = 1, 2, \dots, 2n - 1$  are endowed with some remarkable properties, which define the so-called **Temperley-Lieb algebra** [12].

$$U_i^2 = \sqrt{q} U_i \quad \text{for } i = 1, 2, \dots, 2n - 1 \quad (4.7)$$

$$U_i U_{i-1} U_i = U_i \quad \text{for } i = 2, 3, \dots, 2n - 1 \quad (4.8)$$

$$U_i U_{i+1} U_i = U_i \quad \text{for } i = 1, 2, \dots, 2n - 2 \quad (4.9)$$

$$U_i U_j U_i = U_j \quad \text{for } |i - j| > 1 \quad (4.10)$$

The first property entails that it is possible to define a projection operator associated to  $U_i$ , in fact if we choose  $U'_i = \frac{1}{\sqrt{q}} U_i$  we have the idempotence requirement satisfied. The second and third equations define the special composition rules between operators with indices  $j = i \pm 1$ , whereas the last one states that operators that do not correspond to nearest-neighbouring positions commute among themselves.

We can employ these two sets of operators to express the two transfer matrices, namely:

$$V = \exp \left[ K_1 \frac{1}{\sqrt{q}} \sum_{i=1}^{n-1} U_{2i} \right] \quad (4.11)$$

$$W = \prod_{j=1}^n [v_2 \mathbb{I} + \sqrt{q} U_{2j-1}] \quad (4.12)$$

where  $v_2 = e^{K_2} - 1$ .

There is also an alternative form that exchanges the roles played by the two matrices, making the expression of  $W$  become especially simple this time. That is:

$$V = \prod_{j=1}^{n-1} \left[ \mathbb{I} + v_1 \frac{1}{\sqrt{q}} U_{2j} \right] \quad (4.13)$$

$$W = v_2^n \exp \left[ K_2^* \frac{1}{\sqrt{q}} \sum_{i=1}^n U_{2i-1} \right] \quad (4.14)$$

where  $v_1 = e^{K_1} - 1$ .  $K_2^*$  is the dual lattice coupling constant which can be related to  $K_2$  through following relation:

$$\frac{q}{v} = v^* \equiv e^{K^*} - 1 \quad \Leftrightarrow \quad e^{K^*} = \frac{e^K - 1 + q}{e^K - 1} \quad (4.15)$$

Now, we want to find the **one-dimensional quantum model** linked to the classical Potts model we have just depicted. We need to focus on the transfer matrix of the statistical model because it is the one element that connects the statistical  $d$ -dimensional model to a  $(d - 1)$ -dimensional quantum one.

The first thing to do is imposing periodic boundary condition on one of the two lattice directions, which is going to be turned into a continuous variable and interpreted as the euclidean time for the quantum model to be defined. Periodicity along the vertical direction means that we must add one more  $W$  matrix at the expression for  $\mathcal{Z}_N$  linking the highest row to the lowest one and take the trace over the  $(q^n \times q^n)$ -dimensional space. The formulation (4.13) and (4.12) of the row-to-row transfer matrices  $V$  and  $W$  as products are particularly convenient in order to write the partition function in the following form:

$$\begin{aligned} \mathcal{Z}_N &= \text{Tr}[VWVWVW\dots VWVW] = \text{Tr}[(VW)^m] = \\ &= \left( \prod_{j=1}^n (\mathbb{I} + v_1 \frac{1}{\sqrt{q}} U_{2j}) (v_2 \mathbb{I} + \sqrt{q} U_{2j-1}) \right)^m \end{aligned} \quad (4.16)$$

This allows us to find the critical point of the model, exploiting its self-duality property, i.e. a phase transition, which means that a singularity

occurs in the thermodynamic limit, must be at a fixed point of the duality transformation, otherwise singular points would be mapped into non-singular ones simply switching to the dual coupling. Thus, evaluating the free energy per site in the thermodynamic limit:

$$f(v_1, v_2) = - \lim_{N \rightarrow \infty} \frac{1}{N} \log \mathcal{Z}_N$$

with  $N = nm$ , we get an easy way to the determination of the critical value for the coupling. Mapping the odd sites into even ones, the Temperley-Lieb algebra of operators  $U_i$  is unaffected, therefore we may write the following relation, uncaring of the contingent boundary terms which conveniently disappear in the thermodynamic limit:

$$\lim_{N \rightarrow \infty} \frac{1}{N} \log \mathcal{Z}_N(v_1, v_2) = \lim_{N \rightarrow \infty} \frac{1}{N} \log \mathcal{Z}_N \left( \frac{q}{v_1}, \frac{q}{v_2} \right) + \lim_{N \rightarrow \infty} \frac{1}{N} \log \left( \frac{v_1 v_2}{q} \right)^{nm} \quad (4.17)$$

Hence:

$$f(v_1, v_2) = f(v_1^*, v_2^*) - \log \left( \frac{v_1 v_2}{q} \right) \quad (4.18)$$

Since the system is critical only at fixed points of the dual transformation, we have to fix the additive term to be null, thus:

$$(e^{K_1 c} - 1)(e^{K_2 c} - 1) = q \quad (4.19)$$

If the coupling constants along two axis are different, there is a transition line in the parameters phase diagram. However, the simple case of an isotropic model, can be solved right away and we find the expression for the critical temperature of the phase transition point of the  $q$ -state Potts model [25]:

$$K_c = \frac{J}{T_c} = \log(\sqrt{q} + 1) \quad (4.20)$$

For high temperatures,  $T > T_c \rightarrow K < K_c$  the system is found in a disordered phase, while for low temperatures,  $T < T_c \rightarrow K > K_c$  the system arrange in an ordered configuration. The transition is of the first order for  $q > 4$ , whereas the  $q = 2, 3, 4$  state Potts models display a continuous phase transition and can thus be described near criticality by means of two-dimensional conformal field theories.

Let's go back now to the determination of the quantum Hamiltonian arising from the statistical Potts model. It will be more convenient to choose now the exponential form of the representations of the operators of the Temperley-Lieb algebra (4.11) and (4.14). The transfer matrix, which should be interpreted as an evolution operator for the quantum Hamiltonian we are going to find, is found to have the following expression:

$$T = VW \sim \exp \left[ K_1 \frac{1}{\sqrt{q}} \sum_{i=1}^{n-1} U_{2i} \right] \exp \left[ K_2^* \frac{1}{\sqrt{q}} \sum_{i=1}^n U_{2i-1} \right] \quad (4.21)$$

As lattice anisotropies become irrelevant at the critical point, we are allowed to make the vertical lattice direction continuous reducing to zero the lattice spacing representing the euclidean time for the quantum model. Finally, we take the logarithmic derivative with respect to this variable and we get the one-dimensional quantum Hamiltonian we look for:

$$\mathcal{H}_{q\text{-states}}^{\text{Potts}}(n, K_1, K_2) = -K_1 \frac{1}{\sqrt{q}} \sum_{i=1}^{n-1} U_{2i} - K_2^* \frac{1}{\sqrt{q}} \sum_{i=1}^n U_{2i-1} \quad (4.22)$$

This expression has been inferred at the critical point, given by the relation  $v_1 v_2 = (e^{K_1} - 1)(e^{K_2} - 1) = q$ , but may be interpreted as defining a non-critical model for different values of the couplings, which can be effectively summed up by just one coupling constant, named  $\lambda$ . However, as far as the mapping of the pure-biquadratic Hamiltonian is concerned we can restrict ourselves to the isotropic case  $K_1 = K_2$  at the critical point, identified by the value  $\lambda = 1$ .

We may also write the operators  $U_i$  in terms of a whole new set of operators, namely  $\Omega$  and  $R$ :

$$U_{2i-1} = \frac{1}{\sqrt{q}} \sum_{k=0}^{q-1} \Omega_i^k \quad \text{and} \quad U_{2i} = \frac{1}{\sqrt{q}} \sum_{k=0}^{q-1} R_i^k R_{i+1}^{q-k}$$

which obey a  $Z_q$  algebra, as we will see later on. Now, we display an explicit representations of these matrices [37] in the basis where  $R$  is diagonal, i.e. the classical Potts basis. Setting  $\omega = e^{\frac{2\pi i}{q}}$ :

$$R = \begin{pmatrix} 1 & & & & \\ & \omega & & & \\ & & \omega^2 & & \\ & & & \ddots & \\ & & & & \omega^{q-1} \end{pmatrix} \quad \Omega = \begin{pmatrix} 0 & 1 & 0 & 0 & \cdots \\ 0 & 0 & 1 & 0 & \cdots \\ 0 & 0 & 0 & 1 & \cdots \\ \vdots & & & & \\ 1 & 0 & 0 & 0 & \cdots \end{pmatrix} \quad (4.23)$$

Eventually, we obtain the following quantum Hamiltonian for the  $q$ -state Potts model [2]:

$$\mathcal{H}_{q\text{-states}}^{\text{Potts}}(n, \lambda) = -\frac{\lambda}{q} \sum_{i=1}^{n-1} \sum_{k=1}^{q-1} R_i^k R_{i+1}^{q-k} - \frac{1}{q} \sum_{i=1}^n \sum_{k=1}^{q-1} \Omega_i^k \quad (4.24)$$

in which the summation on  $i$  runs over the sites of a single row of the two-dimensional lattice, which becomes the length of the chain for the quantum model. As we can see, the two sets of different transfer matrices yield two terms in the general  $q$ -state Potts Hamiltonian. The first one, given by

the even-index algebra, is representing the conventional Potts Hamiltonian, which gives an energy contribution of  $-\lambda$  whenever a couple of neighbouring sites on the chain is in the same state of the spin variable, otherwise its contribution is null. It may be written also in the simple form:

$$H^{Potts} = -\lambda \sum_{i=1}^{n-1} \delta(\omega_i - \omega_{i+1}) \quad (4.25)$$

where  $\omega$  is the corresponding eigenstate of the  $R$  matrix, and  $\delta$  is the Kronecker delta previously defined.

The second term can be thought as a transverse field, its elements being  $\Omega_{\omega\omega'} = \delta_{\omega,\omega'+1}$ , which shifts the Potts indices by one, transforming an eigenstate into a linear combination of the others. Alternatively, one can diagonalise the field term and as a consequence the Potts term will result non-diagonal.

## 4.2 Fermionic formulation of $SU(3)$ Heisenberg Hamiltonian

The  $SU(3)$ -invariant Hamiltonian which we introduced as a generalisation of the  $SU(2)$  Heisenberg chain in the form of a bilinear product between the group generators acting on nearest-neighbouring sites:

$$\mathcal{H}^{SU(3)}(J) = J \sum_{i=1}^N \sum_{\alpha=1}^8 \lambda_i^\alpha \lambda_{i+1}^\alpha, \quad (4.26)$$

can effectively be expressed by means of a useful alternative formulation that allows us to prove some of its properties, as we will show later, in a straightforward manner. The Hamiltonian (4.26) or its twin form with alternate conjugated representations on even and odd sites (3.48) may be turned into a peculiar form of a **fermionic system** with a constraint on the number of fermions. For a better understanding of this approach, let's consider at first the simpler case of  $SU(2)$ . The Heisenberg Hamiltonian is:

$$\mathcal{H}_{SU(2)}^{Heis}(-J) = -\frac{J}{2} \sum_{i=1}^N (S_i^+ S_{i+1}^- + S_i^- S_{i+1}^+ + 2 S_i^z S_{i+1}^z) = -J \sum_{i=1}^N H_{i,i+1} \quad (4.27)$$

where  $S = \frac{1}{2}\sigma^\alpha$ ,  $\sigma^\alpha$  being the conventional form of the Pauli matrices and  $\sigma^\pm = \sigma^+ \pm i\sigma^-$ . The remarkable property of this Hamiltonian is that it can be written in the form of either a permutation or an annihilation operator just shifting it by a constant. The permutation operator action is

$$(H_{i,i+1} + \frac{1}{4}) |\alpha\beta\rangle = \frac{1}{2} P_{\alpha\beta} |\alpha\beta\rangle = \frac{1}{2} |\beta\alpha\rangle \quad (4.28)$$

where  $P_{i,i+1}$  is the permutation operator acting on the sites  $i$  and  $i + 1$ .

We can get even the annihilation operator expression performing a particle-hole transformation on half the lattice sites. We conventionally choose even sites and denote this transformation by lowering the index,  $|\alpha\rangle \equiv \varepsilon_{\alpha\beta}|\beta\rangle$ . Thus, the action of the Hamiltonian on this newly defined basis is given by:

$$\left(\mathbf{H}_{i,i+1} + \frac{1}{4}\right)|^\alpha_\beta\rangle = -\frac{1}{2}\delta_\beta^\alpha|\gamma_\gamma\rangle \quad (4.29)$$

Now we can write for both the first and the second action of the Heisenberg Hamiltonian a new expression in terms of fermionic creation and annihilation operators,  $(\psi^\dagger)^\alpha$  and  $\psi_\alpha$  respectively. These operators are conventionally associated to electrons, while holes have their own creation and annihilation operators,  $(\psi^\dagger)_\alpha$  and  $\psi^\alpha$ , respectively. The particle-hole transformation is, of course, given by the substitution  $(\psi_{2i})_\alpha \rightarrow (\psi_{2i}^\dagger)_\alpha$  on even sites. The permutation form of the Hamiltonian:

$$\left(\mathbf{H}_{i,i+1} + \frac{1}{4}\right) = \frac{1}{2}(\psi_i^\dagger)^\alpha(\psi_i)_\beta(\psi_{i+1}^\dagger)^\beta(\psi_{i+1})_\alpha \quad (4.30)$$

commutes a couple of electrons, whereas the annihilation Hamiltonian:

$$\left(\mathbf{H}_{i,i+1} + \frac{1}{4}\right) = -\frac{1}{2}(\psi_i^\dagger)^\alpha(\psi_i)_\beta(\psi_{i+1}^\dagger)_\alpha(\psi_{i+1})^\beta \quad (4.31)$$

destroys a particle-hole couple with the same spin value and recreates a new pair with the same value of spin. The identification of these fermionic Hamiltonians with the  $SU(2)$ -symmetric Heisenberg Hamiltonian works only with an additional constraint, that is given by the demand that *the number of fermions species on each site is bound to be 1*.

This formulation can be generalised to  $SU(n)$  models, for which the spin values can take on  $n$  different values. The two previously described models, however are not equivalent for the general cases with  $n > 2$ . This is due to the fact that the permutation Hamiltonian acts on a state basis with a particle-particle interpretation, i.e. particles are located both on even and on odd sites; on the contrary, the annihilation Hamiltonian acts on a state basis with a particle-hole interpretation, i.e. particles are located on odd sites and holes are located on even sites (one hole corresponding to  $n - 1$  particles).

This generalised models have to be considered as spin- $S$  models, (related to  $n$  through the relation  $n = 2S + 1$ ) for which the Hamiltonian is endowed with a  $SU(n)$ -symmetry property. In the particle-hole case, which is the one we are interested in, the Hamiltonian may be expressed as a sum of projection operators on the singlet state of couples of two neighbouring spins:

$$\mathcal{H}_{SU(n)}^{Heis}(-J) = -J \sum_{i=1}^N \hat{P}_0(\vec{S}_i + \vec{S}_{i+1}) \quad (4.32)$$

where the projection operator is (modulo an additive constant):

$$\hat{P}_0(\vec{S}_i + \vec{S}_{i+1}) = \prod_{j=1}^{2s} \left( 1 - \frac{(\vec{S}_i + \vec{S}_{i+1})^2}{j(j+1)} \right) \quad (4.33)$$

Let's now draw our attention to the case  $n = 3$ , meaning that we are dealing with spin  $S = 1$  operators, which yields the  $SU(3)$ -symmetric biquadratic Hamiltonian, that can take the form of a sum of projection operators on the singlet state of neighbouring sites. A simple evaluation of the formula (4.33), leads to the straightforward identification of this model with the spin-1 pure biquadratic model:

$$\mathcal{H}_{SU(3)}^{Heis}(-J) = \mathcal{H}^{biQ}(-J) = -J \sum_{i=1}^N (\vec{S}_i \cdot \vec{S}_{i+1})^2 + const \quad (4.34)$$

Since we are dealing with singlet projection of pairs of states it is convenient to shift to the valence-bond basis. This peculiar basis, particularly useful in some circumstances, for example in order to solve exactly the AKLT model (1.21), appears immediately clear in a pictorial representation. It basically shows the valence bonds connecting the sites of the chain with suitable links. Different values of the eigenvalue of the total spin  $S_{tot}$  of the couple of spin are marked with different traits, round for the singlet ( $S_{tot} = 0$ ), square for the triplet ( $S_{tot} = 1$ ) and none for the quintet ( $S_{tot} = 2$ ). Here, we will restrict ourselves only to singlet bonds, because they are the only relevant ones in the analysis of the ground state of antiferromagnetic system, which belongs to the  $S_{tot}^z = 0$  sector and has  $S_{tot}^2 = 0$ , too.

In the valence-bond basis it is easy to represent a global singlet of the system. We should contract couples of spins forming singlet bonds among them. There are, indeed, many allowed combinations, but only one is the system ground state, as long as the size of the chain stays finite. We can see it by taking under consideration the action of the Hamiltonian (4.31) on the valence-bond basis, which is usually conveniently normalised to obtain:

$$\mathbb{H}_{i,i+1} |\alpha \beta\rangle = -\frac{1}{n} \delta_{\alpha \beta} |\gamma \gamma\rangle \quad (4.35)$$

Thus, each state formed by pair of sites linked by a valence bond is an eigenstate of the Hamiltonian, with eigenvalue 1,

$$\mathbb{H}_{i,i+1} |\alpha \alpha\rangle = -|\alpha \alpha\rangle \quad (4.36)$$

whereas the action on a link not containing a valence bond is given by:

$$\mathbb{H}_{2,3} |\alpha \alpha \beta \beta\rangle = -\frac{1}{n} |\alpha \beta \beta \alpha\rangle \quad (4.37)$$

which means that, once the valence bonds connecting the sites 2 and 3 with other sites are broken, we build a new valence-bond between them and then connect the two left-out states.

$$\begin{aligned}
 H(\text{---}) &= -(\text{---}) \\
 H_{23}(\text{---}\text{---}) &= (-1/n) \left( \overset{\text{---}}{\text{---}} \right)
 \end{aligned}$$

**Figure 4.2:** Action of the  $SU(n)$  Hamiltonian in its fermionic formulation on generic state expressed in the valence-bond basis. The Hamiltonian acts on couples of neighbouring sites, which may or may not be linked by a valence bond. The first case, refers to the action on a state containing a valence bond, which is an eigenstate of the Hamiltonian with eigenvalue  $-1$ . The second one shows the action of the Hamiltonian on a pair of sites not connected by a valence-bond. In this case, the state is not an eigenstate because it is transformed into an other kind of state through the destruction and recreation of two valence-bonds, in order to build the valence-bond connecting the two sites on which the Hamiltonian is operating. (Picture taken from [2]).

The equations (4.36) and (4.37) completely define the action of the Hamiltonian on a generic state expressed in the valence-bond basis. We have already mentioned that there is one further constraint we need to impose on the system of fermions in order to make it behave exactly in the same manner as the spin-1 Hamiltonian. That is, since a spin-1 chain is made up of a group of localised variables each one attached to its site, we need to make sure that the same occurs in the fermionic system too. Therefore, we should add a suitable device to make sure that we restrict the number of fermion species on each locus to one. If the number of electrons is bound to one on odd sites, the same should happen to holes on even sites.

The formerly discussed **constraint** takes the following form:

$$(\psi_i^\dagger)^\alpha (\psi_i)_\beta (\psi_i^\dagger)^\gamma (\psi_i)_\delta = \delta^\gamma_\beta (\psi_i^\dagger)^\alpha (\psi_i)_\delta \quad (4.38)$$

The general  $SU(n)$ -symmetric Hamiltonian for the alternate fermion-hole representation with open boundary conditions in the fermionic representation becomes:

$$\begin{aligned}
 \mathcal{H}_{SU(n)} &= -\frac{1}{n} \sum_{i=1}^{N/2} (\psi_{2i-1}^\dagger)^\alpha (\psi_{2i-1})_\beta (\psi_{2i}^\dagger)_\alpha (\psi_{2i})^\beta + \\
 &\quad -\frac{\lambda}{n} \sum_{i=1}^{N/2-1} (\psi_{2i}^\dagger)_\alpha (\psi_{2i})^\beta (\psi_{2i+1}^\dagger)^\alpha (\psi_{2i+1})_\beta
 \end{aligned} \quad (4.39)$$

Working with the valence-bond basis it is easy to see that as  $n$  increases so does the the tendency of the system to spontaneously dimerise. This

happens because the contribution of the valence-bond breaking term (4.37) of the Hamiltonian become less important as  $n \rightarrow \infty$ , as its amplitude has a  $\frac{1}{n}$  behaviour. Therefore, the dimerised state, in which odd-even pairs of neighbouring sites connecting  $2i - 1$  to  $2i$  with a singlet bond create  $N/2$  alternate bonds on the  $N$  allowed lattice spaces of the chain, is the exact ground state in the large  $n$  limit. The lowest energy configuration is thus the following one, with contributions coming just from the valence-bonds:

$$\mathcal{H}_{SU(n)}^{Heis} |\alpha \ \beta \ \beta \ \gamma \ \gamma \ \dots\rangle = \sum_{i=1}^N \mathbb{H}_{i,i+1} |\alpha \ \beta \ \beta \ \gamma \ \gamma \ \dots\rangle = -\frac{N}{2} |\alpha \ \beta \ \beta \ \gamma \ \gamma \ \dots\rangle \quad (4.40)$$

In fact, all off-diagonal terms contributions in the Hamiltonian operators are of order  $O(\frac{1}{n})$ . The other singlet states with non-nearest neighbour bonds have an energy gap of  $1 + O(\frac{1}{n})$  and non-singlet states, with missing bonds (uncontracted indices) have at least an equal gap.

Reminding that we keep on working with periodic boundary conditions, in the infinite volume limit, if we impose on the system periodic boundary conditions, the ground state becomes doubly degenerate, because there are two equally probable configurations connected one to another by a translation of all bonds by one lattice constant.

### 4.3 Correspondence between the Potts model and the biquadratic Hamiltonian

The whole purpose of the interpretation in terms of fermionic operators of the pure-biquadratic Hamiltonian was to exploit this formulation to prove the equivalence between the former and the quantum version of the nine-state Potts model. The Hamiltonian version of the latter should be possible only at the critical point, defined by (4.20). However, uncaring of the lattice anisotropy, we could take the continuum limit in one of the two dimensions of the rectangular two-dimensional lattice of the statistical model depicted in section 4.1. Identifying this direction with the time axis, we get the one-dimensional quantum Hamiltonian of the  $q$ -state Potts model near the critical point, which has the following expression:

$$\mathcal{H}_{q\text{-states}}^{Potts}(L, \lambda) = -\frac{\lambda}{q} \sum_{i=1}^{L-1} \sum_{k=1}^{q-1} R_i^k R_{i+1}^{q-k} - \frac{1}{q} \sum_{i=1}^L \sum_{k=1}^{q-1} \Omega_i^k \quad (4.41)$$

for which the critical point corresponds to the critical value of the parameter  $\lambda = 1$ .

We are now on the edge of showing that the biquadratic Hamiltonian may be written in an identical form thanks to the realisation that we can

build a Temperley-Lieb algebra of its operators too. Let us start from the Hamiltonian in the most general form:

$$\mathcal{H}^{biQ}(-J) = -J \sum_{i=1}^{N-1} \epsilon_i (\vec{S}_i \cdot \vec{S}_{i+1})^2 = -J \left[ \sum_{i=1}^{N-1} \epsilon_i (h_i + 1) \right] \quad (4.42)$$

where  $\epsilon_i$  takes different values on even and odd sites, namely  $\epsilon_{2i+1} = 1$  and  $\epsilon_{2i} = \lambda$ , as a measure of the dimerisation tendency of the system. There is one other significant difference from the conventional form of the Hamiltonian used so far: there is in fact one less term in the summation over all sites, due to the choice to deal with open boundary conditions, i.e.  $\vec{S}_{N+1} = 0$ .

We stated previously that the operators  $h_i$  satisfy the relation  $h_i^2 = 3h_i$ . This is just one of the characteristic features of the operators  $h_i$ . It may be shown that they fulfill all the requirements of the Temperley-Lieb algebra definition, namely:

$$h_i^2 = 3h_i \quad \text{for } i = 1, 2, \dots, N \quad (4.43)$$

$$h_i h_{i-1} h_i = h_i \quad \text{for } i = 2, 3, \dots, N \quad (4.44)$$

$$h_i h_{i+1} h_i = h_i \quad \text{for } i = 1, 2, \dots, N-1 \quad (4.45)$$

$$h_i h_j h_i = h_j \quad \text{for } |i - j| > 1 \quad (4.46)$$

which resemble exactly the relations (4.7), (4.8), (4.9) and (4.10) with  $\sqrt{q} = 3$  and  $2n = N$ . These are the first signals that the pure biquadratic spin-1 Hamiltonian may be connected to a *Potts model with  $q = 9$  states defined on a chain of half the length* of the biquadratic one.

Right now, let's proceed by proving that these relations, in fact, hold. It will be really easy to achieve our goal if we make use of the newly introduced representation in terms of fermionic operators. It should be noticed that the  $h_i$  operators are not different from the operators:

$$\mathbf{H}_{i,i+1} = -\frac{1}{3} (\psi_i^\dagger)^\alpha (\psi_i)_\beta (\psi_{i+1}^\dagger)_\alpha (\psi_{i+1})^\beta \quad (4.47)$$

which act according to (4.35) for  $n = 3$ , which means  $S = 1$ . We can start with the first relation, which we can, by the way, check out even from its explicit representation (2.31). Making extensive use of the constraint of one

particle (or hole) per site (4.38), we get:

$$\begin{aligned}
h_i^2 &= \frac{1}{9} \left( (\psi_i^\dagger)^\alpha (\psi_i)_\beta (\psi_{i+1}^\dagger)_\alpha (\psi_{i+1})^\beta \right) \left( (\psi_i^\dagger)^\gamma (\psi_i)_\delta (\psi_{i+1}^\dagger)_\gamma (\psi_{i+1})^\delta \right) = \\
&= \frac{1}{9} \left( (\psi_i^\dagger)^\alpha (\psi_i)_\beta (\psi_i^\dagger)_\gamma (\psi_i)^\delta \right) \left( (\psi_{i+1}^\dagger)^\alpha (\psi_{i+1})_\beta (\psi_{i+1}^\dagger)_\gamma (\psi_{i+1})^\delta \right) = \\
&= \frac{1}{9} \left( \delta^\gamma_\beta (\psi_i^\dagger)^\alpha (\psi_i)_\delta \right) \left( \delta^\beta_\gamma (\psi_{i+1}^\dagger)_\alpha (\psi_{i+1})^\delta \right) = \\
&= 3 \frac{1}{9} (\psi_i^\dagger)^\alpha (\psi_i)_\delta (\psi_{i+1}^\dagger)_\alpha (\psi_{i+1})^\delta = 3 h_i
\end{aligned} \tag{4.48}$$

Let's deal with the second and third relation, which may be treated exactly in the same way:

$$\begin{aligned}
h_i h_{i+1} h_i &= - \frac{1}{27} \left( (\psi_i^\dagger)^\alpha (\psi_i)_\beta (\psi_{i+1}^\dagger)_\alpha (\psi_{i+1})^\beta \right) \left( (\psi_{i+1}^\dagger)_\gamma (\psi_{i+1})^\delta (\psi_{i+2}^\dagger)_\gamma (\psi_{i+2})^\delta \right) \\
&\quad \left( (\psi_i^\dagger)^\varepsilon (\psi_i)_\eta (\psi_{i+1}^\dagger)_\varepsilon (\psi_{i+1})^\eta \right) = \\
&= - \frac{1}{27} \left( \delta_\beta^\varepsilon (\psi_i^\dagger)^\alpha (\psi_i)_\nu \right) \left( \delta^\delta_\varepsilon \delta^\beta_\gamma (\psi_{i+1}^\dagger)_\alpha (\psi_{i+1})^\nu \right) \left( (\psi_{i+2}^\dagger)_\gamma (\psi_{i+2})^\delta \right) = \\
&= - 3 \frac{1}{27} \left( (\psi_i^\dagger)^\alpha (\psi_i)_\nu \right) \left( (\psi_{i+1}^\dagger)_\alpha (\psi_{i+1})^\nu \right) \left( (\psi_{i+2}^\dagger)_\gamma (\psi_{i+2})^\gamma \right) = \\
&= - \frac{1}{3} \left( (\psi_i^\dagger)^\alpha (\psi_i)_\nu (\psi_{i+1}^\dagger)_\alpha (\psi_{i+1})^\nu \right) = h_i
\end{aligned} \tag{4.49}$$

Eventually, the third relation it is clearly inferred from the former one: if there are fermionic operators involved with two or more lattice sites of distance, they obviously have not any common indices, thus they all commute among themselves.

Once the properties of the Temperley-Lieb algebra have been proved, we may connect the spin operators  $h_i$  to the odd and even algebras of the corresponding Potts model. We will finally reach a formulation of the biquadratic Hamiltonian equivalent to the nine-state Potts model. It is sufficient to make the identifications  $h_i = H_{i,i+1} = U_i$  for  $i = 1, 2, \dots, 2n (= N)$ .

According to [9], we should define the two usual odd and even algebras of the Potts model employing the  $h_i = U_i$  operators, which are divided in two classes:

$$h_{2i-1} = \frac{1}{\sqrt{q}} \sum_{k=0}^{q-1} \Omega_i^k \quad \text{and} \quad h_{2i} = \frac{1}{\sqrt{q}} \sum_{k=0}^{q-1} R_i^k R_{i+1}^{q-k} \tag{4.50}$$

with  $i = 1, 2, \dots, N/2$  for the odd part of the algebra and  $i = 1, 2, \dots, N/2 - 1$  for the even part of the algebra. This distinction is due to the fact that we chose to work in the open boundary conditions framework (thus,  $h_N = 0$ ), which makes easier the proof of the equivalence between the two models under examination.

These new sets of operators on each site form a  $Z_q$  algebra, with the following commutation rules:

$$\Omega_i R_i = \omega^{-1} R_i \Omega_i \quad , \quad \Omega_i R_i^\dagger = \omega R_i^\dagger \Omega_i \quad \text{and} \quad \Omega_i^q = R_i^q = 1 \quad (4.51)$$

where we have defined  $\omega = e^{\frac{2\pi i}{q}}$ .

Now, from the comparison between the relation (4.43) on the square of the  $h_i$  operators and the general property (4.7), we realise that  $q = 9$ , thus the biquadratic Hamiltonian turns out to be related to a nine-state Potts model, with its odd- and even-site operators obeying the Temperley-Lieb algebra. Therefore, making use of the substitutions (4.50), we can write:

$$\begin{aligned} \frac{1}{J} \mathcal{H}^{biQ}(-J) &= - \sum_{i=1}^{N-1} \epsilon_i (h_i + 1) = \\ &= - \left( \sum_{i=1}^{N/2} h_{2i-1} + \lambda \sum_{i=1}^{N/2-1} h_{2i} + \frac{1}{2}N + \lambda(\frac{1}{2}N - 1) \right) = \\ &= - \left( \frac{1}{\sqrt{q}} \sum_{i=1}^L \sum_{k=0}^{q-1} \Omega_i^k + \frac{1}{\sqrt{q}} \lambda \sum_{i=1}^{L-1} \sum_{k=0}^{q-1} R_i^k R_{i+1}^{q-k} + L + \lambda(L-1) \right) = \\ &= - \left( \frac{1}{3} \sum_{i=1}^L \sum_{k=1}^8 \Omega_i^k + \frac{1}{3} \lambda \sum_{i=1}^{L-1} \sum_{k=1}^8 R_i^k R_{i+1}^{9-k} + \frac{4}{3}L + \frac{4}{3}\lambda(L-1) \right) = \\ &= 3\mathcal{H}_{9\text{-states}}^{Potts}(L, \lambda) - \frac{4}{3}L - \frac{4}{3}\lambda(L-1) \end{aligned} \quad (4.52)$$

where in the third line we defined  $L = N/2$  and in the fourth line we used the properties of the  $Z_9$  algebra, according to which  $\Omega^9 = R^9 = 1$ . We have thus shown that there is indeed an **equivalence** between the spin-1 antiferromagnetic pure biquadratic model and the **one-dimensional quantum Hamiltonian of the nine-state Potts model**. This correspondence holds thanks to the common underlying algebra of operators characterising both models, that is the Temperley-Lieb algebra, provided that we work under the premise of **open boundary conditions**.

Knowing that the spin-1 pure biquadratic model was also partially mapped into a spin-1/2 XXZ chain (see section 2.1 for further details), we may have a representation of the Temperley-Lieb algebra also in terms of the spin-1/2 operators, i.e the Pauli matrices. That is:

$$U_i = \frac{1}{2}(\sigma_i^x \sigma_{i+1}^x + \sigma_i^y \sigma_{i+1}^y) + \frac{1}{2} \cosh \theta (1 - \sigma_i^z \sigma_{i+1}^z) - \frac{1}{2} \sinh \theta (\sigma_i^z - \sigma_{i+1}^z) \quad (4.53)$$

where the correspondence with the Temperley-Lieb algebra (4.7), (4.8), (4.9) and (4.10) is recovered if we set  $2 \cosh \theta = \sqrt{q}$ . Hence we find that the biquadratic Hamiltonian with open boundary conditions is related to the

spin-1/2 XXZ model by the following equivalence relation. (For simplicity, we will restrict our calculation to the case  $\lambda = 1$ .)

$$\begin{aligned}
\frac{1}{J} \mathcal{H}^{biQ}(-J, N) &= - \sum_{i=1}^{N-1} U_i - (N-1) = \\
&= - \sum_{i=1}^{N-1} \left[ \frac{1}{2} (\sigma_i^x \sigma_{i+1}^x + \sigma_i^y \sigma_{i+1}^y) + \frac{1}{2} \cosh \theta (1 - \sigma_i^z \sigma_{i+1}^z) - \frac{1}{2} \sinh \theta (\sigma_i^z - \sigma_{i+1}^z) \right] + \\
&- (N-1) = \\
&= - \frac{1}{2} \sum_{i=1}^{N-1} [\sigma_i^x \sigma_{i+1}^x + \sigma_i^y \sigma_{i+1}^y - \cosh \theta \sigma_i^z \sigma_{i+1}^z] + \frac{1}{2} \sinh \theta (\sigma_1^z - \sigma_N^z) + \\
&- \left( 1 + \frac{\cosh \theta}{2} \right) (N-1)
\end{aligned} \tag{4.54}$$

Comparing the former expression to the conventional form of the spin-1/2 XXZ Hamiltonian:

$$\mathcal{H}^{XXZ}(J) = \frac{1}{2} J \sum_{i=1}^N [\sigma_i^x \sigma_{i+1}^x + \sigma_i^y \sigma_{i+1}^y + \Delta \sigma_i^z \sigma_{i+1}^z] \tag{4.55}$$

we realise that our spin-1 biquadratic Hamiltonian is equivalent to an antiferromagnetic model (negative coupling), defined on a chain of length  $N$ , with free ends (summation running to  $N-1$ ), its anisotropy parameter being  $\Delta = -\cosh \theta = -\frac{\sqrt{q}}{2} = -\frac{3}{2}$ . Furthermore, external fields of values  $\pm \frac{p}{2} = \pm \frac{\sinh \theta}{2} = \frac{\sqrt{5}}{2}$  are applied to the extremes of the chain. Therefore the correspondence we have established is:

$$\frac{1}{J} \mathcal{H}^{biQ}(-J, N) = \mathcal{H}_{spin-1/2}^{XXZ}(N, \Delta = \frac{3}{2}, \pm p = \pm \frac{\sqrt{5}}{2}) \tag{4.56}$$

This model was solved for the general case in [6] via the Bethe ansatz technique, which yields:

$$E^{XXZ} = -\frac{1}{2}(N-1)\Delta - 2 \sum_{j=1}^n (\cos k_j - \Delta) \tag{4.57}$$

with the quasi-momenta  $k_j$  bound to be solutions of the Bethe ansatz equations [9]:

$$k_j^{2N} = \prod_{l \neq j=1}^n \frac{S(k_l, k_j) S(k_l^{-1}, k_j)}{S(k_j, k_l) S(k_j, k_l^{-1})}, \quad j = 1, 2, \dots, n \tag{4.58}$$

where  $S(k_l, k_j) = 1 + 2\Delta k_j + k_j k_l$ .

From the explicit form of the energy eigenvalues and knowing the values of the parameters which allow the mapping, we can recover information both on the nine-state Potts model and on the spin-1 biquadratic Hamiltonian from which we started. All of the three are mapped one into another with elementary modifications, such as the introduction of a scaling factor and additive constants, which do not alter the spectrum of the model but simply shift and rescale it. Here is the complete equivalence:

$$\begin{aligned} H_{9\text{-states}}^{\text{Potts}}(L, \lambda = 1, \text{free ends}) &\sim \mathcal{H}_{\text{spin-1}}^{\text{biQ}}(2L, \lambda = 1, \text{free ends}) \sim \\ &\sim \mathcal{H}_{\text{spin-1/2}}^{\text{XXZ}}(2L, \Delta = \frac{3}{2}, \pm p = \pm \frac{\sqrt{5}}{2}) \end{aligned} \quad (4.59)$$

The allowed eigenvalues of the three models, are strictly related to the Temperley-Lieb algebra operators, therefore they must be the same set for all of the three models, however the degeneracies may not coincide due to the difference in the dimensions of the representations chosen for the same operator algebra. Both the spin-1 biquadratic and the nine-state Potts model have the same dimension of the Hilbert-space of states, namely  $3^{2L} \times 3^{2L}$  and  $9^L \times 9^L$  respectively, whereas the XXZ spin-1/2 model has a smaller space of states which is  $2^{2L} \times 2^{2L}$  dimensional. This matter has been previously discussed in section 2.4.

We stress once again the importance of the connection between the nine-state Potts model and the XXZ model, condensed in the relation  $\Delta = \cosh \theta = \frac{\sqrt{q}}{2}$ . From this point of view we may get an explanation of the different behaviour of the Potts model at phase transition point for  $q \leq 4$  and  $q > 4$ . In the former case, corresponding to  $0 < \cosh \theta \leq 1$ , in the XXZ interpretation of the model we are going toward the XX-like behaviour, which is located in the massless region of the phase diagram ( $-1 \leq \Delta < 0$ ); while in the latter case,  $\cosh \theta > 1$ , which means we are going towards an Ising anisotropy ( $\Delta < -1$ ) and we are in the gapped region of the phase diagram.

The nine-state Potts model shows a first order phase transition in the thermodynamic limit, which means that its related quantum Hamiltonian at the critical point  $\lambda = 1$  undergoes an ordered-disordered phase transition. In the low-temperature phase ( $\lambda > 1$ ) the ground state is supposed to be nine-fold degenerate. However, when dealing with finite size chains, the symmetry is partially broken resulting in a splitting of the eigenvalues in a two sectors, distinguished by the eigenvalues of  $\Omega$  [9]. The value  $\omega = 0$  is singled out and the eight left eigenvalues remain still degenerate. This  $8 + 1$  splitting reminds us of the  $SU(3)$  multiplet structure of the lowest eigenstates of the biquadratic Hamiltonian which presents a singlet and an octet representation as its lowest energy states (open boundary conditions). Hence, for the nine-state Potts model ( $q > 4$ ) there is a gap between the ground and the first excited state, which is consistent with the fact that the

pure biquadratic Hamiltonian is located in a gapped region of the bilinear-biquadratic phase diagram (fig. 1.1).

This discussion may be extended to encompass even the generic  $SU(n)$ -symmetric system in its fermionic formulation (4.39). The equivalence with the  $q$ -state Potts model is obvious for the  $n$  case too, since the fermion operators were shown to be fulfilling the Temperley-Lieb algebra rules, with  $n = \sqrt{q}$ . For  $q > 4$ , which means  $n > 2$  the first order phase transition guarantees that there are two distinct but coexisting ground states, one ordered and one disordered, which can be mapped one into the other at the critical point ( $\lambda = 1$ ). Therefore, for  $n > 2$  in the infinite volume limit, the ground state is going to be doubly-degenerate meaning that the system is spontaneously dimerised, with its translational symmetry broken.

This does not occur for the case  $n \leq 2$ , i.e.  $q \leq 4$ , because the phase transition is now continuous and the ground state is unique. This behaviour is confirmed by the  $SU(2)$  chain, which is the usual spin-1/2 Heisenberg model, solvable via the Bethe ansatz and having an undimerised and translationally invariant ground state with a zero energy gap [40].

Concluding, it is important to recall that the equivalence of the spin-1 biquadratic Hamiltonian with the Potts model is strictly connected to the choice of **free ends** for both models, which leads to a correspondence with the spin-1/2 XXZ chain previously described, having two opposite external fields applied to the extremes. This might be a problem because in the previous chapters we focused our discussion on periodic boundary conditions only and there is no guarantee that changing the conditions at the extremes would not affect the behaviour of the model.

In particular, choosing periodic boundary conditions in this case leads to a different version of the XXZ spin chain with a defect seam (yielding twisted boundary conditions), which is much more complicated to solve with the Bethe ansatz. As long as the system size remains finite the gap of the biquadratic Hamiltonian is also affected. However, while approaching the thermodynamic limit the discrepancy introduced by the change of boundary conditions must become irrelevant. This statement [9] appears to be confirmed by numerical results, which means that the gap of the biquadratic spin-1 chain in the thermodynamic limit is precisely given by the gap of the spin-1/2 XXZ chain in the thermodynamic limit calculated in [16].

#### 4.4 $q$ -state vertex models correspondence with the biquadratic Hamiltonian

A different approach to the correspondence between the spin-1 pure biquadratic model and the Potts model was proposed by Klumper [27, 28]. In order to connect this equivalence to the others previously examined we need one further passage, that is the the discovered correspondence between

$q$ -state vertex models and  $q^2$ -state Potts models [34]. Having this knowledge at our hand, we now expect the biquadratic model to be equivalent to a **three-state vertex model**. In order to prove that this statement holds we give a brief overview of the demonstration outlined by Klumper, which requires indeed a very intense computational effort. The model under investigation is a bidimensional square lattice model, on each vertex of which a spin variable is located. The variables are allowed to take on  $q$  different values and the energy configuration of the system is determined by mutual interactions among them. We start our discussion from a general  $q$ -state vertex model with only four kinds of vertices allowed.

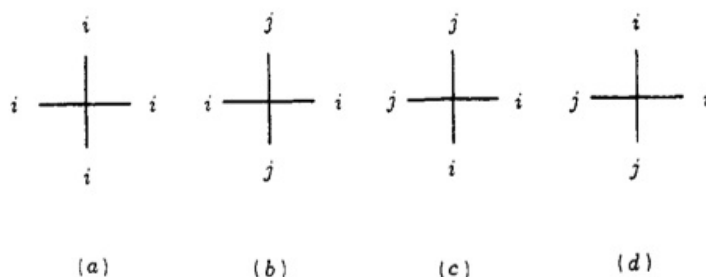


**Figure 4.3:** Graphical representation of the general four types of vertices taken under consideration in the analysis of the  $q$ -state vertex model. Each of them is associated with its related Boltzmann weight, namely  $a, b, c$  and  $d$ . (Picture taken from [27]).

First, we should solve the Yang-Baxter equations for the weights related to each vertex. Some of the families of possible exact solutions were found and are listed in [33]. It is important to say that the solutions change their form and number of free parameters according to the number of possible values  $q$  for the spin variable at each site. We consider just three types of solutions for the Boltzmann weights  $a, b, c, d$  respectively associated to the four vertices of the former picture.

First family:

$$a = 1 \quad b = 0 \quad c = \frac{\omega z + 1 - \omega}{z + 0} \quad d = \frac{(1 - \omega)z + \omega}{z + 1} \quad (4.60)$$

where  $\omega$  was defined by  $\omega = \frac{1}{2} \left( 1 + \sqrt{\frac{q+2}{q-2}} \right)$  and  $z$  is parametrised by means of the spectral variable  $v = \exp(v \log \alpha)$  and  $\alpha = \left( \frac{\omega}{\omega-1} \right)^2$

Second family:

$$a = 1 - \frac{q-2}{2} \left( \frac{1}{4} - v^2 \right) \quad b = \pm \frac{q-2}{2} \left( \frac{1}{4} - v^2 \right) \quad c = \frac{1}{2} + v \quad d = \frac{1}{2} - v \quad (4.61)$$

Third family:

$$a = 1 \quad b = 0 \quad c = \frac{\sqrt{q-1}z-1}{q-2} \quad d = \frac{\sqrt{q-1}z^{-1}-1}{q-2} \quad (4.62)$$

where  $z = \exp(v \log(q-1))$

The symmetry of the transfer matrices in the cases one and two (with minus sign) is  $SO(q)$ , while for the other cases the maximal symmetry is trivially the identity.

Once we have found these parametrised families of solutions for the Boltzmann weights, we need to find the explicit expression of the row-to-row transfer matrix. This operation was performed thanks to some useful symmetry properties of the transfer matrix:

- **symmetry relation:**  $T^\dagger(v) = T(-v^*) \rightarrow \Lambda^*(v) = \Lambda(-v^*)$
- **commutativity:**  $T(v)T(v') = T(v')T(v)$
- **inversion relation:**  $T(v)T(v+1) = \phi(v)^N \mathbb{I} + O(e^{-N}) \rightarrow \Lambda(v)\Lambda(v+1) = \phi(v)^N + O(e^{-N})$

The third and most important property strictly holds just for the points  $v = \pm \frac{1}{2}$ , for which the transfer matrix becomes basically the right or left shift operator. Since these matrices are inverse one of the other, we are allowed to write the inversion relation and we expect it to hold also in the neighbourhood of those points.

Then, we should proceed by computing the function  $\phi$  for the three different families, each one having its own characteristic expression, and exploiting the inversion relation, we may finally be able to find the partition function per site. We should pay attention to the analytical properties of the functions we are dealing with. They have to be meromorphic in the analytical region, i.e.  $-\frac{1}{2} \leq \Re(v) \leq \frac{1}{2}$ , and must satisfy required periodicity or asymptotic behaviour to be well defined. We can then use an ansatz for the partition function based on the previously mentioned properties and finally get its explicit form exploiting the inversion relation.

We have to turn the statistical  $q$ -state vertex model into a one-dimensional quantum model. This is done by taking the logarithmic derivative of the transfer matrix at the shift point ( $v = -\frac{1}{2}$ ), which ensures that the resulting Hamiltonian is a local operator, i.e. the usual sum over operators acting on pairs of neighbouring sites.

Eventually we obtain two remarkable Hamiltonian expressions for the two mentioned families endowed with more symmetry properties (1 and 2<sup>-</sup>). The first set of Boltzmann weights results in the following form:

$$\mathcal{H}^{(1)} = -\frac{2\omega-1}{q^2-4} \log \alpha \sum_{i=1}^N [(\vec{S}_i \cdot \vec{S}_{i+1})^2 - q + 1] \quad (4.63)$$

where  $\vec{S} = \{S^1, S^2, S^3\}$  are the generators of the group  $SO(q)$ . The maximal symmetry group of this Hamiltonian is, however,  $SL(q)$ , which is larger than  $SO(q)$  and contains also the special case  $SU(q)$ , that for  $\mathbf{q} = \mathbf{3}$  reproduces the  $SU(3)$  symmetry which we already know to characterise the **biquadratic model**.

Starting from the second one, choosing the minus sign and selecting the value  $\mathbf{q} = \mathbf{3}$ , we obtain a Hamiltonian reproducing exactly the **Takhtajan-Babujian model** (1.11):

$$\mathcal{H}^{(2^-)} = \frac{1}{2(q-2)} \sum_{i=1}^N [(q-2)^2(\vec{S}_i \cdot \vec{S}_{i+1}) + (q-4)(\vec{S}_i \cdot \vec{S}_{i+1})^2 + q] \quad (4.64)$$

This class of solutions is known to have a  $SO(q)$  maximal symmetry group, which is consistent with what we already know from the bilinear-biquadratic model at  $\Theta = \frac{\pi}{4}$  is not endowed with any more symmetry than the usual  $SU(2)$ .

## Chapter 5

# Two-site, four-site and six-site biquadratic Hamiltonian

In the former chapters we have worked to find a set of good quantum numbers for the biquadratic model both in its  $SU(2)$ -symmetric formulation, in terms of spin-1 operators, and in its  $SU(3)$ -symmetric one, with Gell-Mann matrices as group generators.

Now, it is about time to start a classification of the eigenstates according to these two different points of view. In the  $SU(2)$ -symmetric approach, we may label the eigenstates according to eigenvalue  $S_{tot}^z$ , which is the only good quantum number immediately available to classify the states obtained via the Bethe ansatz technique (see 2.3). In this framework states are, thus, labelled with a number of deviations from the ferromagnetic ground state (the fully aligned one), which is, in fact, the highest excited state for the pure-biquadratic antiferromagnetic model.

We have developed also a different approach exploiting the  $SU(3)$ -symmetry properties of the Heisenberg chain, which led to a fundamental equivalence:

$$\mathcal{H}^{F\otimes A}(J) = -2J \sum_{i=1}^N (\vec{S}_i \cdot \vec{S}_{i+1})^2 + \frac{8}{3} JN \quad (5.1)$$

provided  $S_{2i}^x \rightarrow -S_{2i}^x$  and  $S_{2i}^z \rightarrow -S_{2i}^z$

Relying on this equivalence, we realise that there may be two good quantum numbers for the biquadratic Hamiltonian, which we have proved to be endowed with a  $SU(3)$  symmetry. They are:

- the component of the total spin along the  $z$ -axis, that is

$$S_{tot}^z = \sum_{i=1}^N S_i^z \quad (5.2)$$

- the staggered sum over the square  $z$ -component of spin at each site, that is

$$(S^z)_{stag}^2 = \sum_{i=1}^N (-1)^{i+1} (S_i^z)^2 \quad (5.3)$$

## 5.1 Biquadratic Hamiltonian on a two-site chain

Let's now draw our attention to the simplest case of spin chain, that is a two-site model, which is of fundamental importance mainly because it is essentially the building block of the whole spin-1 chain. In fact, only **nearest-neighbour interactions** are considered, therefore the relevant non trivial pieces in the Kronecker product of spin-1 operators, building up the generic  $N$ -site chain are represented by the matrix of two-spin interaction. The composition by means of Kronecker product of three-dimensional representations leads quickly to a large-sized matrix representing the system Hamiltonian operator. The matter of highly increasing dimension of the Hilbert space of a chain spin-1 variables, which is given by the general expression  $d = 3^N$ , is easily circumvented for finite chains with a few sites, that is  $N = 2, 4, 6$  (since we are considering only even number of sites).

Let's focus, now, on the two-site problem, which can be dealt with even analytically, because we are working within a nine dimensional Hilbert space. Starting with the familiar form of the biquadratic Hamiltonian in terms of spin-1 operators:

$$\mathcal{H}_{2sites}^{biQ}(-J) = -J \sum_{i=1}^2 (\vec{S}_i \cdot \vec{S}_{i+1})^2 \quad (5.4)$$

with periodic boundary conditions  $\vec{S}_{N+1} = \vec{S}_1$ , it gives:

$$\mathcal{H}_{2sites}^{biQ}(-J) = -J \left( (\vec{S}_1 \cdot \vec{S}_2)^2 + (\vec{S}_2 \cdot \vec{S}_1)^2 \right) = -2J (\vec{S}_1 \cdot \vec{S}_2)^2 \quad (5.5)$$

The biquadratic Hamiltonian can be written down explicitly in a matrix form once a suitable basis has been chosen. Recalling our former definition (2.29)

$$|++\rangle | +0\rangle | 0+\rangle | +- \rangle | 00\rangle | -+\rangle | 0-\rangle | -0\rangle | --\rangle \quad (5.6)$$

of the two-site basis we get this expression for the biquadratic Hamiltonian operator, as a  $9 \times 9$  matrix:





	$S_{tot}^2$	$S_{tot}^z$	$\varepsilon'$
QUINTET STATES			
$ ++\rangle$	2	+2	+1
$\frac{1}{\sqrt{2}}( +0\rangle +  0+\rangle)$	2	+1	+1
$\frac{1}{\sqrt{6}}( +-\rangle +  -+\rangle + 2 00\rangle)$	2	0	+1
$\frac{1}{\sqrt{2}}( -0\rangle +  0-\rangle)$	2	-1	+1
$ --\rangle$	2	-2	+1
TRIPLET STATES			
$\frac{1}{\sqrt{2}}( +0\rangle -  0+\rangle)$	1	+1	-1
$\frac{1}{\sqrt{2}}( +-\rangle -  -+\rangle)$	1	0	-1
$\frac{1}{\sqrt{2}}( 0-\rangle -  -0+\rangle)$	1	-1	-1
SINGLET STATE			
$\frac{1}{\sqrt{3}}( +-\rangle +  -+\rangle -  00\rangle)$	0	0	-2

**Table 5.1:** Classification of eigenstates of the two-site spin-1 Heisenberg Hamiltonian according to its good quantum numbers  $S_{tot}^z$  and  $S_{tot}^2$ . Scaled eigenvalues  $\varepsilon' = E/2J$  are displayed in the last column. As a consequence of the  $SU(2)$ -symmetry of the model,  $SU(2)$ -multiplets (singlet, triplet and quintet) precisely correspond to invariant subspaces of the Hamiltonian.

We can immediately see that the singlet, triplet and quintet states with total  $z$ -component null are, in fact, also eigenstates of the biquadratic Hamiltonian. It is easy to verify that, acting with the central non-diagonal block on these states, we get the related eigenvalues, namely +1 for the triplet and the quintet states and +4 for the singlet state.

Let us consider, now, the effect of the action of the biquadratic Hamiltonian on quintet, triplet and singlet states, displayed in table 5.2.

Having a look at the energy eigenvalues, we quickly come up with the idea that there could be an other underlying symmetry structure, which collects together the triplet and quintet states. This observation can be easily understood in terms of  $SU(3)$  representations. In order to do that, we need to change our point of view and interpret the spin-1 chain as a  $SU(3)$  Heisenberg chain with alternate fundamental and antifundamental representations. This procedure can be performed thanks to the equivalence relation (3.47).

	$S_{tot}^2$	$S_{tot}^z$	$\varepsilon$
QUINTET STATES			
$ ++\rangle$	2	+2	+1
$\frac{1}{\sqrt{2}}( +0\rangle +  0+\rangle)$	2	+1	+1
$\frac{1}{\sqrt{6}}( +-\rangle +  -+\rangle + 2 00\rangle)$	2	0	+1
$\frac{1}{\sqrt{2}}( -0\rangle +  0-\rangle)$	2	-1	+1
$ --\rangle$	2	-2	+1
TRIPLET STATES			
$\frac{1}{\sqrt{2}}( +0\rangle -  0+\rangle)$	1	+1	+1
$\frac{1}{\sqrt{2}}( +-\rangle -  -+\rangle)$	1	0	+1
$\frac{1}{\sqrt{2}}( 0-\rangle -  -0+\rangle)$	1	-1	+1
SINGLET STATE			
$\frac{1}{\sqrt{3}}( +-\rangle +  -+\rangle -  00\rangle)$	0	0	+4

**Table 5.2:** Action of the two-site spin-1 pure biquadratic Hamiltonian (5.4) on the Heisenberg Hamiltonian basis of eigenstates (made up of the singlet, triplet and quintet states). Scaled eigenvalues are displayed in the last column  $\varepsilon = E/(-2J)$ . The triplet and quintet states now belong to the same invariant subspace of the Hamiltonian. The presence of eight degenerate eigenstates (octet) suggests an underlying  $SU(3)$  symmetry.

According to our previous conventions (see section 3.3), we should bear in mind that switching from the  $SU(2)$  interpretation to the  $SU(3)$  approach, we need to change the signs of two components on even sites of the chain, namely:

$$S_{2i}^x \rightarrow -S_{2i}^x \quad \text{and} \quad S_{2i}^z \rightarrow -S_{2i}^z \quad (5.12)$$

to make the results obtained through the  $SU(3)$  equivalence match the description in terms of spin-1 operators.

Now, employing the quantum number mapping described in section 3.4 we may classify the biquadratic Hamiltonian eigenstates according to a different set of quantum numbers that is the  $SU(3)$  pair of quantum numbers,  $T_{tot}^3$  and  $Y_{tot}$ , which are related to the spin operators through the relations:

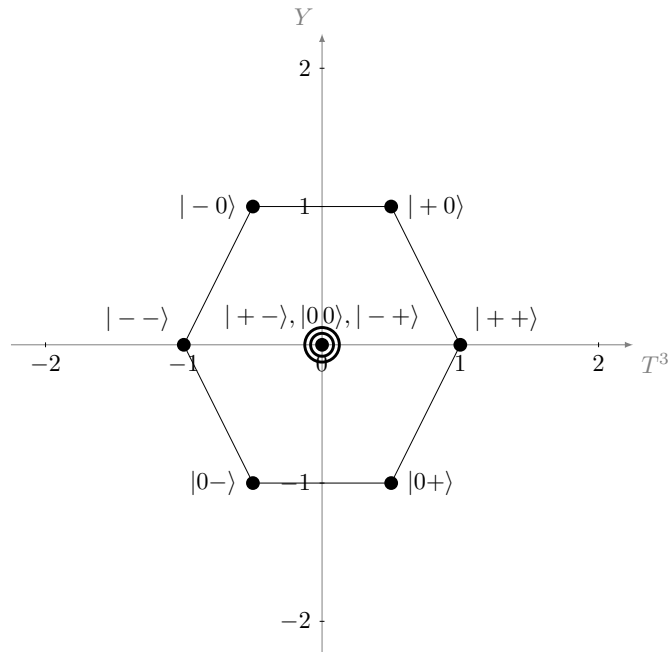
$$T_{tot}^3 = \frac{1}{2} \sum_{i=1}^N S_i^z = S_{tot}^z \quad Y_{tot} = \sum_{i=1}^N (-1)^{i+1} (S_i^z)^2 \equiv (S^z)_{stag}^2 \quad (5.13)$$

Table 5.3 shows the quantum numbers for the nine states of the two-spin basis. Different quantum numbers characterise the six eigenstates with  $S_{tot}^z \neq 0$ , whereas the three states with  $S^z = 0$  show the same set of  $SU(3)$  quantum numbers.

	$T_{tot}^3$	$Y_{tot}$
$ ++\rangle$	+1	0
$ +0\rangle$	1/2	+1
$ 0+\rangle$	1/2	-1
$ +-\rangle$	0	0
$ 00\rangle$	0	0
$ -\rangle$	0	0
$ 0-\rangle$	-1/2	-1
$  - 0 \rangle$	-1/2	+1
$ --\rangle$	-1	0

**Table 5.3:** Classification of the two-state basis (2.29) according to  $SU(3)$  quantum numbers. The states with  $S_{tot}^z = 0$  all have the same set of quantum numbers, i.e.  $(0,0)$ , while the other six states display different couples of quantum numbers, locating them on the vertices of a regular hexagon. See figure 5.1.

The symmetry structure will appear clear as soon as these nine states are displayed on the usual  $T^3 - Y$  plane (fig. 5.1).



**Figure 5.1:** Graphical representation in the  $T^3 - Y$  plane of the nine states of the two-site spin-1 basis labelled by  $S^z$  eigenvalues. They form the characteristic shape of the  $SU(3)$  representations of an octet (regular hexagon with double-degenerate state in its centre) with an additional singlet state (located at the origin).

As we can see, the points on the graph form one of the most typical structures of the  $SU(3)$ -group representations: the regular hexagonal shape of the octet. This happens because the set of nine independent eigenstates of the biquadratic Hamiltonian organise themselves according to the sum of two  $SU(3)$  representations, the **singlet** and the **octet**.

This is the reason why eight of the biquadratic Hamiltonian eigenstates have the same eigenvalue  $\varepsilon = +1$ , while the only one with the different eigenvalue  $\varepsilon = +4$  is the singlet. The former is, actually, the system ground state because its energy is given by  $E = -2J\varepsilon$ , whereas the eigenstates belonging to the octet are all degenerate first-excited states. This is the result of the composition of the  $SU(3)$  representations  $[3]$  and  $[\bar{3}]$ , that we have established to be located respectively on site 1 and 2.

The rules of composition of  $SU(3)$  representations are quite different from the ones for  $SU(2)$  and they are founded on a very efficient pictorial technique. Let's show for now just the simplest case, that is the Kronecker product of one fundamental and one antifundamental representation.

$$[3] \otimes [\bar{3}] = [1] \oplus [8] \quad (5.14)$$

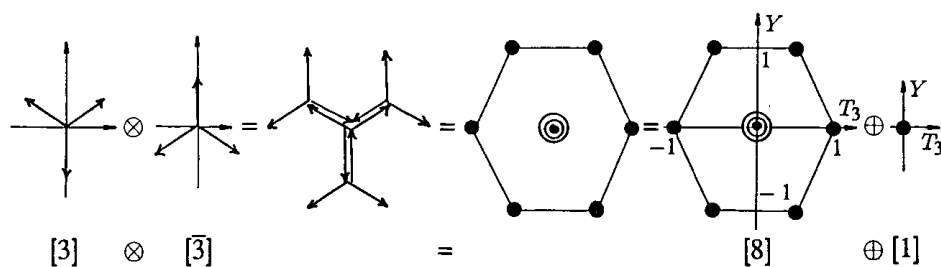


**Figure 5.2:** Graphical composition technique for the fundamental and antifundamental representations. It is shown the reduction method for the Kronecker product of  $[3] \otimes [\bar{3}]$  in the  $T^3 - Y$  plane. The composition of these two representations leads to the direct sum of a singlet and an octet, counting together nine states, just as the product of the two three-dimensional representations we started from. (Picture taken from [22]).

The graphical procedure is based on reproducing one of the two representations centred on each vertex of the other and then connecting the resulting points in order to form  $SU(3)$ -symmetric structures, that must be built upon three different leading symmetry axes, therefore they will be either hexagonal or triangular polygons with internal angles of  $60^\circ$ .

The decomposition of the product of these two representations into a sum of irreducible representations leads us to a classification of the set of eigenstates of the biquadratic Hamiltonian into  $SU(3)$  multiplets, revealing

the inner symmetry structure of the model, hidden under the spin-1 operator formalism.

In table 5.4 we show the biquadratic Hamiltonian eigenstates with their  $SU(3)$  related quantum numbers. As we could already see from the previous tables, there are six eigenstates exactly reproducible with the  $SU(2)$  vector representation employed in the Bethe ansatz approach. They are located precisely on the six vertices of the regular hexagon centred on the origin, with sides measuring one unity (due to the scaling factor on the  $Y$ -axis of  $\frac{\sqrt{3}}{2}$ ).

The other three states are built upon linear combinations in order to form the usual singlet, triplet and quintet states with null  $z$ -component of the total spin. They make up the  $S^z = 0$  sector and are located at the origin in the  $T^3 - Y$  plane, that is a triple-degenerate point. It hosts two states from the  $SU(3)$  octet (that we assume to be the triplet and quintet state with  $S^z = 0$ ) and the  $SU(3)$  singlet, which is also the  $SU(2)$  singlet.

BIQUADRATIC EIGENSTATES	$T_{tot}^3$	$Y_{tot}$
$ ++\rangle$	+1	0
$ +0\rangle$	1/2	+1
$ 0+\rangle$	1/2	-1
$ 0-\rangle$	-1/2	-1
$  - 0\rangle$	-1/2	+1
$ --\rangle$	-1	0
$\frac{1}{\sqrt{2}}( +-\rangle -  -+\rangle)$	0	0
$\frac{1}{\sqrt{6}}( +-\rangle +  -+\rangle + 2 00\rangle)$	0	0
$\frac{1}{\sqrt{3}}( +-\rangle +  -+\rangle -  00\rangle)$	0	0

**Table 5.4:** Two-site pure biquadratic Hamiltonian eigenstates classified according to  $SU(3)$  quantum numbers. The  $S_{tot}^z = 0$  states were linearly combined in order to form the last three eigenstates of the system. The first eight eigenstates assemble the  $SU(3)$  octet [8], while the last one is an  $SU(3)$  singlet, [1].

Once the  $SU(3)$  correspondence of the biquadratic Hamiltonian eigenstates has been established, we may try to enlighten the  $SU(2)$  structure on the  $T^3 - Y$  plane. To this purpose, we should find the  $SU(3)$  expression of the three operators characterising the  $SU(2)$  group multiplets:  $S^+$ ,  $S^-$  and  $S^z$ . We should pay attention to the parity of the site on which the spin is located, because it causes the representation to switch from fundamental to antifundamental and it changes the sign of the  $x$ - and the  $z$ -spin component (cfr. eq. (3.48)).

$$S_{2i-1}^z = 2 T_{2i+1}^3 \quad S_{2i}^z \rightarrow -S_{2i}^z = -2 \bar{T}_{2i}^3 = 2 T_{2i}^3 \quad (5.15)$$

The value of  $S^z$ , which labels the states belonging to a  $SU(2)$  multiplet, can be read on the  $T^3$  axis of the graph, whereas the ladder operators of  $SU(2)$ , which scale the  $z$ -component of spin within the multiplet:

$$\begin{aligned}
S_{2i-1}^+ &= S_{2i-1}^x + iS_{2i-1}^y = \\
&= \frac{1}{\sqrt{2}}(\lambda_{2i-1}^4 + \lambda_{2i-1}^6 + i\lambda_{2i-1}^5 - i\lambda_{2i-1}^7) = \\
&= \sqrt{2}(V_{2i-1}^- + U_{2i-1}^+)
\end{aligned} \tag{5.16}$$

$$\begin{aligned}
S_{2i-1}^- &= S_{2i-1}^x - iS_{2i-1}^y = \\
&= \frac{1}{\sqrt{2}}(\lambda_{2i-1}^4 + \lambda_{2i-1}^6 - i\lambda_{2i-1}^5 + i\lambda_{2i-1}^7) = \\
&= \sqrt{2}(V_{2i-1}^- + U_{2i-1}^+)
\end{aligned} \tag{5.17}$$

$$\begin{aligned}
S_{2i}^+ &= S_{2i}^x + iS_{2i}^y \rightarrow -S_{2i}^x + iS_{2i}^y = \\
&= \frac{1}{\sqrt{2}}(-\bar{\lambda}_{2i}^4 - \bar{\lambda}_{2i}^6 + i\bar{\lambda}_{2i}^5 - i\bar{\lambda}_{2i}^7) = \\
&= \frac{1}{\sqrt{2}}(\lambda_{2i}^4 + \lambda_{2i}^6 + i\lambda_{2i}^5 - i\lambda_{2i}^7) = \\
&= \sqrt{2}(V_{2i}^+ + U_{2i}^-)
\end{aligned} \tag{5.18}$$

$$\begin{aligned}
S_{2i}^- &= S_{2i}^x - iS_{2i}^y \rightarrow -S_{2i}^x - iS_{2i}^y = \\
&= \frac{1}{\sqrt{2}}(-\bar{\lambda}_{2i}^4 - \bar{\lambda}_{2i}^6 - i\bar{\lambda}_{2i}^5 + i\bar{\lambda}_{2i}^7) = \\
&= \frac{1}{\sqrt{2}}(\lambda_{2i}^4 + \lambda_{2i}^6 - i\lambda_{2i}^5 + i\lambda_{2i}^7) = \\
&= \sqrt{2}(V_{2i}^- + U_{2i}^+)
\end{aligned} \tag{5.19}$$

appear as combinations of the ladder operator of the  $SU(3)$  algebra acting on the diagonal directions, as shown in figure 5.3.

The matrix forms of these operators are:

$$\begin{aligned}
U_i^+ &= \begin{pmatrix} 0 & 0 & 0 \\ 0 & 0 & 1 \\ 0 & 0 & 0 \end{pmatrix} & V_i^+ &= \begin{pmatrix} 0 & 0 & 1 \\ 0 & 0 & 0 \\ 0 & 0 & 0 \end{pmatrix} \\
U_i^- &= \begin{pmatrix} 0 & 0 & 0 \\ 0 & 0 & 0 \\ 0 & 1 & 0 \end{pmatrix} & V_i^- &= \begin{pmatrix} 0 & 0 & 0 \\ 0 & 0 & 0 \\ 1 & 0 & 0 \end{pmatrix}
\end{aligned} \tag{5.20}$$

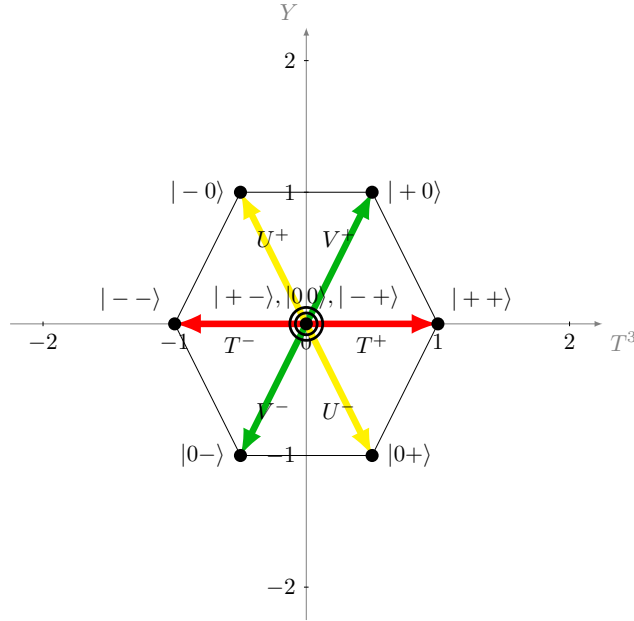


**Figure 5.3:** Graphical representation on the  $T^3$ – $Y$  plane of the action of the ladder operators  $T^\pm$ ,  $U^\pm$  and  $V^\pm$ , related to the three non commuting  $SU(2)$  subalgebras of the  $SU(3)$  group. The units on the  $Y$ -axis are supposed to be rescaled by a factor of  $\frac{\sqrt{3}}{2}$  so that this results a regular hexagon. The directions of action of the three operators exhibit angles of  $60^\circ$  between them all.

Their actions on the usual spin basis (A.11), is immediately inferred from expressions (5.20). Therefore, it is easy to recover some of the usual multiplet relations. For example, from the highest weight state  $|++\rangle$  belonging to the quintet ( $S = 2, s = 2$ ), we should get all the other four states by means of consecutive applications of the operator  $S^-$ . From the picture it is clear that, since  $S^-$  is a linear combination of  $U^+$  and  $V^-$ , the action of this ladder operator leads to the symmetric combination of the two states on the right vertices of the hexagon, which is precisely the second state of the quintet ( $S = 2, s = 1$ ).

Starting from one of the fully aligned states by means of repeated applications of  $SU(3)$  operators, we can reach any state within the  $SU(3)$  octet representation, i.e. the triplet and quintet states, leaving the  $SU(2)$  singlet alone forming its own  $SU(3)$  singlet representation.

Thus,  $U^\pm$  and  $V^\pm$  act on the  $SU(2)$  states increasing and lowering the  $z$ -component by one, i.e. they generate a single deviation, while the  $T^\pm$  operators, acting parallel to the  $T^3 \sim S^z$ -axis create a double deviation, which means a double shift in the  $S^z$  component value. In order to generate a propagating spin pair, i.e. a two-string, we need to act at least once with the  $T^\pm$  starting from the fully aligned states. Each progressive shift of one

unity towards the origin of the plane represents the creation of one further propagating couple, which cannot be identified in general because it is usually defined as a linear combination which has to satisfy the Hamiltonian eigenvalue equation.

Although this is the simplest case of biquadratic Hamiltonian, these latest considerations still hold even for a longer chain, with arbitrary but even number of sites.

In order to get a confirmation of the technique employed, we may try the numerical approach with the  $SU(3)$  Hamiltonian. This will be useful later on, when we will deal with a larger number of sites for which the standard Hamiltonian operator representation is  $(3^N \times 3^N)$ -dimensional.

Focusing right now on the  $N = 2$  site case, the Hamiltonian which we are going to study is the (3.48):

$$\mathcal{H}^{F \otimes A}(J) = J \sum_{\alpha=1}^8 \left[ \lambda_1^\alpha \bar{\lambda}_2^\alpha + \bar{\lambda}_2^\alpha \lambda_1^\alpha \right] \quad (5.21)$$

where we assumed periodic boundary conditions as usual.

Evaluating this operator with the assistance of Mathematica, that provides us with the complete set of eigenstates and eigenvalues of the model, we can see (table 5.6) that the eigenvectors appear in the shape of nine-dimensional vectors, with coefficients representing the decomposition on the canonical  $\mathbb{C}^9$  basis. These nine basis states can be built as the Kronecker product of the three-dimensional vectors corresponding to the states of the two spin variables located on the two sites. Working in the  $SU(3)$  framework we can use the single-site basis states (B.30), (B.31) and (B.32). The two-site joint basis will be the tensor product, organised in a nine-dimensional vector displaying the conventional ordering:

$$\begin{pmatrix} |u\rangle \\ |d\rangle \\ |s\rangle \end{pmatrix} \otimes \begin{pmatrix} |u\rangle \\ |d\rangle \\ |s\rangle \end{pmatrix} = \begin{pmatrix} |uu\rangle \\ |ud\rangle \\ |us\rangle \\ |du\rangle \\ |dd\rangle \\ |ds\rangle \\ |su\rangle \\ |sd\rangle \\ |ss\rangle \end{pmatrix} \quad (5.22)$$

In order to recover the interpretation in terms of spin-1 variables, we must relate the two-spin basis states to the nine canonical basis vectors for the Hilbert space on which the  $SU(3)$  Hamiltonian acts. The correspondence should be based on the single spin basis (A.11), recalling that the order of  $S^z$  eigenstates is slightly different than the usual one (2.29), leading to the



Now, the interpretation of the  $SU(3)$  Heisenberg Hamiltonian with alternate fundamental and antifundamental representations

$$\frac{1}{J}\mathcal{H}^{F\otimes A}(J) = \frac{2}{3} \begin{pmatrix} -2 & 0 & 0 & 0 & -3 & 0 & 0 & 0 & -3 \\ 0 & 1 & 0 & 0 & 0 & 0 & 0 & 0 & 0 \\ 0 & 0 & 1 & 0 & 0 & 0 & 0 & 0 & 0 \\ 0 & 0 & 0 & 1 & 0 & 0 & 0 & 0 & 0 \\ -3 & 0 & 0 & 0 & -2 & 0 & 0 & 0 & -3 \\ 0 & 0 & 0 & 0 & 0 & 1 & 0 & 0 & 0 \\ 0 & 0 & 0 & 0 & 0 & 0 & 1 & 0 & 0 \\ 0 & 0 & 0 & 0 & 0 & 0 & 0 & 1 & 0 \\ -3 & 0 & 0 & 0 & -3 & 0 & 0 & 0 & -2 \end{pmatrix} \quad (5.27)$$

as a spin-1 biquadratic Hamiltonian is based upon the equivalence (3.47) (coupling constants  $J$  for both models were set to 1 and periodic boundary conditions were assumed):

$$\mathcal{H}^{biQ}(-S_{2i}^x, S_{2i}^y, -S_{2i}^z) = \frac{1}{2}\mathcal{H}^{F\otimes A} + \frac{4}{3}N\mathbb{I} \quad (5.28)$$

which leads to an operator representing the biquadratic Hamiltonian with  $x$ - and  $z$ -spin operators with opposite signs.

$$\mathcal{H}^{biQ}(-S_{2i}^x, S_{2i}^y, -S_{2i}^z) = \begin{pmatrix} 2 & 0 & 0 & 0 & 1 & 0 & 0 & 0 & 1 \\ 0 & 1 & 0 & 0 & 0 & 0 & 0 & 0 & 0 \\ 0 & 0 & 1 & 0 & 0 & 0 & 0 & 0 & 0 \\ 0 & 0 & 0 & 1 & 0 & 0 & 0 & 0 & 0 \\ 1 & 0 & 0 & 0 & 2 & 0 & 0 & 0 & 1 \\ 0 & 0 & 0 & 0 & 0 & 1 & 0 & 0 & 0 \\ 0 & 0 & 0 & 0 & 0 & 0 & 1 & 0 & 0 \\ 0 & 0 & 0 & 0 & 0 & 0 & 0 & 1 & 0 \\ 1 & 0 & 0 & 0 & 1 & 0 & 0 & 0 & 2 \end{pmatrix} \quad (5.29)$$

Recovering the true biquadratic Hamiltonian requires the transformation of the matrix (5.29) under the action of the unitary operator  $\mathbb{I} \otimes U$ , switching spins on even sites only.

$$\mathcal{H}^{biQ}(S_{2i}^x, S_{2i}^y, S_{2i}^z) = (\mathbb{I} \otimes U)\mathcal{H}^{biQ}(-S_{2i}^x, S_{2i}^y, -S_{2i}^z)(\mathbb{I} \otimes U)$$

$$\mathcal{H}^{biQ}(S_{2i}^x, S_{2i}^y, S_{2i}^z) = \begin{pmatrix} 1 & 0 & 0 & 0 & 0 & 0 & 0 & 0 & 0 \\ 0 & 2 & 0 & 1 & 0 & 0 & 0 & 0 & -1 \\ 0 & 0 & 1 & 0 & 0 & 0 & 0 & 0 & 0 \\ 0 & 1 & 0 & 2 & 0 & 0 & 0 & 0 & -1 \\ 0 & 0 & 0 & 0 & 1 & 0 & 0 & 0 & 0 \\ 0 & 0 & 0 & 0 & 0 & 1 & 0 & 0 & 0 \\ 0 & 0 & 0 & 0 & 0 & 0 & 1 & 0 & 0 \\ 0 & 0 & 0 & 0 & 0 & 0 & 0 & 1 & 0 \\ 0 & -1 & 0 & -1 & 0 & 0 & 0 & 0 & 2 \end{pmatrix} \quad (5.30)$$

We may notice that this is exactly the same form of the pure biquadratic Hamiltonian we dealt with in section 2.3, concerning the Bethe ansatz approach. We stress the fact that the operator action is perfectly equivalent even though the basis eigenvectors are arranged in a different order (5.23) from usual (2.29).

Let us discuss now the relation among basis vectors of the two models. Thanks to the transformation represented by  $U$  on the even sublattice, we should get the following correspondence among states, symbolically expressed by:

$$| , \rangle_{+,-,0} = (\mathbb{I} \otimes U) | , \rangle_{u,d,s} \quad (5.31)$$

The full mapping between the two basis has been built as shown in table 5.5:

$\mathcal{H}^{biQ}$ basis	$\mathcal{H}^{F \otimes A}$ basis
$  + + \rangle$	$  ud \rangle$
$  + - \rangle$	$-   us \rangle$
$  + 0 \rangle$	$  sd \rangle$
$  - + \rangle$	$  uu \rangle$
$  - 0 \rangle$	$-   ss \rangle$
$  - - \rangle$	$  dd \rangle$
$  0 + \rangle$	$  su \rangle$
$  0 - \rangle$	$-   ds \rangle$
$  0 0 \rangle$	$  du \rangle$

**Table 5.5:** Two site Hamiltonian. Mapping between the  $S^z$  eigenstates spin basis ( $| + \rangle, | - \rangle, | 0 \rangle$ ) of the biquadratic Hamiltonian and the canonical basis built on the states ( $| u \rangle, | d \rangle, | s \rangle$ ) of the fundamental representation [3] of the  $SU(3)$  group. We may switch from one basis to the other by means of the operator  $U$ , which transforms the operators  $S^x$  and  $S^z$  on even sites into  $-S^x$  and  $-S^z$  respectively, allowing the mapping according to (3.47).

Table 5.6 displays the list of the eigenvalues and eigenstates of the  $SU(3)$  Hamiltonian extracted with the help of Mathematica. Hence, it becomes quite easy to read the solutions of the eigenvalue equation as extracted from the diagonalisation of the Hamiltonian (5.27) in terms of the usual spin state basis (2.29). As far as the eigenvectors with only one non-null entry are concerned, the correspondence is certainly immediate; however, eigenvalues built upon linear combinations (involving only  $S_{tot}^z = 0$  states) do not resemble the states we had selected before (cfr. table 5.2), thanks to the help of other quantum numbers to guide our choice.

$E/J$	decomposition coefficients	$\mathcal{H}^{F\otimes A}$ basis	$\mathcal{H}^{biQ}$ basis
$-32/3$	$(1, 0, 0, 0, 1, 0, 0, 0, 1)$	$ uu\rangle +  dd\rangle +  ss\rangle$	$ +-\rangle +  -+\rangle -  00\rangle$
$4/3$	$(-1, 0, 0, 0, 0, 0, 0, 0, 1)$	$- uu\rangle +  ss\rangle$	$- +-\rangle -  00\rangle$
$4/3$	$(0, 0, 0, 0, 0, 0, 0, 1, 0)$	$ sd\rangle$	$ 0+\rangle$
$4/3$	$(0, 0, 0, 0, 0, 0, 1, 0, 0)$	$ su\rangle$	$ 0-\rangle$
$4/3$	$(0, 0, 0, 0, 0, 1, 0, 0, 0)$	$ ds\rangle$	$- -0\rangle$
$4/3$	$(-1, 0, 0, 0, 1, 0, 0, 0, 0)$	$- uu\rangle +  dd\rangle$	$- +-\rangle +  -+\rangle$
$4/3$	$(0, 0, 0, 1, 0, 0, 0, 0, 0)$	$ du\rangle$	$ --\rangle$
$4/3$	$(0, 0, 1, 0, 0, 0, 0, 0, 0)$	$ us\rangle$	$- +0\rangle$
$4/3$	$(0, 1, 0, 0, 0, 0, 0, 0, 0)$	$ ud\rangle$	$ ++\rangle$

**Table 5.6:** Two site Hamiltonian. Energy eigenvalues of the  $SU(3)$  quantum Heisenberg chain with alternate representations ( $[3] \otimes [\bar{3}]$ ), assuming periodic boundary conditions. The table displays in the first column the eigenvalues distinguishing the singlet (ground state) from the eight-fold degenerate states belonging to the octet representation. The second column shows the coefficients arising from the decomposition on the canonical  $\mathbb{C}^9$  basis of the Hilbert space ordered as in (5.22). The third one shows the related linear combinations of states in the  $SU(3)$  canonical basis. The last one column recovers the interpretation of these states as spin-1 variables through the mapping displayed in table 5.5.

The only independent eigenvector must be the singlet, which belongs to an invariant subspace of the Hamiltonian of its own and shows a different eigenvalue. It is important to check that this is eigenstate is independent and orthogonal to all the others, which belong to the same eight-dimensional block of the Hamiltonian, having all the same eigenvalue. This is not really a problem though, because any linear combination of degenerate eigenstates is still an eigenstate with the same eigenvalue. Thus, with suitable combinations we recover the usual forms of the  $S_{tot}^z = 0$  states of the triplet and quintet, as listed in table 5.2.

Finally, we need to test the exact correspondence of the eigenvalues of the two different models as stated by (3.47). Assuming  $N = 2$  and periodic boundary conditions:

$$\begin{aligned}
E(\mathcal{H}^{F\otimes A}(J)) &= -2E(\mathcal{H}^{biQ}(J)) + \frac{8}{3}JN \\
-\frac{32}{3}J &= -2 \cdot 2J(+4) + \frac{8}{3}J \cdot 2 \\
\frac{4}{3}J &= -2 \cdot 2J(+1) + \frac{8}{3}J \cdot 2
\end{aligned} \tag{5.32}$$

## 5.2 Biquadratic Hamiltonian on a four-site chain

Thanks to the assistance of computational devices, the evaluation of the Hamiltonian and the subsequent diagonalisation become a matter of seconds, therefore increasing the number of sites will become very easy. Here, we will present the shortest chains with an even number of sites, namely the four and six-site Hamiltonians.

Let us start with the first one. Recalling the Bethe ansatz approach we should start the classification of states according to the only good quantum number, that is  $S_{tot}^z$ . Thus, we may define them also by the number of deviations from the two possible fully aligned states:

$$|++++\rangle \quad |----\rangle$$

which are, in fact, the doubly-degenerate ground state of ferromagnetic model. The number of deviations  $m$  is immediately related to the  $z$ -component of the total spin, through:

$$m = N - S_{tot}^z, \quad \text{where } N = 4. \quad (5.33)$$

The maximum number of deviations allowed on a fully aligned state of spin-1 variables is  $2N$ , however there is no need to examine all the possible cases  $m = 0, 1, \dots, 2N$ , because there are some symmetries that we can rely on to simplify our work.

The first one is the symmetry of the Hamiltonian under the **exchange of all  $z$ -components of spins**, which halves the number of deviations to be analysed. The symmetry under spin flips, defined by:

$$|+\rangle \longrightarrow |-\rangle \quad |-\rangle \longrightarrow |+\rangle \quad |0\rangle \longrightarrow |0\rangle \quad (5.34)$$

brings an overall minus sign to the  $z$ -component of the total spin, thus making the negative values of  $S_{tot}^z$  redundant, because we may just flip all the spins on the chain and get the corresponding state with opposite value of  $S_{tot}^z$ . Preserving only the positive values of  $S_{tot}^z$ ,  $m$  is bound to span the values from 0 to  $N$ . We will interpret the states with more deviations  $m' > N$  as states with  $m = 2N - m'$  deviations from the opposite fundamental state. Here is an example of the action of the symmetry under spin flips:

$$\begin{array}{ll}
|+-0+\rangle & \longrightarrow \quad | - + 0 + \rangle \\
S_i^z & \longrightarrow \quad -S_i^z \\
S_{tot}^z & \longrightarrow \quad -S_{tot}^z \\
S_{tot}^z = 0, 1, \dots, N & \longrightarrow \quad S_{tot}^z = 0, -1, \dots, -N \\
m = N - S_{tot}^z & \longrightarrow \quad m = N + S_{tot}^z \\
m = 0, 1, \dots, N & \longrightarrow \quad m = N, N + 1, \dots, 2N \\
& \longrightarrow \quad m' = 2N - m = 0, 1, \dots, N
\end{array} \quad (5.35)$$

Now, we may proceed following the same path outlined for the Bethe ansatz (cfr. section 2.3), and then exploit the mapping (3.48) to evaluate the related  $SU(3)$  quantum numbers.

We will make the assumption to start with the state,

$$|++++\rangle$$

and we will later take care of the other possible fundamental state, performing the spin flip and changing the sign of all the  $z$ -component of each of the spins.

- **$m = 0$  deviations**  $\rightarrow \mathbf{S}_{\text{tot}}^z = 4$

There is a unique state that is the fully aligned one. This is the ferromagnetic ground state, but this is the highest excited state for the antiferromagnetic model because of the *complete reversal* of energy eigenstates between the two models.

- **$m = 1$  deviation**  $\rightarrow \mathbf{S}_{\text{tot}}^z = 3$

One single deviation produces a zero on one of the four possible sites. Dealing with the presence of a zero  $z$ -component of the spin, we should distinguish if the deviation occurs on an even or on an odd site, because the action of the  $(S^z)_{\text{stag}}^2$  operator is different in the two cases. So we must split these four states in two groups:

$$|+0++\rangle \quad \text{and} \quad |+++0\rangle$$

in which the deviation is located on an even site, with quantum numbers:

$$T_{\text{tot}}^3 = \frac{3}{2} \quad \text{and} \quad Y_{\text{tot}} = +1$$

and

$$|++0+\rangle \quad \text{and} \quad |0+++ \rangle$$

in which the deviation is located on an odd site, with quantum numbers:

$$T_{\text{tot}}^3 = \frac{3}{2} \quad \text{and} \quad Y_{\text{tot}} = -1$$

- **$m = 2$  deviations**  $\rightarrow \mathbf{S}_{\text{tot}}^z = 2$

Two deviations may occur on the same or on different sites, thus resulting in a minus or two zeroes respectively. In the first case, we get to a state of the form:

$$|++-+\rangle$$

where there are four possible locations for the minus on the chain, all of them having the same quantum numbers

$$T_{\text{tot}}^3 = 1 \quad \text{and} \quad Y_{\text{tot}} = 0$$

because the  $(S^z)_{stag}^2$  operator does not distinguish a minus from a plus since their square  $z$ -component is exactly the same.

The distinction has to be made for the case of two zeroes, which can be located both on even sites (one state):

$$|+ 0 + 0\rangle$$

$$T_{tot}^3 = 1 \quad \text{and} \quad Y_{tot} = +2$$

both on odd sites (one state):

$$|0 + 0 +\rangle$$

$$T_{tot}^3 = 1 \quad \text{and} \quad Y_{tot} = -2$$

or one on an odd site and one on an even one (four states):

$$|0 0 + +\rangle, | + 0 0 +\rangle, | + + 0 0\rangle, |0 + + 0\rangle$$

$$T_{tot}^3 = 1 \quad \text{and} \quad Y_{tot} = 0$$

• **m = 3 deviations**  $\rightarrow \mathbf{S}_{tot}^z = 1$

Three deviations may be either a minus and a zero or three zeroes. Here we have to distinguish again according to the parity of the sites hosting the zero  $z$ -components among the four sites of the chain.

When there is only one zero it can be located either on an even site or on an odd one, leading to the quantum numbers:

$$T_{tot}^3 = \frac{1}{2} \quad \text{and} \quad Y_{tot} = \pm 1$$

There are six states for both the even and the odd case, given by the permutations of the other three elements (two plus and one minus).

When there are three zeroes, they can be arranged on two even and one odd site or on two odd and one even site, because we have to pay attention to the fact that on a four site chain we cannot find more than two odd or two even positions. There are two possible states for each of the two cases, with quantum numbers:

$$T_{tot}^3 = \frac{1}{2} \quad \text{and} \quad Y_{tot} = \pm 1$$

- **m = 4 deviations** →  $S_{tot}^z = 0$

Let's focus now on the last subspace of states, that is the  $S_{tot}^z = 0$  one, which is actually the largest and the most important one, as it contains the ground state for the antiferromagnetic model. The four deviations can be arranged to form two minus, one minus and two zeroes or four zeroes. In the first case there are six possible states with the same quantum numbers:

$$T_{tot}^3 = 0 \quad \text{and} \quad Y_{tot} = 0$$

In the second case, uncaring of the minus location, we can arrange the two zeroes both on even sites (2 states):

$$T_{tot}^3 = 0 \quad \text{and} \quad Y_{tot} = +2$$

both on odd sites (2 states):

$$T_{tot}^3 = 0 \quad \text{and} \quad Y_{tot} = -2$$

or one on an odd and one on an even site (8 states):

$$T_{tot}^3 = 0 \quad \text{and} \quad Y_{tot} = 0$$

Finally the third case, that is two minus, yields six different states, with the same quantum numbers:

$$T_{tot}^3 = 0 \quad \text{and} \quad Y_{tot} = 0$$

Throughout this discussion, we should notice that there is one additional symmetry of the model that we have not used before. Having a look at the quantum numbers of the previously listed states, we can see that, **exchanging odd sites with even ones**, we get an overall change of sign of the value of  $Y_{tot}$ . Thus, the translation of one lattice constant applied to all the spins on the chain produces the corresponding state with an opposite value of the second  $SU(3)$  quantum number. This entire line of reasoning which allows the mapping of even sites into odd ones works only if periodic boundary conditions hold. The action of this symmetry can be summarised as follows:

$$\begin{aligned}
 |+-0+\rangle &\longrightarrow |++-0\rangle \\
 i &\longrightarrow i+1 \\
 S_i^z &\longrightarrow S_{i+1}^z \\
 (S_i^z)^2 &\longrightarrow (S_{i+1}^z)^2 \\
 (S^z)_{stag}^2 &\longrightarrow -(S^z)_{stag}^2
 \end{aligned} \tag{5.36}$$

Here, we have a little recap of the symmetries of the biquadratic Hamiltonian and their action on the  $SU(3)$  quantum numbers.

- $\mathbf{S}_i^z \rightarrow -\mathbf{S}_i^z$  symmetry under spin flip

$$T_{tot}^3 \rightarrow -T_{tot}^3 \quad \text{and} \quad Y_{tot} \rightarrow Y_{tot} \quad (5.37)$$

In the  $T^3 - Y$  plane this is a symmetry with respect to the  $y$ -axis.

- $\mathbf{S}_i^z \rightarrow \mathbf{S}_{i+1}^z$  symmetry under site-parity exchange

$$T_{tot}^3 \rightarrow T_{tot}^3 \quad \text{and} \quad Y_{tot} \rightarrow -Y_{tot} \quad (5.38)$$

In the  $T^3 - Y$  plane this is a symmetry with respect to the  $x$ -axis.

In conclusion, the  $SU(3)$  representation of a biquadratic spin-1 chain, with an even number of sites and periodic boundary conditions, should be symmetric with respect to the origin. It is sufficient, thus, to draw the diagram in one quarter of the plane and then use the symmetry properties for the remaining three.

These symmetry properties allow a remarkable simplification of the classification process. The complete set of states organised according to the number of deviations is listed in the table 5.7 displaying the related  $SU(3)$  quantum numbers, which we are going to represent later on the  $T^3 - Y$  plane.

$m$	$S_{tot}^z$	zeroes	minus	zeroes parity	$T_{tot}^3$	$Y_{tot}$	multiplicity
0	4	0	0	—	2	0	1
1	3	1	0	1 even	$\frac{3}{2}$	1	2
1	3	1	0	1 odd	$\frac{3}{2}$	-1	2
2	2	2	0	2 even	1	2	1
2	2	2	0	1 even 1 odd	1	0	4 (♥)
2	2	2	0	2 odd	1	-2	1
2	2	0	1	—	1	0	4 (♥)
3	1	3	0	2 even 1 odd	$\frac{1}{2}$	1	2 (★)
3	1	3	0	2 odd 1 even	$\frac{1}{2}$	-1	2 (◇)
3	1	1	1	1 even	$\frac{1}{2}$	1	6 (★)
3	1	1	1	1 odd	$\frac{1}{2}$	-1	6 (◇)
4	0	4	0	2 odd 2 even	0	0	1 (♣)
4	0	2	1	2 even	0	2	2
4	0	2	1	1 even 1 odd	0	0	8 (♣)
4	0	2	1	2 odd	0	-2	2
4	0	0	2	—	0	0	6 (♣)

$m$	$S_{tot}^z$	zeroes	minus	zeroes parity	$T_{tot}^3$	$Y_{tot}$	multiplicity
5	-1	3	1	2 even 1 odd	$-\frac{1}{2}$	1	2 ( $\star$ )
5	-1	3	1	2 odd 1 even	$-\frac{1}{2}$	-1	2 ( $\diamond$ )
5	-1	1	2	1 even	$-\frac{1}{2}$	1	6 ( $\star$ )
5	-1	1	2	1 odd	$-\frac{1}{2}$	-1	6 ( $\diamond$ )
6	-2	2	2	2 even	-1	2	1
6	-2	2	2	1 even 1 odd	-1	0	4 ( $\heartsuit$ )
6	-2	2	2	2 odd	-1	-2	1
6	-2	0	3	—	-1	0	4 ( $\heartsuit$ )
7	-3	1	3	1 even	$-\frac{3}{2}$	1	2
7	-3	1	3	1 odd	$-\frac{3}{2}$	-1	2
8	-4	0	4	—	-2	0	1

**Table 5.7:** Four-site pure biquadratic Hamiltonian. Classification of states according to the number of deviations  $m$  (Bethe ansatz approach) and correspondence with quantum numbers  $T^3$  and  $Y$  ( $SU(3)$ -Heisenberg chain approach). Number of spin variables with  $S_i^z = 0, -1$ , and parity of the zeroes site location are needed to calculate the quantum numbers through mapping (3.47). The last column displays the multiplicity of the states.

The graphical representation 5.4 shows perfectly the  $SU(3)$ -symmetric structure of the classification of states according to the number of deviations. However, not all of these states can be classified according to  $SU(2)$  quantum numbers, because they are not eigenstates of the operator  $S_{tot}^2$  and acting on them with the ladder operators  $S^\pm$  we cannot recover the conventional  $SU(2)$  multiplet structure. Fulfilling this purpose requires linear combinations of them, with coefficients extracted using the Bethe ansatz technique.

So, we can clearly identify only the points on the diagram corresponding to eigenstates that are represented by a single state basis also in the  $SU(2)$  classification according to the number of deviations. This is actually possible only for states located on the external hexagon, hosting the states with the lowest or highest number of deviations, which correspond to the most excited states.

For  $m = 0, 8$  at the right and left extremes on the  $x$ -axis, we have the two fully aligned states (blue in the picture). For  $m = 1, 7$  we have the states with just one zero (green in the picture), lying on the half edge of the external sides of the outer hexagon. We have identified even some of the states located on the upper and lower vertices of the outer hexagon, with  $m = 2, 6$  deviations (yellow in the picture) having two isolated zeroes. We can also find states with  $m = 4$  deviations on the upper and lower half-edges of this hexagon.

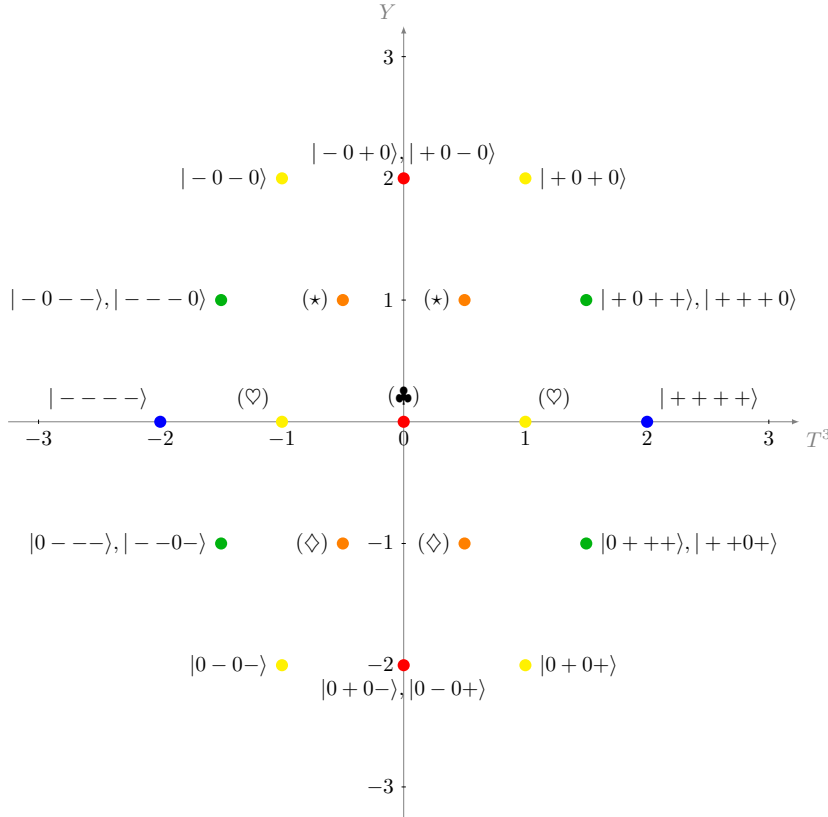


**Figure 5.4:** Four-site Hamiltonian. Graphical representation on the  $T^3 - Y$  plane of the spin-1 four-sites basis states classified by number of deviations  $m$  from the  $|++++\rangle$  state. Symmetry with respect to the spin flip allows the states with  $m$  and  $m' = 8 - m$  deviations to be treated equally. The key to the interpretation of the coloured points in the figure is given by:  $m = 0, 8 \rightarrow$  colour: blue;  $m = 1, 7 \rightarrow$  colour: green;  $m = 2, 6 \rightarrow$  colour: yellow;  $m = 3, 5 \rightarrow$  colour: orange;  $m = 4 \rightarrow$  colour: red.

The only states which certainly belong to the set of eigenstates of the biquadratic model are, in fact, the ones on which the biquadratic Hamiltonian matrix (2.31) does not yield any effect of propagation. As a consequence, they turn out to be degenerate with the fully aligned states. These eigenstates have only isolated zeroes, which entails the absence on the entire chain of pairs of neighbouring spins belonging to the set:

$$|+-\rangle, |-+\rangle, |00\rangle$$

Let us, now, deal with the states of the internal hexagon; its vertices are all eight-fold degenerate, each of them hosting linear combinations of the eight independent states labelled by the corresponding symbols ( $(\diamond)$ ,  $(\heartsuit)$ ,  $(\star)$ ) in the table of states 5.7. They have  $m = 2, 6$  (colour: yellow) deviations

in the right and left external vertices and  $m = 3, 5$  deviations for the upper and lower vertices (colour: orange).

Finally, the most internal point shows an even higher multiplicity: it contains fifteen degenerate Hamiltonian eigenstates built from combinations of states with  $m = 4$  and the corresponding  $SU(3)$  quantum numbers null; they are labelled by the symbol ( $\clubsuit$ ) in table 5.7. Among them we expect to find the singlet, that represents the ground state.

In order to classify thoroughly the structure of the spectrum of the biquadratic Hamiltonian we are supposed to be able to find the decomposition into irreducible representations. These representations form the energy multiplets that we may compare with the numerical results given by the diagonalisation of the equivalent  $SU(3)$  Heisenberg model.

The  $SU(3)$  Heisenberg chain on four sites with periodic boundary conditions  $\lambda_{N+1}^\alpha = \lambda_1^\alpha$ , has the following Hamiltonian

$$\mathcal{H}^{F \otimes A}(J) = J \sum_{\alpha=1}^8 \left[ \lambda_1^\alpha \bar{\lambda}_2^\alpha + \bar{\lambda}_2^\alpha \lambda_3^\alpha + \lambda_3^\alpha \bar{\lambda}_4^\alpha + \bar{\lambda}_4^\alpha \lambda_1^\alpha \right] \quad (5.39)$$

which is the result of the direct product of four  $SU(3)$  representations, two fundamental ones for the odd sites and two antifundamental ones for the even sites. Therefore, we may decompose the Hamiltonian Hilbert space of states into the direct sum of smaller  $SU(3)$  irreducible representations by making use of the graphical technique of composition of representations.

$$\mathfrak{H}^{4sites} = [3] \otimes [\bar{3}] \otimes [3] \otimes [\bar{3}]$$

Starting from the elementary decomposition (two-site chain):

$$[3] \otimes [\bar{3}] = [1] \oplus [8]$$

we may proceed one representation at a time. Here we add the first site:

$$[3] \otimes [\bar{3}] \otimes [3] = ([1] \oplus [8]) \otimes [3]$$

First, let's deal with  $[8] \otimes [3]$ . Figure 5.5 clearly suggests that:

$$[8] \otimes [3] = [15] \oplus [\bar{6}] \oplus [3] \quad (5.40)$$

Therefore, the three-site Hamiltonian Hilbert space is decomposed as follows:

$$[3] \otimes [\bar{3}] \otimes [3] = [3] \oplus ([15] \oplus [\bar{6}] \oplus [3]) \quad (5.41)$$

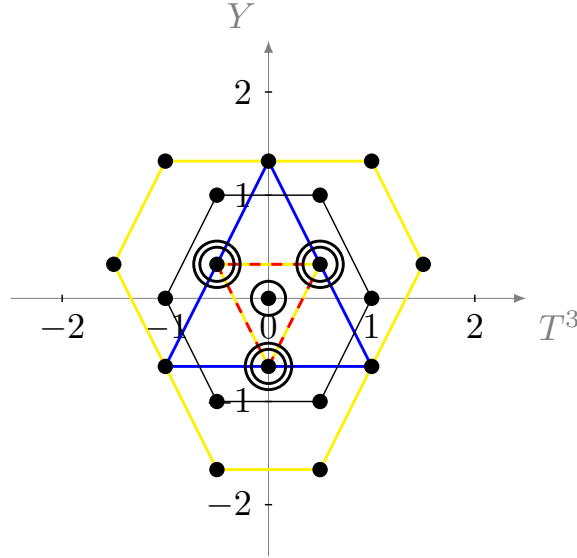


**Figure 5.5:**  $[8] \otimes [3]$  reduction scheme. The decomposition into the sum of irreducible representations is performed employing the graphical technique (see appendix C for examples and explanation). Dots represent states and circles around them indicate the presence of eventual degeneracies. The octet  $[8]$  is drawn in black and the resulting composition with the triplet  $[3]$  gives the sum of three new representations. Colour code:  $[15] \rightarrow$  yellow solid line;  $[\bar{6}] \rightarrow$  blue solid line;  $[3] \rightarrow$  red dashed line.

Let's try a dimensional check, recalling the general formula (B.33) for the dimension of a  $SU(3)$  representation.

$$\begin{aligned} [3] \otimes [\bar{3}] \otimes [3] &\longrightarrow 3^3 = 27 \\ [3] \oplus [15] \oplus [\bar{6}] \oplus [3] &\longrightarrow 3 + 15 + 6 + 3 = 27 \end{aligned} \quad (5.42)$$

Now, we add one further site with antifundamental representation:

$$[3] \otimes [\bar{3}] \otimes [3] \otimes [\bar{3}] = (2[3] \oplus [15] \oplus [\bar{6}]) \otimes [\bar{3}] \quad (5.43)$$

Again, we deal with each product separately, starting with  $[\bar{6}] \otimes [\bar{3}]$ , which yields (figure 5.6):

$$[\bar{6}] \otimes [\bar{3}] = [\bar{10}] \oplus [8] \quad (5.44)$$

Let's proceed then with  $[15] \otimes [\bar{3}]$ , (figure 5.7):

$$[15] \otimes [\bar{3}] = [27] \oplus [10] \oplus [8] \quad (5.45)$$

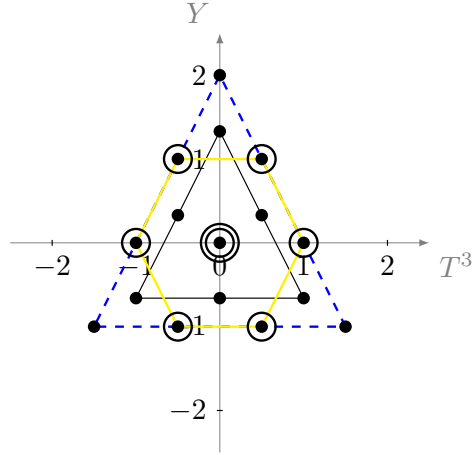


**Figure 5.6:**  $[\bar{6}] \otimes [\bar{3}]$  reduction scheme. Degeneracies are indicated by circled dots. Colour code:  $[\bar{10}] \rightarrow$  blue dashed line;  $[8] \rightarrow$  yellow solid line.

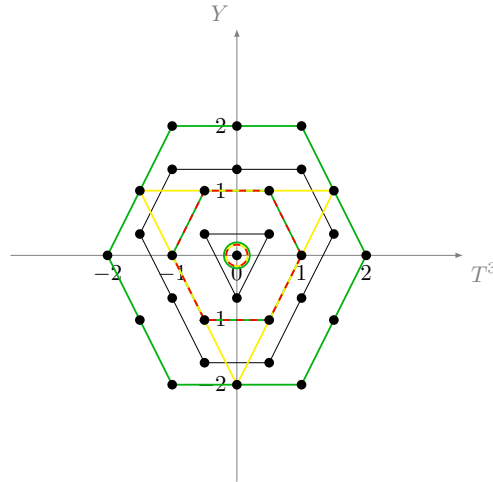


**Figure 5.7:**  $[15] \otimes [\bar{3}]$  reduction scheme. Degeneracies have been withdrawn. Colour code:  $[\bar{10}] \rightarrow$  yellow solid line;  $[8] \rightarrow$  red dashed line;  $[27] \rightarrow$  green solid line.

The final result of the total decomposition for the Hilbert space of a four-site Hamiltonian is:

$$\begin{aligned}
 [3] \otimes [\bar{3}] \otimes [3] \otimes [\bar{3}] &= \\
 &= 2([1] \oplus [8]) \oplus ([27] \oplus [10] \oplus [8]) \oplus ([\bar{10}] \oplus [8]) = \quad (5.46) \\
 &= 2[1] \oplus 4[8] \oplus [\bar{10}] \oplus [10] \oplus [27]
 \end{aligned}$$

Again, let's try a dimensional check:

$$\begin{aligned} [3] \otimes [\bar{3}] \otimes [3] \otimes [\bar{3}] &\longrightarrow 3^4 = 81 \\ 2[1] \oplus 4[8] \oplus [\bar{10}] \oplus [10] \oplus [27] &\longrightarrow 2 + 32 + 10 + 10 + 27 = 81 \end{aligned} \quad (5.47)$$

In the following picture we show the representation decomposition (5.46), where the vertex of the external hexagon are single-degenerate states, the points lying on the half edges are doubly-degenerate, the inner hexagonal vertices are eight-fold degenerate and finally the origin is fifteen-fold degenerate. Summing all over these states, we obtain the 81 eigenstates of the biquadratic Hamiltonian, that correspond to the 81 independent states classified in table 5.7 according to the number of deviations.

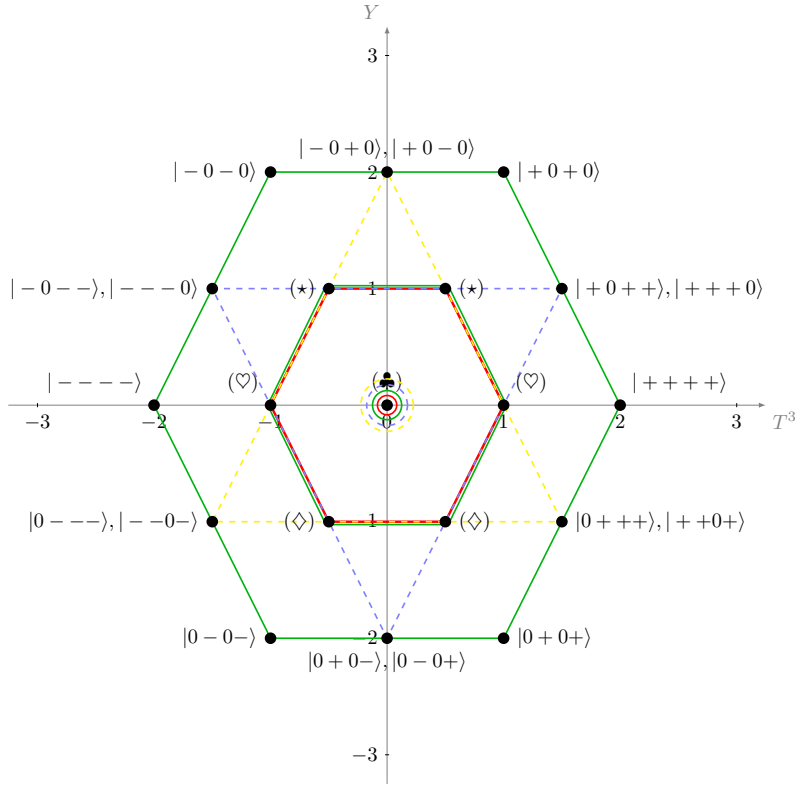


**Figure 5.8:** Four-site pure biquadratic Hamiltonian.  $SU(3)$ -symmetric structure and decomposition into a sum of irreducible representations. Eigenstates in the outer hexagon can be identified in the usual  $S^z$ -eigenstate basis. Eigenstates lying on the inner hexagon result from linear combinations of states of the table 5.7 labelled by the same symbol. Coloured lines display the patterns of the multiplets occurring in eq. (5.46). Degeneracies were thoroughly discussed before because they are too high to be shown as circled dots on the diagram. Colour code is the following one:  $[8] \rightarrow$  red solid;  $[10] \rightarrow$  light blue dashed;  $[\bar{10}] \rightarrow$  yellow dashed;  $[27] \rightarrow$  green solid.

Concluding our analysis of this model, we may have Mathematica evaluate for us the energy eigenvalues for the  $81 \times 81$  matrix representing the Hamiltonian operator. The results are listed in table 5.8:

eigenvalue $E/J$	multiplicity	$SU(3)$ multiplets
$-40/3$	1	[1]
$-22/3$	8	[8]
$-16/3$	1	[1]
$-10/3$	16	[8] $\oplus$ [8]
$2/3$	8	[8]
$2/3$	47	[27] $\oplus$ [10] $\oplus$ [10]

**Table 5.8:** Four-site  $SU(3)$  Heisenberg chain with alternate representations and periodic boundary conditions. Diagonalisation of the Hamiltonian and counting of the energy eigenvalue degeneracies. The eigenstates gather into invariant subspaces with dimensions corresponding to the sum of the  $SU(3)$  multiplets resulting from decomposition (5.46). Note the structure of the lowest energy eigenstates: the first excited state is eight-fold degenerate (octet) followed by an other singlet as the second excited state.

### 5.3 Biquadratic Hamiltonian on a six-site chain

The shortest non trivial chain, which may show the general properties of the model is made up of six sites. In fact, in the four-site case, there is no room for other than a couple of two-strings, which prevents us from detecting any interaction among them. The Bethe ansatz classification of states according to the number of deviations is listed in the following table.

$m$	$S_{tot}^z$	zeroes	minus	zeroes parity	$T_{tot}^3$	$Y_{tot}$	multiplicity
0	6	0	0	—	3	0	1
1	5	1	0	1 even	$\frac{5}{2}$	1	3
1	5	1	0	1 odd	$\frac{5}{2}$	-1	3
2	4	2	0	2 even	2	2	3
2	4	2	0	1 even 2 odd	1	0	9
2	4	2	0	2 odd	2	-2	3
2	4	0	1	—	2	0	6
3	3	3	0	3 even	$\frac{3}{2}$	3	1
3	3	3	0	2 even 1 odd	$\frac{3}{2}$	1	9
3	3	3	0	2 odd 1 even	$\frac{3}{2}$	-1	9
3	3	3	0	3 odd	$\frac{3}{2}$	-3	1
3	3	1	1	1 even	$\frac{3}{2}$	1	15
3	3	1	1	1 odd	$\frac{3}{2}$	-1	15
4	2	4	0	3 even 1 odd	1	2	3
4	2	4	0	2 odd 2 even	1	0	9
4	2	4	0	3 odd 1 even	1	-2	3
4	2	2	1	2 even	1	2	12
4	2	2	1	1 even 1 odd	1	0	36
4	2	2	1	2 odd	1	-2	12
4	2	0	2	—	1	0	15
5	1	5	0	3 even 2 odd	$\frac{1}{2}$	1	3
5	1	5	0	3 odd 2 even	$\frac{1}{2}$	-1	3
5	1	3	1	3 even	$\frac{1}{2}$	3	3
5	1	3	1	2 even 1 odd	$\frac{1}{2}$	1	27
5	1	3	1	2 odd 1 even	$\frac{1}{2}$	-1	27
5	1	3	1	3 odd	$\frac{1}{2}$	-3	3
5	1	1	2	1 even	$\frac{1}{2}$	1	30
5	1	1	2	1 odd	$\frac{1}{2}$	-1	30

$m$	$S_{tot}^z$	zeroes	minus	zeroes parity	$T_{tot}^3$	$Y_{tot}$	multiplicity
6	0	6	1	3 even 3 odd	0	0	1
6	0	4	1	3 even 1 odd	0	2	6
6	0	4	1	2 even 2 odd	0	0	18
6	0	4	1	3 even 1 odd	0	-2	6
6	0	2	2	2 even	0	2	18
6	0	2	2	1 even 1 odd	0	0	54
6	0	2	2	2odd	0	-2	18
6	0	0	3	-	0	0	20
7	-1	5	1	3 even 2 odd	$-\frac{1}{2}$	1	3
7	-1	5	1	3 odd 2 even	$-\frac{1}{2}$	-1	3
7	-1	3	2	3 even	$-\frac{1}{2}$	3	3
7	-1	3	2	2 even 1 odd	$-\frac{1}{2}$	1	27
7	-1	3	2	2 odd 1 even	$-\frac{1}{2}$	-1	27
7	-1	3	2	3 odd	$-\frac{1}{2}$	-3	3
7	-1	1	2	1 even	$-\frac{1}{2}$	1	30
7	-1	1	2	1 odd	$-\frac{1}{2}$	-1	30
8	2	4	2	3 even 1 odd	-1	2	3
8	2	4	2	2 odd 2 even	-1	0	9
8	2	4	2	3 odd 1 even	-1	-2	3
8	2	2	3	2 even	-1	2	12
8	2	2	3	1 even 1 odd	-1	0	36
8	2	2	3	2 odd	-1	-2	12
8	2	0	4	-	-1	0	15
9	-3	3	3	3 even	$-\frac{3}{2}$	3	1
9	-3	3	3	2 even 1 odd	$-\frac{3}{2}$	1	9
9	-3	3	3	2 odd 1 even	$-\frac{3}{2}$	-1	9
9	-3	3	3	3 even	$-\frac{3}{2}$	-3	1
9	-3	1	4	1 even	$-\frac{3}{2}$	1	15
9	-3	1	4	1 odd	$-\frac{3}{2}$	-1	15
10	-4	2	4	2 even	-2	2	3
10	-4	2	4	1 even 1 odd	-2	0	9
10	-4	2	4	2 odd	-2	-2	3
10	-4	0	5	-	-2	0	6
11	-5	1	5	1 even	$-\frac{5}{2}$	1	3
11	-5	1	5	1 odd	$-\frac{5}{2}$	-1	3
12	-6	0	6	-	-3	0	1

**Table 5.9:** Six-site Hamiltonian. Classification of states according to the number of deviations  $m$  (Bethe ansatz approach) and correspondence with quantum numbers  $T^3$  and  $Y$  ( $SU(3)$  Heisenberg chain approach). Number of spin variables with  $S_i^z = 0, -1$ , and parity of the zeroes site location are needed to calculate the quantum numbers with the mapping (3.47). The last column displays the multiplicity of the states.

The same method of evaluating the  $SU(3)$  quantum numbers was employed, using the mapping (3.47). However, this time the degeneracies are indeed higher because of the increasing allowed permutations of spins along the chain. The total number of independent states is given by  $3^6 = 729$ . The  $S_{tot}^z = 0$  alone contains 141 independent states that have to be linearly combined in order to find the proper ground state of the model.

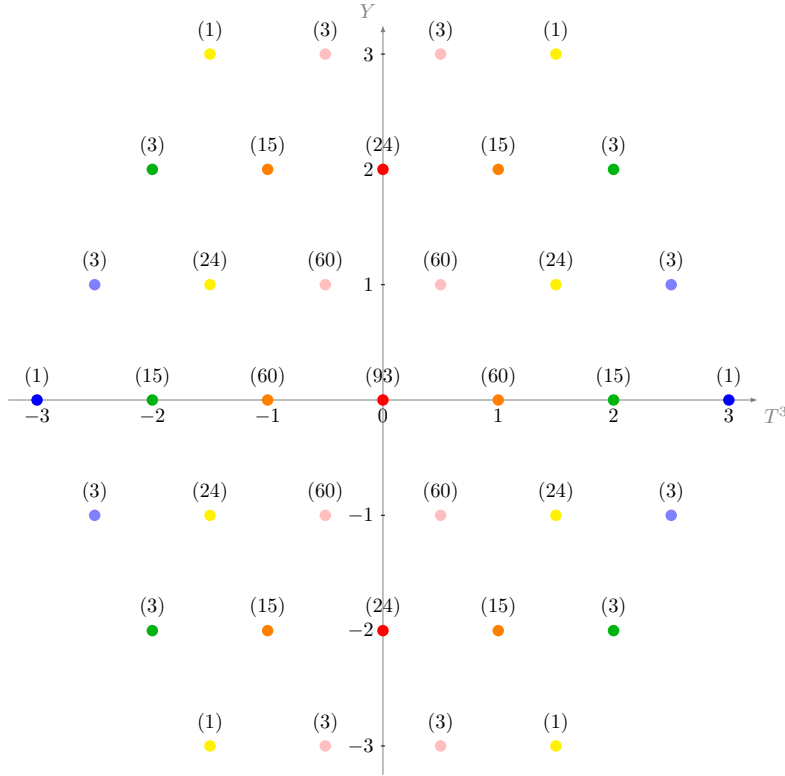


**Figure 5.9:** Six-site Hamiltonian. Graphical representation on the  $T^3 - Y$  plane of the spin-1 six-sites basis states classified by number of deviations  $m$  from the  $|+++++)\rangle$  state. Degeneracies of each couple of  $SU(3)$  quantum numbers is indicated just over each point of the diagram. The key to the interpretation of the coloured points in the figure is given by:  $m = 0, 12 \rightarrow$  colour: blue;  $m = 1, 11 \rightarrow$  colour: light blue;  $m = 2, 10 \rightarrow$  colour: green;  $m = 3, 9 \rightarrow$  colour: yellow;  $m = 4, 8 \rightarrow$  colour: orange;  $m = 5, 7 \rightarrow$  colour: pink;  $m = 6 \rightarrow$  colour: red.

The technique employed to decompose the Hilbert space of eigenstates of the biquadratic Hamiltonian is exactly the same outlined in the former sections. We just need to add two more representations (a fundamental and an antifundamental one) which correspond to the two spin-1 variables located on the two additional sites of the chain.

$$\mathfrak{H}^{6sites} = [3] \otimes [\bar{3}] \otimes [3] \otimes [\bar{3}] \otimes [3] \otimes [\bar{3}]$$

This requires some effort in the composition of  $SU(3)$  representations, but it is definitely worth it, because the results achieved by means of the graphical method previously explained, show the  $SU(3)$  multiplet structure of the eigenstates of the biquadratic model.

Starting from the four sites Kronecker product (see (5.46)):

$$[3] \otimes [\bar{3}] \otimes [3] \otimes [\bar{3}] = 2[1] \oplus 4[8] \oplus [\bar{10}] \oplus [10] \oplus [27]$$

we add one site, that is represented by the fundamental representation  $[3]$ . We need to evaluate the the product:

$$[27] \otimes [3] = [42] \oplus [\bar{24}] \oplus [15]$$

that may be written according to the notation presented in appendix C, as:

$$D(2, 2) \otimes D(1, 0) = D(3, 2) \oplus D(1, 3) \oplus D(2, 1)$$

This notation is necessary to distinguish among representations with the same dimensions, but different structure, such as  $[15]$  and  $[15]^*$ , which have indeed different shapes because the first one is hexagonal and the second one is triangular.

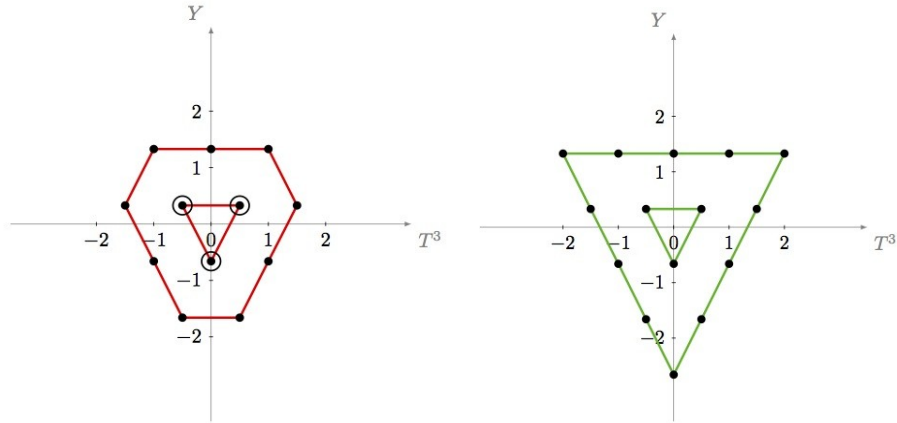


**Figure 5.10:** Two different  $SU(3)$  representations with the same dimensions, but different internal structure. The structure of the representation  $D(p, q)$  is uniquely determined by the two numbers  $p$  and  $q$ , which indicate the numbers of points on two consecutive edges of the general hexagonal form of the  $SU(3)$  multiplet.  $D(2, 1) = [15]$  has an hexagonal shape, while  $D(4, 0) = [15]^*$  has a triangular shape. (Further details on  $SU(3)$  representations may be found in appendix C).

Other useful relations for the decomposition are given by:

$$[10] \otimes [3] = [15] \oplus [15]^* \Leftrightarrow D(3,0) \otimes D(1,0) = D(2,1) \oplus D(4,0)$$

$$[\overline{10}] \otimes [3] = [\overline{24}] \oplus [\overline{6}] \Leftrightarrow D(0,3) \otimes D(1,0) = D(1,3) \oplus D(0,2)$$

Hence, the final form of the five-site Hilbert space decomposition:

$$\begin{aligned} [3] \otimes [3] \otimes [3] \otimes [3] \otimes [3] = \\ 2[3] \oplus 4([15] \oplus [\overline{6}] \oplus [3]) \oplus ([\overline{24}] \oplus [\overline{6}]) \oplus ([15] \oplus [15]^*) \oplus ([42] \oplus [\overline{24}] \oplus [15]) \end{aligned} \quad (5.48)$$

We need now to add the last one site, that means a Kronecker product with an antifundamental representation. The missing pieces we need to accomplish this purpose are:

$$[15]^* \otimes [\overline{3}] = [35] \oplus [10] \Leftrightarrow D(4,0) \otimes D(0,1) = D(4,1) \oplus D(3,0)$$

$$[\overline{24}] \otimes [\overline{3}] = [\overline{35}] \oplus [27] \oplus [\overline{10}] \Leftrightarrow D(1,3) \otimes D(0,1) = D(1,4) \oplus D(2,2) \oplus D(0,3)$$

$$[42] \otimes [\overline{3}] = [27] \oplus [35] \oplus [64] \Leftrightarrow D(3,2) \otimes D(0,1) = D(2,2) \oplus D(4,1) \oplus D(3,3)$$

Finally, we get the ultimate decomposition of the Hilbert space of the six-site biquadratic Hamiltonian into  $SU(3)$  irreducible representations:

$$\begin{aligned} \mathfrak{H}^{6sites} &= [3] \otimes [\overline{3}] \otimes [3] \otimes [\overline{3}] \otimes [3] \otimes [\overline{3}] \\ &= 6[1] \oplus 17[8] \oplus 7[10] \oplus 7[\overline{10}] \oplus 9[27] \oplus 2[35] \oplus 2[\overline{35}] \oplus [64] \end{aligned} \quad (5.49)$$

which has been calculated via the graphical composition technique and is displayed in fig. 5.11.

The irreducible representations forming the  $SU(3)$  multiplets are nothing other than the degenerate eigenstates in the energy spectrum of the biquadratic Hamiltonian. The related eigenvalues will be calculated with the assistance of Mathematica working on the diagonalisation of the equivalent  $SU(3)$  Heisenberg chain (3.48) with  $N = 6$ .

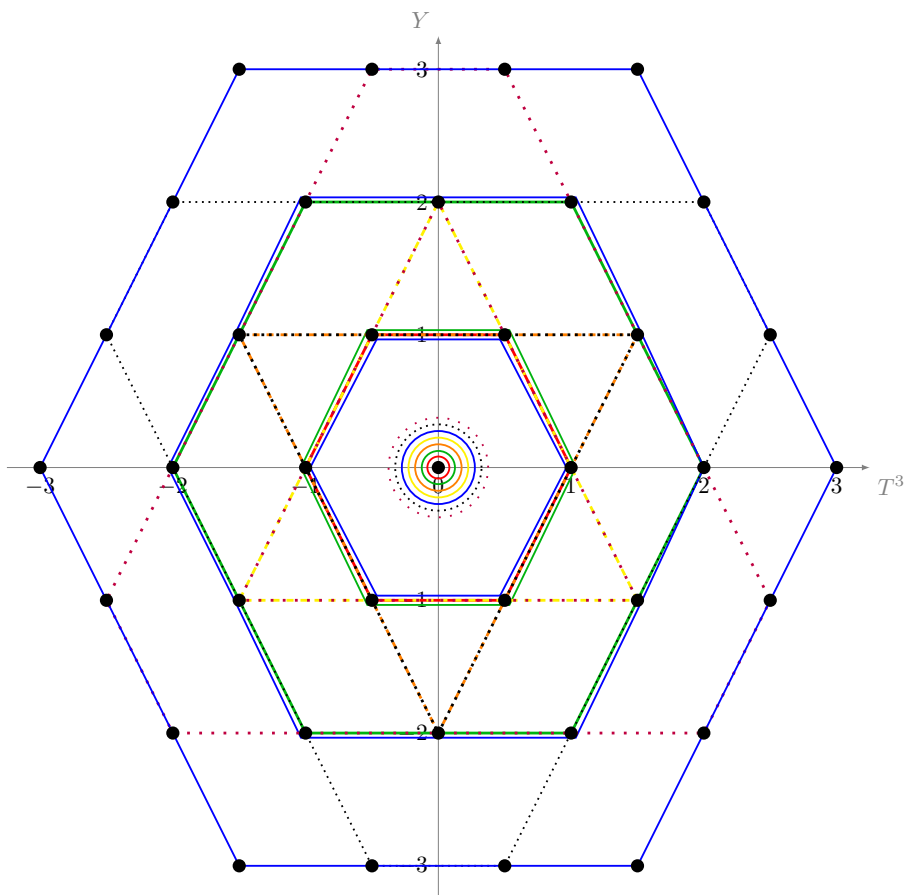


**Figure 5.11:** Six-site Hamiltonian.  $SU(3)$ -symmetric structure and decomposition into a sum of irreducible representations. Coloured lines display the patterns of the multiplets occurring in eq. (5.49). Degeneracies are not shown as circled dots, because they are very high indeed (see fig. 5.9 for degeneracies). Colour code is the following one:  $[8] \rightarrow$  red dashed;  $[10] \rightarrow$  orange dashed;  $[\overline{10}] \rightarrow$  yellow dashed;  $[27] \rightarrow$  green solid;  $[35] \rightarrow$  black dotted;  $[\overline{35}] \rightarrow$  purple dotted;  $[64] \rightarrow$  blue solid.

Table 5.10 lists the energy eigenvalues with the related degeneracies. This time, making the identification with the  $SU(3)$  multiplets is a little bit trickier because of the increasing number of allowed combinations of representations. For example, the ten-fold degenerate eigenstate with  $E/J = -8$  may be actually given by  $[8] \oplus [1] \oplus [1]$  or by  $[10]$ . Making the assumption that non centrally symmetric representations, that are conjugated one of the other ( $[10]$  and  $[\overline{10}]$ ), should appear always in pairs, because of the global central symmetry of the entire chain with an even number of sites, and comparing the lowest excited state with the eight-site Hamiltonian spectrum 6.1 that shows the same behaviour, we may establish that this is most likely the composition of an octet and two singlets.

$E/J$	multiplicity	$SU(3)$ multiplets
-18.5498	1	[1]
-14.3421	8	[8]
-14.	1	[1]
-11.0578	16	[8] $\oplus$ [8]
-9.58258	16	[8] $\oplus$ [8]
-8.	10	[8] $\oplus$ [1] $\oplus$ [1]
-6.	27	[27]
-5.6651	16	[8] $\oplus$ [8]
-5.4641	40	[10] $\oplus$ [10] $\oplus$ [10] $\oplus$ [10]
-4.62317	8	[8]
-4.	54	[27] $\oplus$ [27]
-3.45017	1	[1]
-2.	48	[10] $\oplus$ [10] $\oplus$ [10] $\oplus$ [10] $\oplus$ [8]
-1.227706	16	[8] $\oplus$ [8]
-0.417424	16	[8] $\oplus$ [8]
0.	54	[27] $\oplus$ [27]
0.965226	8	[8]
1.4641	40	[10] $\oplus$ [10] $\oplus$ [10] $\oplus$ [10]
2.	27	[27]
4.	322	[1] $\oplus$ 2[8] $\oplus$ [10] $\oplus$ [10] $\oplus$ 3[27] $\oplus$ 2[35] $\oplus$ 2[35] $\oplus$ [64]

**Table 5.10:** Six-site  $SU(3)$  Heisenberg chain with alternate representations and periodic boundary conditions. Diagonalisation of the Hamiltonian and counting of the energy eigenvalue degeneracies. Some suppositions have been made on the possible correspondence between invariant subspaces and the  $SU(3)$  multiplets resulting from decomposition (5.49). Note the structure of the lowest energy eigenstates: the first excited state once again eight-fold degenerate (octet) followed by an other singlet as the second excited state.



## Chapter 6

# Eight-site Hamiltonian and new results

In this chapter we will deal with the eight-site biquadratic chain mainly employing a numerical approach, thanks to the assistance of Mathematica, which allows us to diagonalise the matrix representing the Hamiltonian operator, even though its dimension ( $3^8 \times 3^8$ ) becomes too high to evaluate even the decomposition coefficients of the eigenvectors on the Hilbert space canonical basis.

We will focus our analysis on the ground state and the gap with the lowest excited states. It is clear that, since we are far away from the thermodynamic limit, the ground state is single-degenerate, however the lowest excited is represented by another singlet which will become degenerate with it in the infinite-volume limit.

The remaining part is dedicated to the perturbation of the pure-biquadratic interaction by means of the introduction of a **bilinear term**, having the form of the usual spin-1 **Heisenberg Hamiltonian**. We will analyse the influence created by the additional term, which breaks the  $SU(3)$  symmetry of the model, leading to a splitting of the degenerate states of the biquadratic spectrum. We will examine at first small and then larger values of the coupling for the bilinear term, moving away from the biquadratic point in the phase diagram, towards the two nearest known points, namely the antiferromagnetic-ferromagnetic phase transition (point D;  $\Theta = \frac{3}{4}\pi$ ) and the Tahkhtajan and Babudjian model (point B;  $\frac{\pi}{4}$ ).

### 6.1 Comments on the ground state of the pure-biquadratic model

The ground state for the biquadratic spin-1 Hamiltonian in the infinite volume limit is supposed to be doubly degenerate [17, 26]. In fact, the purely

biquadratic model (point C) lies in the dimerised region of the phase diagram (cfr. fig.1.1).

On the other hand, for a finite size chain the ground state is unique and it can be identified with a singlet representation according to the  $SU(3)$  classification. For the two- four- and six-site cases we have shown explicitly that the lowest excited state belongs to an  $SU(3)$  octet representation, thus it is eight-fold degenerate. The second excited state in the four- and six-site chains is represented by a singlet again, however this pattern is broken once we come to the eight-site case.

In fact, somewhere between the six-site and the eight-site model there is a crossing of the energy levels of the octet and the second singlet, that is perfectly consistent with the numerical work displayed in [15].

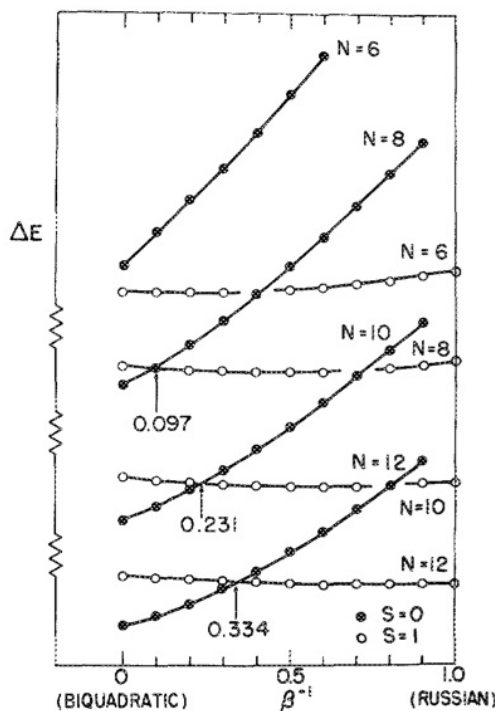


**Figure 6.1:** Spin-1 bilinear-biquadratic Hamiltonian. The image displays, on different energy scales, the trend of the singlet and triplet excitations of a spin-1 chain with an even number of sites and periodic boundary conditions showing the dependence of the excitation gap on the coupling  $\beta$ , determining the characteristic behaviour of the bilinear-biquadratic Hamiltonian (6.2). The range of  $\beta$  covers the phase space (fig. 1.1) included between the Takhtajan and Babudjian model (point B) and the pure-biquadratic antiferromagnetic model (point C). Different lengths of the chain ( $N = 6, 8, 10, 12$ ) are plotted and the corresponding value of the parameter  $\beta$ , where the crossing between the singlet and the triplet excitation occurs, is pointed out. (Picture taken from [15]).

In the analysis of the bilinear-biquadratic model for the parameter range  $0 < \beta^{-1} < 1$ , the singlet excitation was found to cross the triplet one, becoming the lowest excited states for  $N > 6$ . This behaviour could suggest the progressive closure of the energy gap between the first and the second singlet for increasing number of sites leading to a doubly-degenerate ground states in the  $N \rightarrow \infty$  limit. This hypothesis is further confirmed by numerical results obtained in [13], where longer chains ( $N = 8, 10, 12$ ) have been studied. Those numerical simulations support the results obtained analytically by means of the equivalence with other known integrable models (spin 1/2 XXZ and nine-state Potts model). In particular, approaching the thermodynamic limit we should find a small but **non vanishing gap** ( $\Delta = 0.173178\dots$ ) between the ground-state, being doubly-degenerate, and the first excited one. These states are represented respectively by two  $SU(3)$  singlets and eight degenerate states belonging to the octet representation.

Picturing this phenomenon by means of the valence-bond representation [17, 2], we can immediately see that, imposing periodic boundary conditions on a chain with an even number of sites we may have two graphically equivalent ground states, that are mapped one into the other performing a translation of one lattice constant.

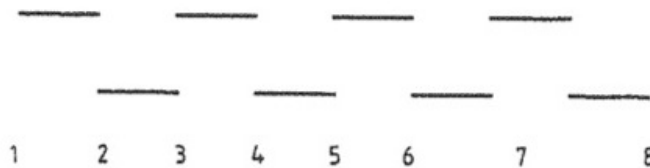


**Figure 6.2:** Two degenerate ground states of the pure biquadratic spin-1 Hamiltonian in the infinite volume limit  $N \rightarrow \infty$ . The ground state is dimerised, i.e. valence bonds occur between couples of spins lying on adjacent sites. Imposing periodic boundary conditions on a chain with an even number of sites, there are two equally probable configurations given by  $N/2$  valence bonds between sites with indices  $2i-1$  and  $2i$  (upper configuration displayed in the figure) or an equal number of bonds between sites with indices  $2i$  and  $2i+1$  (lower configuration). (Picture taken from [2]).

These two states become degenerate only in the limit  $N \rightarrow \infty$  and under the assumptions of even number of sites and periodic boundary conditions. Otherwise, i.e. while dealing with finite size chains, the two singlets are not degenerate. We have previously discussed the cases  $N = 4, 6$ , for which the second singlet is located at even higher energies than the octet, but increasing the number of sites ( $N \geq 8$ ), it crosses the octet line becoming the lowest excited state. The reason behind the finite-size energy splitting between the two thermodynamically equivalent singlets is always represented by symmetry. We may find that the finite-size ground state is given by a

*totally symmetric* linear combination under the translation of one lattice, whereas the second singlet proves to be *totally antisymmetric* under the translation of one lattice constant. Working in the the conventional  $SU(3)$  notation with the basis  $(|u\rangle, |d\rangle, |s\rangle)$  and recalling the equivalence with  $S^z$  eigenstates, this symmetries can be checked out easily for the shortest cases of chains, for which it is possible to have Mathematica calculate the Hamiltonian eigenvectors.

## 6.2 Eight-site Hamiltonian

In this section we will discuss the eight-site Hamiltonian, starting from the numerical diagonalisation of the pure-biquadratic model, which we focused on until now. The number of sites is sufficiently large to guarantee that the most of the characteristic features of the spin-1 biquadratic Hamiltonian will emerge. The number of eigenstates ( $3^8 = 6561$ ) has definitely become very large, but we draw attention just on the lowest energy states, which can always be classified according to  $SU(3)$  representations. Table 6.1 collects the first lowest energy eigenvalues of the  $SU(3)$  Heisenberg model related to the spin-1 biquadratic Hamiltonian.

$E/J$	multiplicity	$SU(3)$ multiplets
-12.0608	1	[1]
-10.5503	8	[1]
-10.4191	8	[8]
-9.13004	16	[8] $\oplus$ [8]
-8.29042	16	[8] $\oplus$ [8]
-7.86913	8	[8]
-7.74755	2	[1] $\oplus$ [1]
-7.70059	16	[8] $\oplus$ [8]
-7.33333	2	[1] $\oplus$ [1]
-6.91356	27	[27]
-6.64186	16	[8] $\oplus$ [8]

**Table 6.1:** Eight-site  $SU(3)$  Heisenberg chain with alternate representations and periodic boundary conditions. Numerical diagonalisation of the Hamiltonian and counting of the energy eigenvalue degeneracies. The total number amounts to 6561, but only the first ones have been displayed, with the associated  $SU(3)$  decomposition into irreducible representations. Note that the structure of the lowest energy eigenstates has changed: now the first excited is an other singlet, while the eight degenerate states of the octet form the second excited state.

Here we have a numerical confirmation of the doubly-degenerate structure of the ground state in thermodynamic limit; in fact, the two lowest

lying states of the spectrum are singlets, which represent the formerly discussed symmetric and antisymmetric combinations, the antisymmetric one being the first excited state in this finite-size system.

Let's introduce now the bilinear interaction term in order to study the behaviour of the spin-1 model under small perturbations from the biquadratic antiferromagnetic point. The additional Hamiltonian will be expressed according to the convenient mapping outlined in section 3.3, which leads to the equivalence relation (3.47), which holds once the substitutions  $S_{2i}^x \rightarrow -S_{2i}^x$  and  $S_{2i}^z \rightarrow -S_{2i}^z$  have been performed. Operating in the same way we find the formulation of the spin-1 bilinear Hamiltonian in terms of Gell-Mann matrices:

$$\begin{aligned} \mathcal{H}_{8sites}^{bil}(J) &= J \sum_{i=1}^8 (-S_i^x \cdot S_{i+1}^x + S_i^y S_{i+1}^y - S_i^z S_{i+1}^z) = \\ &= \sum_{i=1}^8 \left[ -\frac{1}{2} (-\lambda_i^4 \lambda_{i+1}^4 + \lambda_i^6 \lambda_{i+1}^6 + \lambda_i^4 \lambda_{i+1}^6 + \lambda_i^4 \lambda_{i+1}^4) + \right. \\ &\quad \left. + \frac{1}{2} (\lambda_i^5 \lambda_{i+1}^5 + \lambda_i^7 \lambda_{i+1}^7 - \lambda_i^5 \lambda_{i+1}^7 - \lambda_i^7 \lambda_{i+1}^5) - \lambda_i^3 \lambda_{i+1}^3 \right] \end{aligned} \quad (6.1)$$

We will proceed by evaluating the now bilinear-biquadratic Hamiltonian eigenstates gradually increasing the contribution of the bilinear term.

$$\mathcal{H}(J, \beta) = \mathcal{H}_{8sites}^{bil}(J) - \beta \mathcal{H}_{8sites}^{biQ}(J) = J \beta \sum_{i=1}^8 \left[ \beta^{-1} \vec{S}_i \cdot \vec{S}_{i+1} - (\vec{S}_i \cdot \vec{S}_{i+1})^2 \right] \quad (6.2)$$

The coupling is represented by  $\beta = \tan \Theta$ , where  $\Theta$  is the usual parameter employed to describe the spin-1 bilinear-biquadratic phase space in chapter 1. In this parametrisation, the biquadratic Hamiltonian corresponds to the limit  $\beta \rightarrow \infty$ .

We may start with small perturbations  $|\beta| < 0.1$ , in both directions of the round phase space, recalling that with  $\beta > 0$  we are moving towards the Haldane phase transition, which is represented by the (Tahkhtajan Babudjian) russian model, corresponding to the value  $\beta = 1$ , i.e. equal contributions but opposite signs in the bilinear and biquadratic terms; on the contrary with  $\beta < 0$  we are moving towards the antiferromagnetic-ferromagnetic phase transition, which is an  $SU(3)$ -symmetric model, corresponding to the value  $\beta = -1$ , i.e. equal contributions and concurring signs in the bilinear and biquadratic terms.

The first basic observation we can make when the exchange is not purely biquadratic anymore, is that the **SU(3) symmetry is broken**. In the following analysis we will restrict ourselves to the ten lowest energy eigenstates which correspond to the  $SU(3)$  representations  $[1] \oplus [1] \oplus [8]$  in the

biquadratic model. The octet states, decomposing into its elements, cause a split of the energy spectrum. However, since the global bilinear-biquadratic model is still  $SU(2)$ -invariant, the splitting of the octet yields the sum of a two  $SU(2)$  multiplets, i.e. a **triplet** and a **quintet**. In the case  $\beta > 0$  the triplet states lie under the quintet ones, while for  $\beta < 0$  the quintet states are in fact the ones with lower energy.

The triplet and the quintet configurations are clearly recognisable in the spectrum as long as the coupling constant  $\beta^{-1}$  of the bilinear model stays in the range  $|\beta| < 0.1$ . Figure 6.3 shows the energy gap between the first nine excited states and the ground state. Only three leading deviation directions manifestly appear in this picture. This is due to the fact that, other than the quintet and the triplet states, one more state, the **second singlet**, is accounted into these pictures. Its energy does not cross the two lower lines of the triplet and the quintet, for  $\beta > 0$  and  $\beta < 0$  respectively. Thus, it remains the first excited state in this range of the parameter. As  $|\beta^{-1}|$  increases, its value comes closer to the triplet one (for  $\beta > 0$ ) and to the quintet one (for  $\beta < 0$ ).

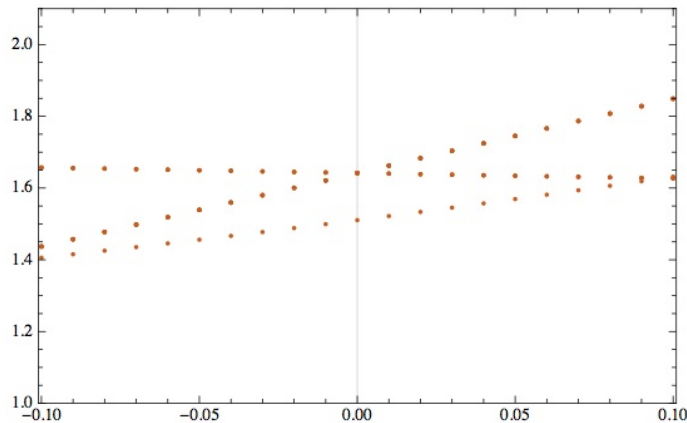


**Figure 6.3:**  $SU(3)$  equivalent model to the bilinear-biquadratic Hamiltonian. Dependence of the first nine excited states of the model (plotted with their relative gap from the ground state singlet) on the value of the parameter  $\beta^{-1}$  spacing the range  $[-0.1, 0.1]$ . Small perturbations from the pure-biquadratic model cause the splitting of the octet into triplet and quintet states, the former lying lower in the  $\beta > 0$  case, the latter in the  $\beta < 0$  case. The second singlet (i.e. the antisymmetric one) is still the first excited state in this parameter range. It will cross the triplet line approximately at  $\beta^{-1} = 0.1$  and the quintet line at  $\beta^{-1} = -0.2$ , becoming then a higher excited state.

Extending the range of the parameter to reach the two transition points at  $\beta = \pm 1$  we can observe two very different behaviours of the energy gap of the first excited states, displayed in figure 6.4.

Let's start with the  $\beta > 0$  region. Increasing the influence of the bilinear

term of the Hamiltonian going from  $\beta = \infty$  to  $\beta = 1$ , we notice a **crossing point** between the triplet state and the second singlet, which from  $\beta^{-1} = 0.01$  on lies above the triplet. We stress the fact that this result is consistent with what was found in [15] where  $\beta^* = 0.97$  for a chain of eight sites. This location of the singlet between the triplet and the quintet remains fixed while increasing the value of  $\beta^{-1}$  until we reach the russian model. This point of the phase diagram (B in fig. 1.1) is endowed with a  $SU(2)_2$  symmetry with  $k = 2$ , which means that in the thermodynamic limit it is supposed to have a four-fold degenerate ground state. In the finite-size case we are dealing with at the moment, we may see a hint at this kind of behaviour of the system, in the fact that the triplet state remains the lowest excited state for the system at  $\beta > 0$ , while the second singlet and the quintet state are the second and third excited states, respectively. The gap between the latter ones and the triplet manifestly increases as  $\beta$  decreases towards one. The triplet state gap, on the contrary, actually stays constant in the whole  $0 < \beta^{-1} < 1$  range, while the gap with the other excited states rapidly increases. This is a strong suggestion that in the thermodynamic limit the first-excited gap may close leading to the expected four-fold degenerate ground state for the the critical point at  $\beta = 1$ .

Let's see, now what happens in the opposite region of the phase space, namely  $\beta < 0$ . In the near biquadratic region, the same pattern as before is displayed, apart from the fact that the lowest lying states among the octet are now belonging to the quintet (coupling reversal leads to energy eigenstate structure reversal), until we reach the crossing line of these states at  $\beta^{-1} = 0.02$ . Expanding further on our parameter range it is possible to single out the behaviour of the singlet state just until we reach the value  $\beta^{-1} = -0.60$ , because from there on the singlet does not belong to the ten first excited states anymore, but higher multiplets begin to descend under its energy line. Eventually we come to a point represented by  $\beta = -1$  in which the ground state appears to be forty-five-fold degenerate. This happens because the antiferromagnetic-ferromagnetic phase transition point is again characterised by a  $SU(3)$  symmetry (45 may be decomposed into  $SU(3)$  centrally symmetric representations like  $2[1] \oplus 2[8] \oplus [27]$ ).

The occurrence of this symmetry is traceable in the finite-size systems too, because it is essentially built on the equivalence to the  $SU(3)$ -Heisenberg chain with the same kind of representation on each site (see appendix C). As a consequence of this symmetry a large amount of previously higher excited states cross the singlet line as we move towards  $\beta = -1$  and come together to build the fundamental state of the bilinear-biquadratic model at  $\beta = -1$ .

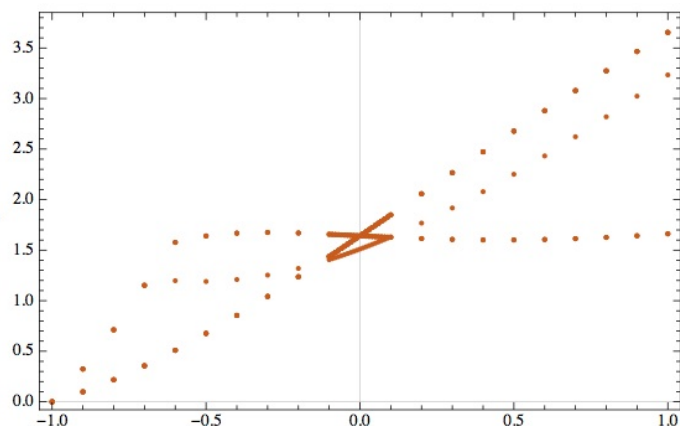


**Figure 6.4:**  $SU(3)$  equivalent model to the bilinear-biquadratic Hamiltonian. Dependence of the first nine excited states of the model (plotted with their relative gap from the ground state singlet) on the value of the parameter  $\beta^{-1}$  spacing the range  $[-1, 1]$ . Expanding the graph to include larger perturbations from the pure biquadratic model, we get very different results for the two parts of the energy spectrum. While for  $\beta > 0$  the triplet gap is almost constant and the singlet and the quintet, which are the second and third excited states, gradually increase their gap; when  $\beta < 0$  the first nine excited state show a rapidly decreasing energy gap with the ground state, all of them lying under the singlet state line from  $\beta^{-1} = -0.6$  down.

The set of images figg. 6.5, 6.6 and 6.7 conclude our analysis of spectrum of the bilinear-biquadratic model reproducing the gap between the ground state and the first excited state as a function of  $\beta^{-1}$ . However, that the lowest excite state is different in each region of the parameter space, because of the increasing influence of the bilinear term, which causes the splitting of the lines of the biquadratic spectrum. Here's a sketch of the gap structure according to our analysis:

- $-0.9 \leq \beta^{-1} \leq -0.2 \rightarrow$  the first excited state is a **quintet**, its gap with the singlet ground state rapidly decreasing as  $\beta$  approaches the value  $-1$ .
- $-0.2 < \beta^{-1} < 0.1 \rightarrow$  the first excited state an other **singlet**, just as it happens for the biquadratic model  $\beta^{-1} = 0$ .
- $0.1 \leq \beta^{-1} \leq 1 \rightarrow$  the first excited state is a **triplet** state and its gap with the ground state is nearly constant throughout this whole range.

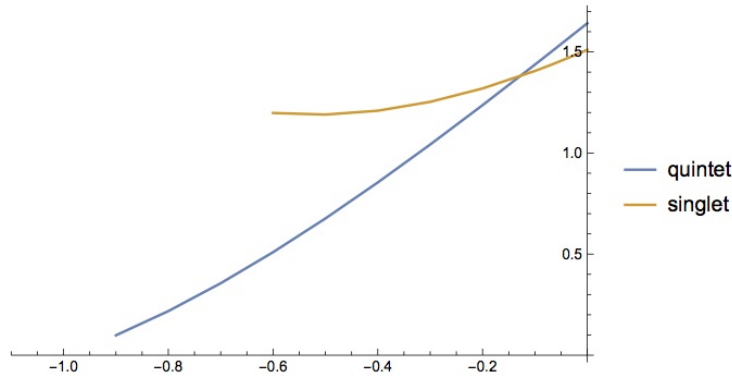


**Figure 6.5:**  $SU(3)$  equivalent model to the bilinear-biquadratic Hamiltonian. Gap of the second singlet and the quintet states for  $\beta < 0$ . The singlet can be traced back only until the value  $\beta = -0.6$  for which the singlet last appears among the nine lowest excited states of the Hamiltonian. The quintet, however, remains the first excited state until we come to  $\beta = -1$ , where the states organise once again according to the representations of the recovered  $SU(3)$  symmetry. The gap between the ground state and the first excited state (quintet) rapidly decreases in the range  $\beta^{-1} \leq -0.2$  approaching  $\beta = -1$ .

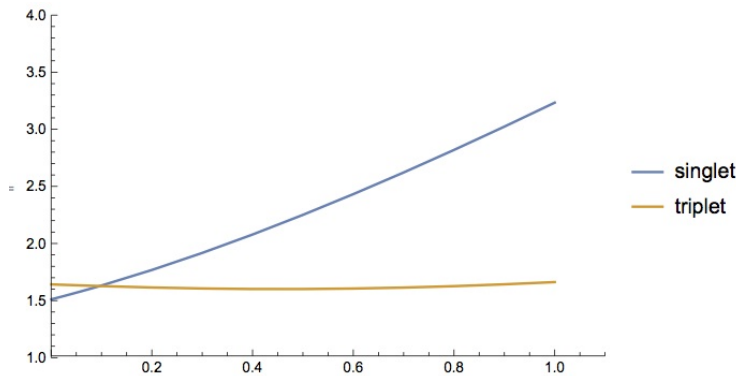


**Figure 6.6:**  $SU(3)$  equivalent model to the bilinear-biquadratic Hamiltonian. Gap of the second singlet and the triplet states for  $\beta > 0$ . The singlet line crosses the triplet one at  $\beta^{-1} = 0.1$  and remains between the triplet and the quintet states from there on. The gap between the the ground state and the first excited state (triplet) remains almost constant in the range  $0.1 \leq \beta^{-1} \leq 1$ , while the gap of the second singlet increases as we approach  $\beta = 1$ .

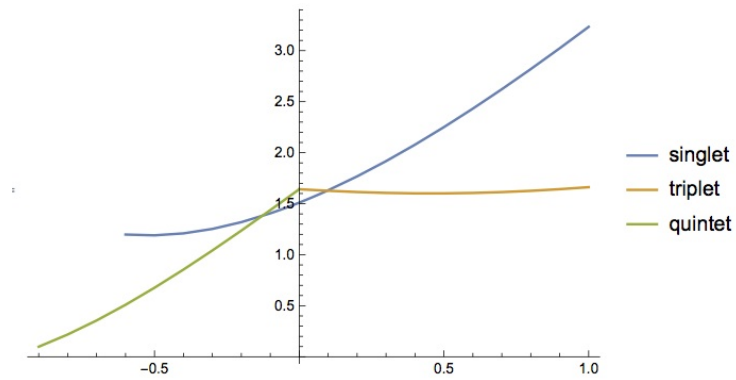


**Figure 6.7:**  $SU(3)$  equivalent model to the bilinear-biquadratic Hamiltonian. Global representation of the gap of the lowest excited states (singlet and triplet for  $\beta > 0$ ; quintet and singlet for  $\beta < 0$ ) in the entire parameter range  $\beta \in [-1, 1]$ , covering the phase space region between the russian model  $\beta = 1$  and the antiferromagnetic-ferromagnetic transition point  $\beta = -1$ .

# Appendix A

## Spin-1 Representations

The main topics dealt with in this thesis lay their foundations on spin-1 chains, which are essentially one dimensional models, where the relevant interactions occur among spin variables positioned on each locus of the chain. This appendix tries to give a quick overview of the very basic properties of the spin-1 representations.

It is crucial to have a full understanding of the elementary properties of spin-1 operators on each site, because we will then consider a system of spin variables interacting through a Hamiltonian, that connects the various spins belonging to the chain. This results into a very large Hilbert space for the system under consideration, which is essentially built up by Kronecker products of representations of spin-1, as many as the number of sites on the chain.

A primary aim of this appendix is trying to establish a conventional notation, which we will follow consistently throughout the whole work.

### A.1 Spin variables

Spin is an intrinsic degree of freedom of fundamental particles, which spontaneously arises in the definition of fields behaviour under the action of the rotation group. Therefore, spin may be thought as an intrinsic angular momentum of elementary particles, which acts differently on each type of field, modifying the field form by means of position independent operators.

Different kinds of fields transform according to different types of spin representations; namely spinor fields transform under the fundamental representation, meanwhile vector fields transform under the spin-1 one representation. This is the reason why vector fields are essentially employed to describe spin-1 particles.

Different representations correspond to different operators and matrix dimensions, but with one underlying common feature, that is determined by the universal behaviour of operators under commutation. The spin relation

with angular momentum appears immediately clear when we check that the commutation relations among spin group generators obey the  $SU(2)$  Lie algebra, that is exactly the same algebra as the rotation group  $SO(3)$ .

This is the physical context in which spin emerges, but for our purposes we shall focus on spin degrees of freedom only, separately from the other physical features related to particles.

## A.2 Spin-1 operators

The spin-1 operators form a representation of the spin group of dimension three and are related to classical variables, which can take on three different values, which we conventionally set to  $-1, 0, +1$ . The three cartesian components of the spin vector are conventionally represented by  $3 \times 3$  matrices:

$$S^x = \frac{1}{\sqrt{2}} \begin{pmatrix} 0 & 1 & 0 \\ 1 & 0 & 1 \\ 0 & 1 & 0 \end{pmatrix} \quad S^y = \frac{1}{\sqrt{2}} \begin{pmatrix} 0 & -i & 0 \\ i & 0 & -i \\ 0 & i & 0 \end{pmatrix} \quad S^z = \begin{pmatrix} 1 & 0 & 0 \\ 0 & 0 & 0 \\ 0 & 0 & -1 \end{pmatrix} \quad (\text{A.1})$$

We may interpret the generators of the spin group as the three hermitian traceless generators of the special unitary group  $SU(2)$ , which is isomorphic to the rotations group in three dimensions  $SO(3)$ . They, in fact, obey the same Lie algebra, that has the following commutation relations:

$$[S^\alpha, S^\beta] = i \varepsilon_{\alpha\beta\gamma} S^\gamma \quad \text{with} \quad \alpha, \beta, \gamma = x, y, z \quad (\text{A.2})$$

We may introduce two new operators:

$$S^\pm = S^x \pm iS^y \quad (S^\pm)^\dagger = S^\mp \quad (\text{A.3})$$

$$S^+ = \sqrt{2} \begin{pmatrix} 0 & 1 & 0 \\ 0 & 0 & 1 \\ 0 & 0 & 0 \end{pmatrix} \quad S^- = \sqrt{2} \begin{pmatrix} 0 & 0 & 0 \\ 1 & 0 & 0 \\ 0 & 1 & 0 \end{pmatrix} \quad (\text{A.4})$$

which we call ladder operators, since their action on the eigenstates of  $S^z$  has the effect of respectively raising or lowering by one unity the eigenvalue of  $S^z$ .

$$\begin{aligned} S^+ |+\rangle &= 0 & S^+ |0\rangle &= \sqrt{2} |+\rangle & S^+ |-\rangle &= \sqrt{2} |0\rangle \\ S^- |+\rangle &= \sqrt{2} |0\rangle & S^- |0\rangle &= \sqrt{2} |-\rangle & S^- |-\rangle &= 0 \end{aligned} \quad (\text{A.5})$$

This property can be seen immediately by the following commutation rules, which may equally be taken as a definition of the  $SU(2)$  group:

$$[S^z, S^\pm] = \pm S^\pm \quad \text{and} \quad [S^+, S^-] = 2S^z \quad (\text{A.6})$$

Since none of the generators commute with the others, we may indifferently represent the states on a basis of eigenstates of a single one of the three

generators. It is convenient to choose  $S^z$ , which is diagonal with eigenvalues  $\lambda = 0, \pm 1$ . Therefore, we can decompose a generic state on the following basis, which is the canonical basis:

$$|+\rangle = \begin{pmatrix} 1 \\ 0 \\ 0 \end{pmatrix} \quad |0\rangle = \begin{pmatrix} 0 \\ 1 \\ 0 \end{pmatrix} \quad |-\rangle = \begin{pmatrix} 0 \\ 0 \\ 1 \end{pmatrix} \quad (\text{A.7})$$

The formerly outlined representation of the spin-1 operators is the best physical picture and usually the most widely employed. However, we may choose different representations as long as they satisfy the same commutation rules and, thus, the same Lie algebra, given by (A.2).

An other useful spin representation, which spontaneously arise from the interpretation of spin as a rotation group, may be given by the antisymmetric generators of rotations in three dimensions times  $i\hbar$ :

$$S_1 = i\hbar \begin{pmatrix} 0 & 0 & 0 \\ 0 & 0 & -1 \\ 0 & 1 & 0 \end{pmatrix} \quad S_2 = i\hbar \begin{pmatrix} 0 & 0 & 1 \\ 0 & 0 & 0 \\ -1 & 0 & 0 \end{pmatrix} \quad S_3 = i\hbar \begin{pmatrix} 0 & -1 & 0 \\ 1 & 0 & 0 \\ 0 & 0 & 0 \end{pmatrix} \quad (\text{A.8})$$

(In order to make them dimensionless we may drop the  $\hbar$  dependence). Now, since all of the three matrices are non-diagonal, the eigenvalues of them being  $\lambda = 0, \pm 1$ , we may write down the eigenstates of  $S^3$  as linear combinations of the canonical basis vectors in the following way:

$$|+\rangle = \frac{1}{\sqrt{2}} \begin{pmatrix} -i \\ 1 \\ 0 \end{pmatrix} \quad |0\rangle = \begin{pmatrix} 0 \\ 0 \\ 1 \end{pmatrix} \quad |-\rangle = \frac{1}{\sqrt{2}} \begin{pmatrix} i \\ 1 \\ 0 \end{pmatrix} \quad (\text{A.9})$$

This choice may be not very practical as long as we need to classify the states according to the  $S^z$  eigenvalues, because we have to deal with linear combinations, but it turns out to be a very useful representation to prove the equivalence of the biquadratic Hamiltonian with an  $SU(3)$  spin chain with alternate fundamental and antifundamental representations. (See Appendix C)

Eventually, let's introduce one last spin representation which has been massively employed throughout this work, even though it is not really widespread. However, it allows an immediate classification of eigenstates of a spin chain because  $S^z$  has a diagonal form exactly corresponding to the third Gell-Mann matrix. (see Appendix B and sections 3.3 and 3.4)

$$S^x = \frac{1}{\sqrt{2}} \begin{pmatrix} 0 & 0 & 1 \\ 0 & 0 & 1 \\ 1 & 1 & 0 \end{pmatrix} \quad S^y = \frac{1}{\sqrt{2}} \begin{pmatrix} 0 & 0 & -i \\ 0 & 0 & i \\ i & -i & 0 \end{pmatrix} \quad S^z = \begin{pmatrix} 1 & 0 & 0 \\ 0 & -1 & 0 \\ 0 & 0 & 0 \end{pmatrix} \quad (\text{A.10})$$

The eigenvalues and eigenstates of  $S^z$  are exactly the same as (A.7), but they appear in a slightly different order on the canonical basis:

$$|+\rangle = \begin{pmatrix} 1 \\ 0 \\ 0 \end{pmatrix} \quad |0\rangle = \begin{pmatrix} 0 \\ 0 \\ 1 \end{pmatrix} \quad |-\rangle = \begin{pmatrix} 0 \\ 1 \\ 0 \end{pmatrix} \quad (\text{A.11})$$

The same definitions (A.3), (A.4) and considerations (A.5) about the ladder operators apply also in this case, with:

$$S^+ = \sqrt{2} \begin{pmatrix} 0 & 0 & 1 \\ 0 & 0 & 0 \\ 0 & 1 & 0 \end{pmatrix} \quad S^- = \sqrt{2} \begin{pmatrix} 0 & 0 & 0 \\ 0 & 0 & 1 \\ 1 & 0 & 0 \end{pmatrix} \quad (\text{A.12})$$

We may check that the commutation relations (A.6) and (A.2) still hold too.

### A.3 $SU(2)$ -multiplets

$SU(2)$  is a continuous symmetry group of dimension  $2^2 - 1 = 3$ , isomorphic to the rotations group in three dimensions,  $SO(3)$ . Their common Lie algebra is built upon three generators, none of which commute with the others, as established by (A.2). The corresponding maximum number of commuting operators, that defines the group rank is thus one. By Racach theorem we have only one Casimir operator, that is:

$$S^2 = (S^x)^2 + (S^y)^2 + (S^z)^2, \quad (\text{A.13})$$

which is a bilinear function of all the generators having the property of commuting with all the former and thus with all the elements of the symmetry group.

Now we may start a classification of the  $SU(2)$ -symmetric states by labelling them with the corresponding  $S^2$  eigenvalue.

The problem that arises in this picture is that  $S^2$  eigenvalues are not sufficient to point out a unique state, because in the generic representation of spin  $S$ ,  $S^2$  eigenstates are  $(2S + 1)$ -fold degenerate. These  $2S + 1$  states transform among themselves under the action of the ladder operator  $S^+$  and  $S^-$ , closing the  $SU(2)$  algebra (A.2). The set of degenerate states which transform among themselves under the action of a symmetry group form an invariant subspace, called a multiplet. The Casimir operators of a group uniquely characterize the multiplets.

Focusing on the particular case  $S = 1$ , we find three different eigenstates, each of them with an eigenvalue of  $S^2 = S(S + 1) = 2$ , but we are allowed to label them thanks to an other good quantum number, which has been chosen to be the  $S^z$  eigenvalue. They turn out to be:

$$\begin{aligned} |+\rangle &= |S^2 = 2, S^z = +1\rangle \\ |0\rangle &= |S^2 = 2, S^z = 0\rangle \\ |-\rangle &= |S^2 = 2, S^z = -1\rangle \end{aligned} \quad (\text{A.14})$$

The action of the ladder operators on a generic state of the multiplet generates the whole set of degenerate states belonging to the associated multiplet. The case of a single particle of spin  $S$  is elementary; the application of  $S^\pm$

$$S^\pm |S, s\rangle = \sqrt{S(S+1) - s(s \pm 1)} |S, s \pm 1\rangle \quad (\text{A.15})$$

on the eigenstates (A.14), reproduces in the spin-1 case the relations established in (A.5). This is, however, generally true for any representation of spin  $S$ , for which we get a set of  $2S+1$  degenerate eigenstates belonging to the multiplet.

## A.4 Useful commutation rules for spin operators

Commutation rules of squares and mixed products of the spin components with  $S^z$ :

$$[(S^x)^2, S^z] = -i(S^x S^y + S^y S^x) \quad (\text{A.16})$$

$$[(S^y)^2, S^z] = i(S^x S^y + S^y S^x) \quad (\text{A.17})$$

$$[S^x S^y, S^z] = i(S^x)^2 - i(S^y)^2 \quad (\text{A.18})$$

$$[S^y S^x, S^z] = i(S^x)^2 - i(S^y)^2 \quad (\text{A.19})$$

$$[S^x S^z, S^z] = -iS^y S^z \quad (\text{A.20})$$

$$[S^z S^x, S^z] = -iS^z S^y \quad (\text{A.21})$$

$$[S^y S^z, S^z] = iS^x S^z \quad (\text{A.22})$$

$$[S^z S^y, S^z] = iS^z S^x \quad (\text{A.23})$$

Commutation rules of squares and mixed products of the spin components with  $(S^z)^2$ :

$$[(S^x)^2, (S^z)^2] = -i(S^x S^y + S^y S^x)S^z - iS^z(S^x S^y + S^y S^x) \quad (\text{A.24})$$

$$[(S^y)^2, (S^z)^2] = i(S^x S^y + S^y S^x)S^z + iS^z(S^x S^y + S^y S^x) \quad (\text{A.25})$$

$$[S^x S^y, (S^z)^2] = i((S^x)^2 - (S^y)^2)S^z + iS^z((S^x)^2 - (S^y)^2) \quad (\text{A.26})$$

$$[S^y S^x, (S^z)^2] = i((S^x)^2 - (S^y)^2)S^z + iS^z((S^x)^2 - (S^y)^2) \quad (\text{A.27})$$

$$[S^x S^z, (S^z)^2] = -iS^y(S^z)^2 - iS^z S^y S^z \quad (\text{A.28})$$

$$[S^z S^x, (S^z)^2] = -iS^z S^y S^z - i(S^z)^2 S^y \quad (\text{A.29})$$

$$[S^y S^z, (S^z)^2] = iS^x(S^z)^2 - iS^z S^x S^z \quad (\text{A.30})$$

$$[S^z S^y, (S^z)^2] = iS^z S^x S^z + i(S^z)^2 S^x \quad (\text{A.31})$$



# Appendix B

## $SU(3)$ group

$SU(3)$  is the special unitary group in  $n = 3$  dimensions. The group dimension is established by the number of generators, which is known to be given by  $n^2 - 1 = 8$ . It is also a remarkable fact that  $SU(3)$  contains  $SU(2)$  as a subgroup. We may, in fact, assemble three different copies of  $SU(2)$ , using some of the generators of  $SU(3)$ .

### B.1 Group generators

The eight group generators of  $SU(3)$  in the group fundamental representation of dimension three are the well-known Gell-Mann matrices, which are universally defined as follows:

$$\lambda^1 = \begin{pmatrix} 0 & 1 & 0 \\ 1 & 0 & 0 \\ 0 & 0 & 0 \end{pmatrix} \quad \lambda^2 = \begin{pmatrix} 0 & -i & 0 \\ i & 0 & 0 \\ 0 & 0 & 0 \end{pmatrix} \quad \lambda^3 = \begin{pmatrix} 1 & 0 & 0 \\ 0 & -1 & 0 \\ 0 & 0 & 0 \end{pmatrix} \quad (\text{B.1})$$

$$\lambda^4 = \begin{pmatrix} 0 & 0 & 1 \\ 0 & 0 & 0 \\ 1 & 0 & 0 \end{pmatrix} \quad \lambda^5 = \begin{pmatrix} 0 & 0 & -i \\ 0 & 0 & 0 \\ i & 0 & 0 \end{pmatrix} \quad \lambda^6 = \begin{pmatrix} 0 & 0 & 0 \\ 0 & 0 & 1 \\ 0 & 1 & 0 \end{pmatrix} \quad (\text{B.2})$$

$$\lambda^7 = \begin{pmatrix} 0 & 0 & 0 \\ 0 & 0 & -i \\ 0 & i & 0 \end{pmatrix} \quad \lambda^8 = \frac{1}{\sqrt{3}} \begin{pmatrix} 1 & 0 & 0 \\ 0 & 1 & 0 \\ 0 & 0 & -2 \end{pmatrix} \quad (\text{B.3})$$

We should notice that these matrices are all hermitian, as required for the generators of a unitary group, and traceless, to guarantee the condition on the determinant, that is bound to be 1. The Lie algebra obeyed by the Gell-Mann matrices is more complicated than the corresponding  $SU(2)$  one and it can be summarised by the commutation and anticommutation rules:

$$[\lambda^\alpha, \lambda^\beta] = 2if^{\alpha\beta\gamma}\lambda_\gamma \quad (\text{B.4})$$

$$\{\lambda^\alpha, \lambda^\beta\} = \frac{4}{3}\delta^{\alpha\beta}\mathbb{I} + 2d^{\alpha\beta\gamma}\lambda_\gamma \quad (\text{B.5})$$

where  $\alpha, \beta, \gamma$  run from 1 to 8 and  $f_{\alpha\beta\gamma}$  are the structure constants of the group, which are completely antisymmetric with respect to the exchange of the three indices, meanwhile the coefficients  $d_{\alpha\beta\gamma}$  are completely symmetric.

$$f^{\alpha\beta\gamma} = -f^{\beta\alpha\gamma} = -f^{\alpha\gamma\beta} = -f^{\gamma\beta\alpha} = f^{\beta\gamma\alpha} = f^{\gamma\alpha\beta} \quad (\text{B.6})$$

$$d^{\alpha\beta\gamma} = d^{\beta\alpha\gamma} = d^{\alpha\gamma\beta} = d^{\gamma\beta\alpha} = d^{\beta\gamma\alpha} = d^{\gamma\alpha\beta} \quad (\text{B.7})$$

A complete outline of the non-zero structure constants and the symmetry coefficients can be found in table B.1.

$\alpha\beta\gamma$	$f^{\alpha\beta\gamma}$	$\alpha\beta\gamma$	$d^{\alpha\beta\gamma}$
123	1	118	$\frac{1}{\sqrt{3}}$
145	$\frac{1}{2}$	146	$\frac{1}{2}$
156	$-\frac{1}{2}$	157	$\frac{1}{2}$
246	$\frac{1}{2}$	228	$\frac{1}{\sqrt{3}}$
257	$\frac{1}{2}$	247	$-\frac{1}{2}$
345	$\frac{1}{2}$	256	$\frac{1}{2}$
367	$-\frac{1}{2}$	338	$\frac{1}{\sqrt{3}}$
458	$\frac{\sqrt{3}}{2}$	344	$\frac{1}{2}$
678	$\frac{\sqrt{3}}{2}$	355	$\frac{1}{2}$
		366	$-\frac{1}{2}$
		377	$-\frac{1}{2}$
		448	$-\frac{1}{2\sqrt{3}}$
		558	$-\frac{1}{2\sqrt{3}}$
		668	$-\frac{1}{2\sqrt{3}}$
		778	$-\frac{1}{2\sqrt{3}}$
		888	$-\frac{1}{\sqrt{3}}$

**Table B.1:** Non-zero structure constants  $f^{\alpha\beta\gamma}$  and symmetry coefficients  $d^{\alpha\beta\gamma}$  for the  $SU(3)$  group. Antisymmetric and symmetric permutations of indices are understood.

An other useful property, which can be checked via explicit calculation, involves the trace of the  $SU(3)$  generators:

$$\text{Tr}[\lambda^\alpha \lambda^\beta] = \delta^{\alpha\beta} \quad (\text{B.8})$$

## B.2 Lie Subalgebras of $SU(3)$

We may redefine the generators of the  $SU(3)$  group, just as we usually do for the spin operators of the  $SU(2)$  group, as  $F^\alpha = \frac{1}{2}\lambda^\alpha$  and rewrite the

commutation relation (B.4) as:

$$[F^\alpha, F^\beta] = iF^{\alpha\beta\gamma} F_\gamma \quad \text{with} \quad \alpha, \beta, \gamma = 1, 2, \dots, 8. \quad (\text{B.9})$$

Following the same pattern outlined for the  $SU(2)$  case, let's define, then, ladder operators of three different types  $T$ ,  $U$ ,  $V$ , using the six operators which have a non-diagonal matrix representation:

$$T^\pm = F^1 \pm i F^2 \quad V^\pm = F^4 \pm i F^5 \quad U^\pm = F^6 \pm i F^7. \quad (\text{B.10})$$

We should pay special attention to the two diagonal Gell-Mann matrices:

$$T^3 = F^3 \quad Y = \frac{2}{\sqrt{3}} F^8 \quad (\text{B.11})$$

which will be later used as good quantum numbers to describe the states belonging to  $SU(3)$  multiplets. The commutation relations will be subsequently modified as follows:

$$[T^3, T^\pm] = \pm T^\pm \quad [T^+, T^-] = 2 T^3 \quad (\text{B.12})$$

$$[T^3, V^\pm] = \pm \frac{1}{2} V^\pm \quad [V^+, V^-] = \frac{3}{2} Y + T^3 \quad (\text{B.13})$$

$$[T^3, U^\pm] = \mp \frac{1}{2} U^\pm \quad [U^+, U^-] = \frac{3}{2} Y - T^3 \quad (\text{B.14})$$

$$[Y, T^\pm] = 0 \quad [Y, V^\pm] = V^\pm \quad [Y, U^\pm] = U^\pm \quad (\text{B.15})$$

$$[T^+, V^-] = -U^- \quad [T^+, U^+] = V^+ \quad [U^+, V^-] = T^- \quad (\text{B.16})$$

$$[T^-, V^+] = +U^+ \quad [T^-, U^-] = -V^- \quad [U^-, V^+] = -T^+ \quad (\text{B.17})$$

$$[T^+, V^+] = 0 \quad [T^+, U^-] = 0 \quad [U^+, V^+] = 0 \quad (\text{B.18})$$

$$[T^-, V^-] = 0 \quad [T^-, U^+] = 0 \quad [U^-, V^-] = 0 \quad (\text{B.19})$$

$$[T^3, Y] = 0 \quad (\text{B.20})$$

It is immediately understood from the complete set of the commutation rules that the maximum number of commuting generators for the  $SU(3)$  group is two. This property sets the group rank at two, and, as a consequence of the Racah's theorem, we should be able to build two Casimir operators. These conventionally are defined by:

$$C^1 = -\frac{2}{3} i \sum_{\alpha, \beta, \gamma=1}^8 f_{\alpha\beta\gamma} F^\alpha F^\beta F^\gamma = \sum_{\alpha=1}^8 (F^\alpha)^2 \quad (\text{B.21})$$

$$C^2 = \sum_{\alpha, \beta, \gamma=1}^8 d_{\alpha\beta\gamma} F^\alpha F^\beta F^\gamma \quad (\text{B.22})$$

Once given the former definitions, setting  $V^3 = \frac{3}{4} Y + \frac{1}{2} T^3$  and  $U^3 = \frac{3}{4} Y - \frac{1}{2} T^3$ , we notice from (B.12), (B.13) and (B.14) that the T, V and

$U$  algebras are closed under the commutator operation, therefore they form subalgebras of the  $SU(3)$  Lie algebra.

They are indeed three different copies of the  $SU(2)$  algebra (A.6), which do not commute among themselves, as we can see from (B.16) and (B.17); which is a consequence of the fact that  $SU(3)$  cannot be built as a direct product of  $SU(2)$  representations.

As previously anticipated, we can classify  $SU(3)$  states by means of two quantum numbers and, according to the common use, the eigenvalues of the commuting operators  $T^3$  and  $Y$  take on this role. Thus, we can represent the  $SU(3)$  symmetric states on a  $T^3 - Y$  plane, on which the action of the shift operators is defined by the commutation rules (B.12), (B.13), (B.14) and (B.14). Aiming to immediately visualise the action of the  $T^\pm$ ,  $V^\pm$  and  $U^\pm$  operators on the common eigenstates of  $T^3$  and  $Y$ , a pictorial representation may be very useful.

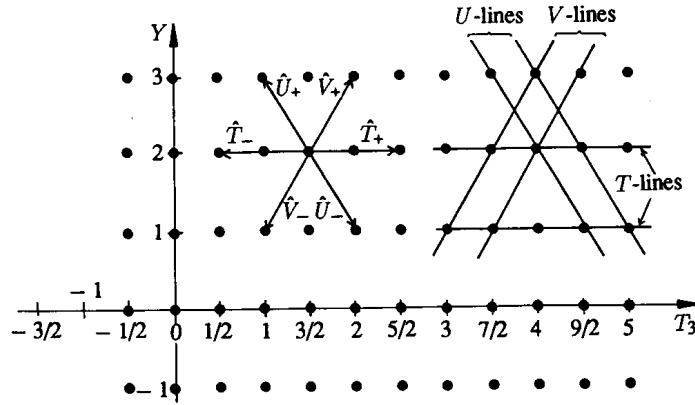


**Figure B.1:** Action of the  $SU(3)$  ladder operators on the  $T^3 - Y$  plane. Their directions cross forming angles of  $60^\circ$  that ensure the  $SU(3)$  symmetric structure of the multiplets built up by the action of these operators. Commutation rules (B.12), (B.13), (B.14) and (B.14) of the Lie algebra define the relations among them, which are now easier to visualise on the  $T^3 - Y$  plane. (Picture taken from [22]).

Rescaling on the  $Y$ -axis by a factor of  $\frac{\sqrt{3}}{2}$  is due to the fact that the arrows representing  $U^\pm$  and  $V^\pm$  operators are bound to have the same length of the  $T$  vector, which lies parallel to the  $T^3$ -axis. The resulting geometrical construction is an equilateral triangle, that perfectly embodies the required symmetry with respect to the three axes established by the three different  $SU(2)$  spin representations. Regarding symmetries, we know that each  $SU(2)$ -multiplet is bound to be symmetric with respect to three symmetry axes rotated by  $120^\circ$ , fixed by the directions of action of the three types of shift operators defining the  $SU(2)$  subalgebras included in  $SU(3)$ .

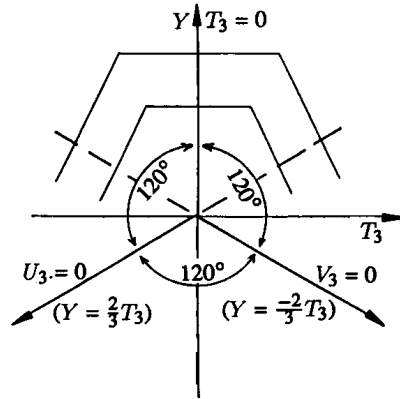


**Figure B.2:** Symmetry axes of an  $SU(3)$  multiplet. Multiplets must obey strict symmetry constraints which bind them to have rather characteristic shapes on the  $T^3 - Y$  plane. The only geometrical figures which fit these criteria, in particular the internal angles of  $60^\circ$ , are equilateral triangles and hexagon with at least two alternatively equal sides. (Picture taken from [22]).

### B.3 $SU(3)$ -multiplets

The same properties and definitions formerly outlined for the  $SU(2)$  group still apply in the  $SU(3)$  more complicated case, but with some reservations. In fact, the notion of multiplet as an invariant subspace under the action of the symmetry group operators is unaffected by the change of the symmetry group to which we relate, but the structure of the multiplet itself depends explicitly on the symmetry group under investigation.

Thus, important modifications are due, since  $SU(3)$  has rank two and, therefore, two different Casimir operators (B.21) (B.22). In order to univocally characterise the multiplet, we should choose a couple of commuting operators, that are usually  $T^3$  and  $Y$ . Their eigenvalues are exactly what we need to classify the degenerate eigenstates belonging to a  $SU(3)$  multiplet. Let's see now what happens in the case of a single  $SU(3)$ -symmetric variable.

The fundamental representation for  $SU(3)$  is three-dimensional, but there are two inequivalent representations with the same dimension, namely the fundamental [3] and antifundamental one  $[\bar{3}]$ , which cannot be related via unitary transformations. [22]

It is a well-known property of a Lie group that each operator is the result of an exponential mapping with the group generators:

$$U(\vec{c}) = \exp \left[ i \sum_{\alpha=1}^8 c^\alpha F^\alpha \right] \tag{B.23}$$

where  $c^\alpha$  are real parameters, collected in an eight dimensional vector, which

forms a linear combination of the generators  $F^\alpha$  of  $SU(3)$ . Now, we define the antifundamental representation as the one having conjugated operators:

$$\bar{U}(\vec{c}) = \exp\left[-i \sum_{\alpha=1}^8 c^\alpha (F^\alpha)^*\right] = \exp\left[i \sum_{\alpha=1}^8 c^\alpha \bar{F}^\alpha\right] \quad (\text{B.24})$$

Thus, the generators of the antifundamental representation will be the opposite of the conjugated:

$$\bar{F}^\alpha = -(F^\alpha)^* \quad \alpha = 1, 2, \dots, 8 \quad (\text{B.25})$$

Here we show the two different resulting diagrams in the  $T^3 - Y$  plane for the triplets of fundamental (red) and antifundamental (blue) representation.

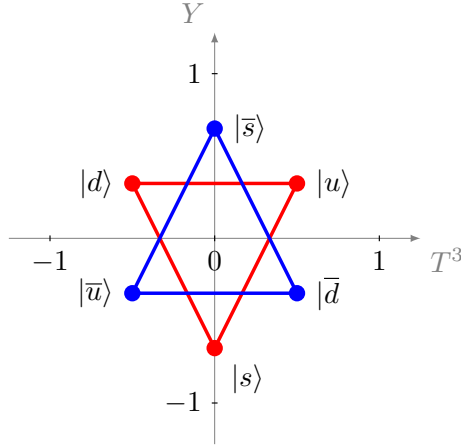


**Figure B.3:** Fundamental  $[3]$  and antifundamental  $[\bar{3}]$  representations of the  $SU(3)$  group. The first one (colour: red) is conventionally employed to represent quarks (up, down and strange); the second one (colour: blue) represents the related set of antiparticles (anti-up, anti-down and anti-strange). The two representations can be mapped one into the other exchanging both the signs of the quantum numbers  $T^3$  and  $Y$ . This corresponds to a central symmetry around the origin of the plane.

Just having a quick look at the geometry of the picture we can notice that, firstly, the structure of the triplets is that one of an equilateral triangle, that is symmetric, as expected, with respect to three axes of symmetry rotated by  $120^\circ$ . Secondly, we can see that it is possible to obtain the  $[\bar{3}]$  graphical representation starting from  $[3]$  and performing a point reflection around the origin.

This is the consequence of the fact that the two quantum numbers we have chosen to employ in order to classify the states belonging to  $SU(3)$ -

multiplets are the eigenvalues of the two real operators:

$$T^3 = \frac{1}{2} \begin{pmatrix} 1 & 0 & 0 \\ 0 & -1 & 0 \\ 0 & 0 & 0 \end{pmatrix} \quad Y = \frac{1}{3} \begin{pmatrix} 1 & 0 & 0 \\ 0 & 1 & 0 \\ 0 & 0 & -2 \end{pmatrix} \quad (\text{B.26})$$

Their antifundamental is, according to (B.25), the opposite of the conjugated matrix operator, resulting in a change of sign for all quantum numbers.

The composite effect of these two axial symmetries with respect to the two cartesian axes, gives a central symmetry with the origin as the reflection point.

The states individuated by the vertices of the equilateral triangles have their own quantum numbers classifying them as follows:

$$|u\rangle = |T^3 = \frac{1}{2}, Y = \frac{1}{3}\rangle \quad (\text{B.27})$$

$$|d\rangle = |T^3 = -\frac{1}{2}, Y = \frac{1}{3}\rangle \quad (\text{B.28})$$

$$|s\rangle = |T^3 = 0, Y = -\frac{2}{3}\rangle \quad (\text{B.29})$$

conventionally labelled by the name of quarks -up, down, strange- they are related to when we deal with  $SU(3)$  as a QCD symmetry group. A similar interpretation is given to the antifundamental representation states, which we may see as the respective antiparticles: anti-up, anti-down and anti-strange.

$$|\bar{u}\rangle = |T^3 = -\frac{1}{2}, Y = -\frac{1}{3}\rangle \quad (\text{B.30})$$

$$|\bar{d}\rangle = |T^3 = \frac{1}{2}, Y = -\frac{1}{3}\rangle \quad (\text{B.31})$$

$$|\bar{s}\rangle = |T^3 = 0, Y = \frac{2}{3}\rangle \quad (\text{B.32})$$

Higher dimensional multiplets will appear in the operation of composition of representations by means of Kronecker products, that mix the fundamental and antifundamental types of representations.

Here we will show some of the lowest dimensional irreducible representations of the  $SU(3)$  group.

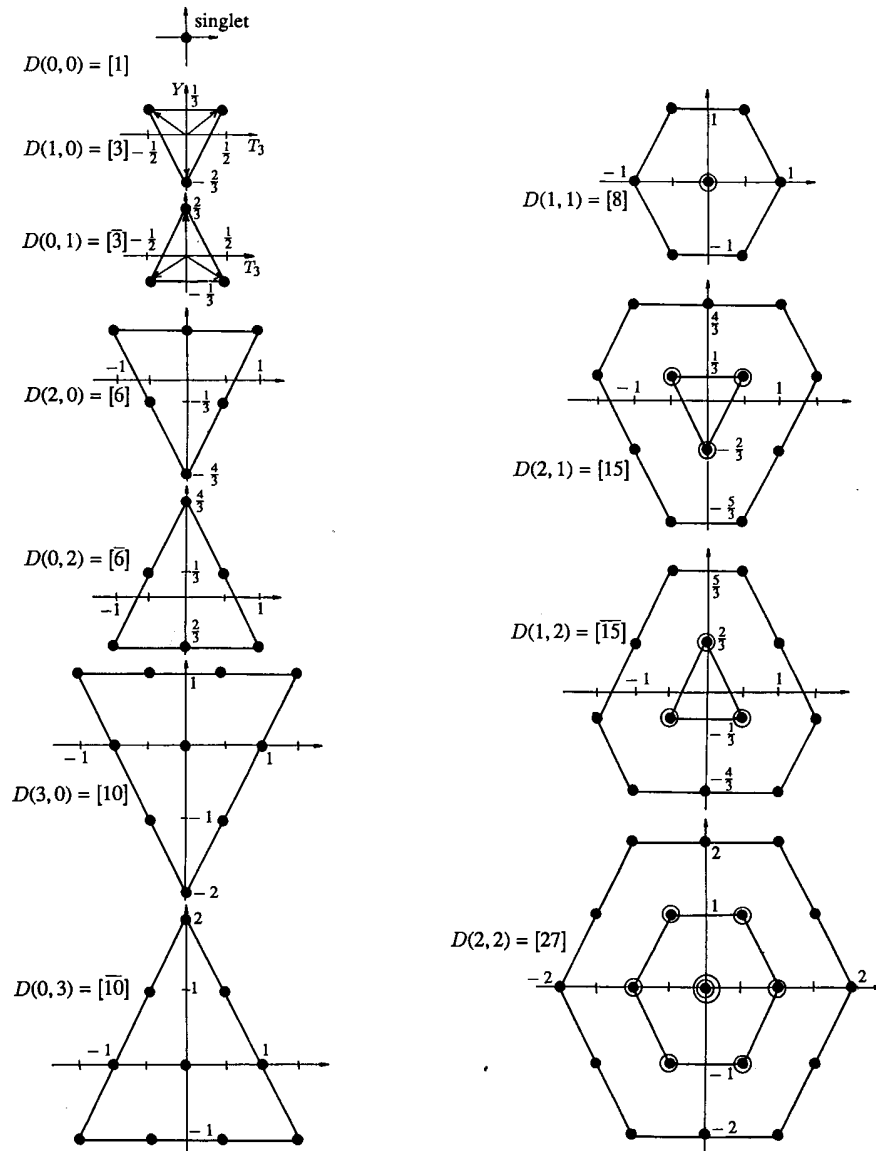


**Figure B.4:** Some of the lowest dimensional  $SU(3)$  representations. They are labelled by two indices  $p$  and  $q$  which graphically represent the lengths of the two possible different sides of the hexagonal shape of the representation. The internal structure of the multiplets and the state degeneracies are determined by these parameters. Note that a conjugated representation does not have the origin as its centre of symmetry, nevertheless it is mapped into its conjugated one by the central symmetry with the origin as the inversion point. (Picture taken from [22]).

Since the multiplets are bound to be symmetric with respect to the three axes, determined by the orthogonal directions to  $T$ ,  $U$  and  $V$  operator lines. There are essentially just three directions to form the edges of the multiplet

polygon, therefore two adjacent edges are sufficient to define the  $SU(3)$  representation.

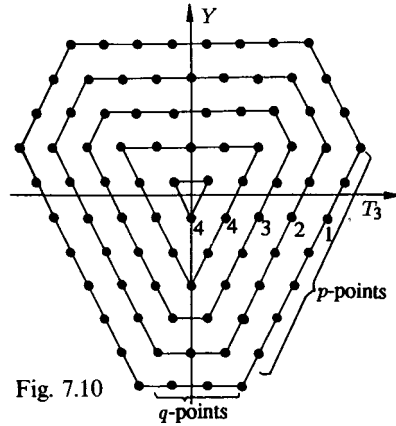


Fig. 7.10

**Figure B.5:** Definition of the  $p$  and  $q$  parameters for a generic  $SU(3)$  representation labelled by the name  $D(p, q)$ .  $p$  is the number of consecutive allowed applications of the operator  $V^-$  to the maximal weight state before getting zero as a result and  $q$  represents the number of allowed consecutive applications from there on of the operator  $T^-$  before getting zero again. See (B.33) for the formula which determines the dimension of the generic representation on  $SU(3)$  given the value of  $p$  and  $q$ . (Picture taken from [22]).

Starting from the furthest state on the right, named the maximal weight state, on which the application of the operators  $T^+, U^+$  and  $V^-$  is null, we may define two numbers  $p$  and  $q$ , that are the numbers of consecutive applications of the operators  $V^-$  and  $T^-$  respectively necessary to get the null vector. The  $SU(3)$  representations  $D(p, q)$  are thus defined by the two boundary variables  $p$  and  $q$ , which allow us to find easily the dimension of the representation given by:

$$d(q, p) = \frac{1}{2}(p + 1)(q + 1)(p + q + 2) \tag{B.33}$$

This formula is based on the following basic rule [22]: whereas the highest weight states may be proved to be unique, each time we reach a inner shell the multiplicity of the states is increased by one, if the outer shell is still hexagonal-shaped, on the contrary the degeneration of states is preserved, if it is triangular-shaped.



# Appendix C

## Alternative mapping

In this appendix we propose an alternative mapping of the purely biquadratic spin-1 model into a  $SU(3)$  Heisenberg chain, which makes it considerably easier to prove the equivalence between the two models, but eventually yields to a non-diagonal form of the operator  $T_i^3$  acting on each site. This further complicates the interpretation of  $T_{tot}^3$  in terms of  $SU(2)$  quantum numbers, preventing us from fulfilling our purpose to map the Bethe ansatz classification of eigenstates in a wider  $SU(3)$ -symmetric structure.

### C.1 Alternative form of the $SU(3)$ Heisenberg chain

It may be convenient to deal with the  $SU(3)$  Heisenberg Hamiltonian in a slightly different formulation from the usual one in terms of Gell-Mann matrices. We will restrict our analysis to the most relevant case for our discussion, that is:

$$\begin{aligned} \mathcal{H}^{F\otimes A}(\pm J) = \pm J \sum_{i=1}^N [ & -\lambda_i^8 \lambda_{i+1}^8 - \lambda_i^3 \lambda_{i+1}^3 + \\ & - \lambda_i^1 \lambda_{i+1}^1 + \lambda_i^2 \lambda_{i+1}^2 - \lambda_i^4 \lambda_{i+1}^4 + \lambda_i^5 \lambda_{i+1}^5 - \lambda_i^6 \lambda_{i+1}^6 + \lambda_i^7 \lambda_{i+1}^7 ] \end{aligned} \quad (\text{C.1})$$

which has alternate fundamental and antifundamental representations on odd and even sites.

Since for the spin-1/2 operators it is possible to express the combination  $S_i^x S_{i+1}^x + S_i^y S_{i+1}^y$  in terms of the  $SU(2)$  ladder operators, namely  $\frac{1}{2}(S_i^- S_{i+1}^+ + S_i^+ S_{i+1}^-)$ , we may attempt to do the same for the spin-1 operators too. In order to do so, all the ladder operators  $T^\pm, U^\pm$  and  $V^\pm$  characterising the three  $SU(2)$  subalgebras included in the  $SU(3)$  group have to be employed.

By means of definition (B.10) we get to the identity:

$$\begin{aligned}
T_i^+ T_{i+1}^+ + T_i^- T_{i+1}^- &= \\
&= \frac{1}{4}(\lambda_i^1 + i\lambda_i^2)(\lambda_{i+1}^1 + i\lambda_{i+1}^2) + \frac{1}{4}(\lambda_i^1 - i\lambda_i^2)(\lambda_{i+1}^1 - i\lambda_{i+1}^2) = \\
&= \frac{1}{2}(\lambda_i^1 \lambda_{i+1}^1 - \lambda_i^2 \lambda_{i+1}^2)
\end{aligned} \tag{C.2}$$

Similarly for the other two cases:

$$U_i^+ U_{i+1}^+ + U_i^- U_{i+1}^- = \frac{1}{2}(\lambda_i^6 \lambda_{i+1}^6 - \lambda_i^7 \lambda_{i+1}^7) \tag{C.3}$$

$$V_i^+ V_{i+1}^+ + V_i^- V_{i+1}^- = \frac{1}{2}(\lambda_i^4 \lambda_{i+1}^4 - \lambda_i^5 \lambda_{i+1}^5) \tag{C.4}$$

Eventually, the  $SU(3)$  Heisenberg Hamiltonian (C.1) can be rewritten in the following form:

$$\begin{aligned}
\mathcal{H}^{F \otimes A}(\pm J) &= \mp J \sum_{i=1}^N [T_i^+ T_{i+1}^+ + T_i^- T_{i+1}^- + U_i^+ U_{i+1}^+ + U_i^- U_{i+1}^- + \\
&+ V_i^+ V_{i+1}^+ + V_i^- V_{i+1}^- + 2T_i^3 T_{i+1}^3 + \frac{3}{2}Y_i Y_{i+1}]
\end{aligned} \tag{C.5}$$

where the last two Gell-Mann matrices  $\lambda^3$  and  $\lambda^8$  have been replaced by their related  $SU(3)$  operators  $T^3$  and  $Y$  (B.11).

## C.2 Mapping between spin-1 operators and Gell-Mann matrices

The following pages outline the complete mapping between the  $SU(3)$ -symmetric Heisenberg chain and two special cases of the spin-1 bilinear-biquadratic models, i.e. the pure biquadratic and the Lai-Sutherland models. As previously stated, this mapping [13] is indeed the easiest way to prove the equivalence between the models under investigation. In fact, the equivalence between the two Hamiltonians follows immediately, once the basic equivalence with the generators of  $SU(2)$  algebra has been established. Namely:

$$S^1 = \lambda^7 \quad S^2 = -\lambda^5 \quad S^3 = \lambda^2 \tag{C.6}$$

Let's make now, the correspondence with the  $SU(3)$  operators for some operators which turn out to be part of the bilinear-biquadratic model. Firstly the squares of the spin components:

$$(S^1)^2 = \frac{1}{2} \left( -\lambda^3 - \frac{1}{\sqrt{3}}\lambda^8 + \frac{4}{3} \right) \tag{C.7}$$

$$(S^2)^2 = \frac{1}{2} \left( \lambda^3 - \frac{1}{\sqrt{3}} \lambda^8 + \frac{4}{3} \right) \quad (\text{C.8})$$

$$(S^3)^2 = \frac{1}{3} \left( \sqrt{3} \lambda^8 + 2 \right) \quad (\text{C.9})$$

and then the mixed products of components:

$$S^1 S^2 = -\frac{1}{2} (\lambda^1 - i\lambda^2) \quad S^2 S^1 = -\frac{1}{2} (\lambda^1 + i\lambda^2) \quad (\text{C.10})$$

$$S^1 S^3 = -\frac{1}{2} (\lambda^4 - i\lambda^5) \quad S^3 S^1 = -\frac{1}{2} (\lambda^4 + i\lambda^5) \quad (\text{C.11})$$

$$S^2 S^3 = -\frac{1}{2} (\lambda^6 - i\lambda^7) \quad S^3 S^2 = -\frac{1}{2} (\lambda^6 + i\lambda^7) \quad (\text{C.12})$$

Let us start with the bilinear form of the  $SU(2)$ -symmetric Heisenberg Hamiltonian, having the following expression in terms of spin-1 operators:

$$\mathcal{H}^{Heis}(J) = J \sum_{i=1}^N \left( (S_i^1)(S_{i+1}^1) + (S_i^2)(S_{i+1}^2) + (S_i^3)(S_{i+1}^3) \right) \quad (\text{C.13})$$

Using the mapping (C.6), it is easy to see that:

$$(S_i^1)(S_{i+1}^1) + (S_i^2)(S_{i+1}^2) + (S_i^3)(S_{i+1}^3) = \lambda_i^7 \lambda_{i+1}^7 + \lambda_i^5 \lambda_{i+1}^5 + \lambda_i^2 \lambda_{i+1}^2 \quad (\text{C.14})$$

Now, let's deal with the biquadratic term of the Hamiltonian, which yields nine different terms:

$$\begin{aligned} \mathcal{H}^{biQ}(-J) = -J \sum_{i=1}^N & \left( (S_i^1)^2 (S_{i+1}^1)^2 + (S_i^2)^2 (S_{i+1}^2)^2 + (S_i^3)^2 (S_{i+1}^3)^2 + \right. \\ & + (S_i^1 S_i^2)(S_{i+1}^1 S_{i+1}^2) + (S_i^2 S_i^1)(S_{i+1}^2 S_{i+1}^1) + (S_i^1 S_i^3)(S_{i+1}^1 S_{i+1}^3) + \\ & \left. + (S_i^3 S_i^1)(S_{i+1}^3 S_{i+1}^1) + (S_i^2 S_i^3)(S_{i+1}^2 S_{i+1}^3) + (S_i^3 S_i^2)(S_{i+1}^3 S_{i+1}^2) \right) \end{aligned} \quad (\text{C.15})$$

In order to complete the mapping we need the biquadratic terms and the quadratic mixed products. Using the identities (C.7), (C.8) and (C.9), we get:

$$\begin{aligned} (S_i^1)^2 (S_{i+1}^1)^2 = \frac{1}{4} & \left( \lambda_i^3 \lambda_{i+1}^3 + \frac{1}{3} \lambda_i^8 \lambda_{i+1}^8 + \frac{16}{9} + \right. \\ & \left. + \frac{1}{\sqrt{3}} \lambda_i^3 \lambda_{i+1}^8 + \frac{1}{\sqrt{3}} \lambda_i^8 \lambda_{i+1}^3 - \frac{4}{3\sqrt{3}} \lambda_i^8 - \frac{4}{3\sqrt{3}} \lambda_{i+1}^8 - \frac{4}{3} \lambda_i^3 - \frac{4}{3} \lambda_{i+1}^3 \right) \end{aligned} \quad (\text{C.16})$$

$$\begin{aligned} (S_i^2)^2 (S_{i+1}^2)^2 = \frac{1}{4} & \left( \lambda_i^3 \lambda_{i+1}^3 + \frac{1}{3} \lambda_i^8 \lambda_{i+1}^8 + \frac{16}{9} + \right. \\ & \left. - \frac{1}{\sqrt{3}} \lambda_i^3 \lambda_{i+1}^8 - \frac{1}{\sqrt{3}} \lambda_i^8 \lambda_{i+1}^3 - \frac{4}{3\sqrt{3}} \lambda_i^8 - \frac{4}{3\sqrt{3}} \lambda_{i+1}^8 + \frac{4}{3} \lambda_i^3 + \frac{4}{3} \lambda_{i+1}^3 \right) \end{aligned} \quad (\text{C.17})$$

$$(S_i^3)^2(S_{i+1}^3)^2 = \frac{1}{3}\lambda_i^8\lambda_{i+1}^8 + \frac{4}{9} + \frac{2}{3\sqrt{3}}\lambda_i^8 + \frac{2}{3\sqrt{3}}\lambda_{i+1}^8 \quad (\text{C.18})$$

Now, using the identities (C.10), (C.11) and (C.12), we may deal with the mixed products, for which a convenient cancellation of terms occurs, leading to the following relations:

$$(S_i^1 S_i^2)(S_{i+1}^1 S_{i+1}^2) + (S_i^2 S_i^1)(S_{i+1}^2 S_{i+1}^1) = \frac{1}{2}(\lambda_i^1 \lambda_{i+1}^1 - \lambda_i^2 \lambda_{i+1}^2) \quad (\text{C.19})$$

$$(S_i^1 S_i^3)(S_{i+1}^1 S_{i+1}^3) + (S_i^3 S_i^1)(S_{i+1}^3 S_{i+1}^1) = \frac{1}{2}(\lambda_i^4 \lambda_{i+1}^4 - \lambda_i^5 \lambda_{i+1}^5) \quad (\text{C.20})$$

$$(S_i^2 S_i^3)(S_{i+1}^2 S_{i+1}^3) + (S_i^3 S_i^2)(S_{i+1}^3 S_{i+1}^2) = \frac{1}{2}(\lambda_i^6 \lambda_{i+1}^6 - \lambda_i^7 \lambda_{i+1}^7) \quad (\text{C.21})$$

Finally, collecting these results all together we may write the most general form of the bilinear-biquadratic spin-1 Hamiltonian, parametrised by means of two coefficients  $\alpha$  and  $\beta$ . Suitable choices of their values correspond to different models represented in the phase space of fig. 1.1.

$$\begin{aligned} \mathcal{H}(\alpha, \beta) &= \alpha \mathcal{H}^{Heis} + \beta \mathcal{H}^{biQ} = \\ &= \sum_{i=1}^N \alpha (\lambda_i^2 \lambda_{i+1}^2 + \lambda_i^5 \lambda_{i+1}^5 + \lambda_i^7 \lambda_{i+1}^7) + \\ &+ \sum_{i=1}^N \frac{1}{2} \beta \left( \lambda_i^8 \lambda_{i+1}^8 + \lambda_i^3 \lambda_{i+1}^3 + \frac{8}{3} + \right. \\ &\left. + \lambda_i^1 \lambda_{i+1}^1 - \lambda_i^2 \lambda_{i+1}^2 + \lambda_i^4 \lambda_{i+1}^4 - \lambda_i^5 \lambda_{i+1}^5 + \lambda_i^6 \lambda_{i+1}^6 - \lambda_i^7 \lambda_{i+1}^7 \right) \end{aligned} \quad (\text{C.22})$$

In order to recover the pure-biquadratic exchange Hamiltonian we need to select the value  $\alpha = 0$  in (C.22), which erases the presence of the bilinear interaction. The resulting expression in terms of standard  $SU(3)$  generators can be interpreted as a  $SU(3)$  Heisenberg chain with alternate fundamental and antifundamental representations on odd and even sites, which cause the signs to change in some given products of Gell-Mann matrices.

$$\begin{aligned} \mathcal{H}^{biQ}(\pm J) &= \mathcal{H}(\alpha = 0, \beta = \pm J) = \pm \frac{1}{2} J \sum_{i=1}^N [ \lambda_i^8 \lambda_{i+1}^8 + \lambda_i^3 \lambda_{i+1}^3 + \\ &+ \lambda_i^1 \lambda_{i+1}^1 - \lambda_i^2 \lambda_{i+1}^2 + \lambda_i^4 \lambda_{i+1}^4 - \lambda_i^5 \lambda_{i+1}^5 + \lambda_i^6 \lambda_{i+1}^6 - \lambda_i^7 \lambda_{i+1}^7 ] \pm \frac{4}{3} J N = \\ &= -\frac{1}{2} \mathcal{H}^{F \otimes A}(\pm J) \pm \frac{4}{3} J N \end{aligned} \quad (\text{C.23})$$

In order to recover the Lai-Sutherland model, we need the coefficients of the bilinear and biquadratic terms to be equal, thus we may select  $\alpha = \beta$  in equation (C.22) to finally get:

$$\begin{aligned}
\mathcal{H}^{LS}(\pm J) &= \mathcal{H}(\alpha = \beta = \pm J) \pm \frac{1}{2}J \sum_{i=1}^N [ \lambda_i^8 \lambda_{i+1}^8 + \lambda_i^3 \lambda_{i+1}^3 + \\
&+ \lambda_i^1 \lambda_{i+1}^1 + \lambda_i^2 \lambda_{i+1}^2 + \lambda_i^4 \lambda_{i+1}^4 + \lambda_i^5 \lambda_{i+1}^5 + \lambda_i^6 \lambda_{i+1}^6 + \lambda_i^7 \lambda_{i+1}^7 ] \pm \frac{4}{3}JN = \\
&= \frac{1}{2}\mathcal{H}^{F \otimes F}(\pm J) \pm \frac{4}{3}JN
\end{aligned} \tag{C.24}$$

which clearly represents a  $SU(3)$  Heisenberg model with the same type of representation on both even and odd sites.



# Bibliography

- [1] I. Affleck, *Exact critical exponents for quantum spin chains, non-linear  $\sigma$ -models at  $\theta = \pi$  and the quantum Hall effect*, Nucl. Phys. B265, 409-447, (1986).
- [2] I. Affleck, *Exact results on the dimerisation transition in  $SU(n)$  antiferromagnetic chains*, J. Phys. 2, 405-415, (1990).
- [3] I. Affleck, T. Kennedy, E. H. Lieb, H. Tasaki, *Rigorous results on valence-bond ground states in antiferromagnets*, Phys. Rev. Lett. 59, 799-802, (1987).
- [4] I. Affleck, T. Kennedy, E. H. Lieb, H. Tasaki, *Valence bond ground states in isotropic quantum antiferromagnets*, Commun. Math. Phys. 115, 477-528, (1988).
- [5] F. C. Alcaraz, M. N. Barber, M. T. Batchelor, *Conformal invariance, the XXZ chain and the operator content of two-dimensional critical systems*, Ann. Phys. N.Y. 182, 280-343, (1988).
- [6] F. C. Alcaraz, M. N. Barber, M. T. Batchelor, *Surface exponents of the quantum XXZ, Ashkin-Teller and Potts models*, J. Phys. A 20, 6397-6409, (1987)
- [7] M. Andres, I. Schneider, S. Eggert, *Highest weight state description of the isotropic spin-1 chain*, Phys. Rev. B 77, 014429 1-7, (2008).
- [8] H. M. Babujian, *Exact solution of the one-dimensional isotropic Heisenberg chain with arbitrary spin  $s$* , Phys. Lett.90A, 479-482, (1982).
- [9] M. N. Barber, M. T. Batchelor, *Spectrum of the biquadratic spin-1 antiferromagnetic chain*, Phys. Rev. B 40, 4621-4626, (1989).
- [10] M. N. Barber, M. T. Batchelor, *Spin- $s$  quantum chains and Temperley-Lieb algebras*, J. Phys. A, L15-L21, (1990).
- [11] R. J. Baxter, *Exactly solved models in statistical mechanics*, Academic Press, (1982).

- [12] R. J. Baxter, H. N. V. Temperley, S. E. Ashley *Triangular Potts Model at its Transition Temperature, and Related Models*, Proc. Roy. Soc. London 358A, 535-559, (1978).
- [13] C. Benassi, *SU(3) lattice gauge theories and spin chains*, <http://amslaurea.unibo.it>, (2014).
- [14] E. Berkcan, *On the order-disorder variables, duality and the functional inversion relation*, Nucl. Phys. B215, 68-82, (1983).
- [15] J. C. Bonner, J. B. Parkinson, J. Oitmaa, H. W. J. Blote, *Unusual critical behavior in a bilinear-biquadratic exchange Hamiltonian*, J. Appl. Phys. 61, 4432-4434, (1987).
- [16] J. Des Cloizeaux, M. Gaudin, H. W. J. Blote, *Anisotropic Linear Magnetic Chain*, J. Math. Phys. 7, 1384-1400 (1966).
- [17] K. Chang, I. Affleck, G. W. Hayden, Z. G. Soos, *A study of the bilinear-biquadratic spin-1 antiferromagnetic chain using the valence-bond basis*, J. Phys. 1, 153-167, (1989).
- [18] P. Di Francesco, P. Mathieu, D. Senechal, *Conformal field theory*, Springer, (1997).
- [19] G. Fath, J. Solyom, *Isotropic spin-1 chain with twisted boundary condition*, Phys. Rev. B 47, 872-881, (1993).
- [20] G. Fath, J. Solyom, *Solitonic excitations in the Haldane phase of an S=1 chain*, J. Phys. 5, 8983-8998, (1993).
- [21] G. Fath, J. Solyom, *Search for the nondimerized quantum nematic phase in the spin-1 chain*, Phys. Rev. B 51, 3620-3625, (1995).
- [22] W. Greiner, B. Muller, *Quantum mechanics symmetries*, Springer, (1994).
- [23] F. D. M. Haldane, *Continuum dynamics of the 1-D Heisenberg antiferromagnet: identification with the O(3) nonlinear sigma model*, Phys. Lett. 93A, 463-468, (1983).
- [24] F. D. M. Haldane, *Nonlinear Field Theory of Large-Spin Heisenberg Antiferromagnets: Semiclassically Quantized Solitons of the One-Dimensional Easy-Axis Néel State*, Phys. Rev. Lett. 50, 1153-1156, (1983).
- [25] M. Henkel, *Conformal invariance and critical phenomena*, Springer, (1999).

- 
- [26] T. Kennedy, H. Tasaki, *Hidden symmetry breaking and the Haldane phase in  $S=1$  quantum spin chains*, Commun. Math. Phys. 147, 431-484, (1992).
- [27] A. Klumper, *The spectra of  $q$ -state vertex models and related antiferromagnetic quantum spin chain*, J. Phys. A23, 809-823, (1989).
- [28] A. Klumper, *New results for  $q$ -state vertex models and pure biquadratic spin-1 Hamiltonian*, Europhys. Lett.9, 815-820, (1989).
- [29] C. K. Lai, *Lattice gas with nearest neighbor interaction in one dimension with arbitrary statistics*, J. Math. Phys. 15, 1675-1676, (1974).
- [30] M. P. Nightingale, H. J. Blote, *Gap of the linear spin-1 Heisenberg antiferromagnet: a Monte Carlo calculation*, Phys. Rev B 33, 659-661, (1986).
- [31] J. B. Parkinson, *The  $S = 1$  quantum spin chain with pure biquadratic exchange*, J.Phys. C 20, L1029-L1032, (1987).
- [32] J. B. Parkinson, *The  $S = 1$  quantum spin chain with pure biquadratic exchange*, J.Phys. C 21, 3793-3806, (1988).
- [33] J. H. H. Perk, C. L. Schultz, *Families of commuting transfer matrices in  $q$ -state vertex models*, Yang-Baxter equation in integrable systems, Michio Jimbo, (1989).
- [34] J. H. H. Perk, F. Y. Wu, *Nonintersecting String Model and Graphical Approach: Equivalence with a Ports Model*, J. Stat. Phys. 42, 727-742, (1986).
- [35] U. Schollwock, Th. Jolicoeur, T. Garel, *Onset of incommensurability at the valence-bond-solid point in the  $S=1$  quantum spin chain*, Phys. Rev. B 53, 3304-3311, (1995).
- [36] J. Solyom, *Competing bilinear and biquadratic exchange couplings in spin-1 Heisenberg chains*, Phys. B 36, 8642-8648, (1987).
- [37] J. Solyom, P. Pfeuty, *Renormalization-group study of Hamiltonian version of the Potts model*, Phys. Rev. B 24, 147, 218-229, (1981).
- [38] Yu. G. Stroganov, *A new calculation method for partition functions in some lattice models*, Phys. Lett. 74A, 116-118, (1979).
- [39] B. Sutherland, *Model for a multicomponent quantum system*, Phys. Rev. B 12, 3795-3805, (1975).
- [40] M. Takahashi, *Thermodynamics of one-dimensional solvable models*, Cambridge University Press, (1999).

- [41] L. A. Takhtajan, *The picture of low-lying excitations in the isotropic Heisenberg chain of arbitrary spin*, Phys. Lett. 87A, 479-482, (1982).